Belo Horizonte

2013

Mariana Noyma Xavier

MECHANISMS OF *BRUCELLA ABORTUS* SURVIVAL DURING CHRONIC INFECTION: THE ROLE OF IL-10 AND PPARγ

Tese apresentada à UFMG, como requisito parcial para a obtenção do título de Doutor.
Curso: Doutorado em Ciência Animal
Área de Concentração: Patologia Animal
Orientador: Renato de Lima Santos

Belo Horizonte

Escola de Veterinária – UFMG

2013

Tese defendida em 25 de junho de 2013, pela comissão examinadora constituída por:

_____

Prof. Renato de Lima Santos

(orientador)

_____

Prof. Sérgio Costa Oliveira

_____

Dr. Andreas J. Bäumler

_____

Dr. Sebastian E. Winter

_____

Dra. Lis Ribeiro do Vale Antonelli

A minha família, meus maiores amores: meu pai Paulo Afonso, minha mãe Wilma, minhas irmãs Thaís e Sílvia, meus cunhados Alexandre e Paulo Emílio e meus sobrinhos Laura, Arthur, Marina e Elisa (nosso anjinho) - Obrigada pela compreensão e por acreditarem junto comigo que mais esta conquista seria possível.

“(...) nem entendo aquilo que entendo: pois estou infinitamente maior do que eu mesma, e não me alcanço. "

(Clarice Linspector)

Agradecimentos

A Deus, por ser a luz que ilumina meu caminho.

Ao Frank, por todo o seu apoio e companheirismo. Você e sua família tornaram meus anos nos EUA muito mais especiais.

Ao prof. Renato de Lima Santos, por sua orientação, preocupação com meu crescimento e por ter aberto as portas para um novo mundo de aprendizagem e descobertas.

A Dra. Renée Tsolis, por abrir as portas do seu laboratório e por acreditar nas minhas idéias. Eu não tenho como medir a admiração e o respeito que eu tenho por você como ser humano e como cientista.

A professora Tatiane Paixão, pela confiança e por todos os anos de ensinamento. Você foi um modelo para mim desde quando trabalhamos juntas na iniciação científica.

A Maria Winter, Vydia Atluri, Alanna Spees, Kim Nguyen e Teane Silva, por sua ajuda em todos os experimentos, e por dedicarem parte do seu precioso tempo aos meus projetos.

Ao Dr. Andreas Den Hartigh, pelo treinamento e paciência durante o meu treinamento no laboratório da Dra. Tsolis.

A todos os membros odo laboratório ABRT, especialmente Maria Winter, Sebastian Winter, Marijke Keestra, Jason Mooney, Tobias Kerrinnes, Franziska Faber and Alanna Spees, por fazerem da ida diária ao trabalho uma experiência tão prazerosa. A amizade de vocês foi o meu maior presente durante esta aventura.

A Nicole Sotak, por me acolher em sua casa e por ser uma amiga tão especial ao longo desta caminhada.

Summary

SUPPLEMENTARY MATERIAL LIST

FIGURE LIST

RESUMO

A evasão de resposta imune do hospedeiro é um pré-requisito para doenças bacterianas crônicas. No entanto, os mecanismos subjacentes não são totalmente compreendidos. Neste estudo foi demonstrado que a *Brucella abortus*, impede a ativação dos macrófagos ao induzir a produção de interleucina-10 (IL-10) por células T $CD4^{+}CD25^{+}$ durante a infecção aguda. Além disso, falha na produção de IL-10 por células T ou a incapacidade de macrófagos em responder a esta citocina resultou num aumento da capacidade de camundongos em controlar a infecção por *B. abortus*, apesar da indução elevada de citocinas pró-inflamatórias, e de grave patologia no fígado e no baço de camundongos infectados. Apesar dos avanços significativos na compreensão da sobrevivência intracelular de *B. abortus in vitro*, pouco se sabe sobre o nicho intracelular de *B. abortus in vivo*. Este estudo demonstra que *B. abortus* é capaz de sobreviver e replicar preferencialmente em macrófagos alternativamente ativados (AAM), que aumentam em número durante a infecção crônica. O mecanismo desta maior sobrevivência em AAM é uma mudança no metabolismo induzido por *"peroxisome proliferator activated receptor gamma"* (PPARγ), o que aumenta a disponibilidade de glucose intracelular. A capacidade de transportar glicose foi crucial para persistência, e para aumento da replicação de *B. abortus* em AAM. Em conjunto, os nossos resultados sugerem que a produção de IL-10 por células T $CD4^{+}CD25^{+}$ modula a função de macrófagos, a fim de promover infecção persistente por *B. abortus*. Além disso, tal persistência, também foi determinada por uma mudança na disponibilidade intracellular de nutrientes induzida por PPARy em AAM.

Palavras-Chave: Brucelose, persistência, macrófago, metabolismo

ABSTRACT

Evasion of host immune responses is a prerequisite for chronic bacterial diseases; however, the underlying mechanisms are not fully understood. This study demonstrated that Brucella abortus prevents immune activation of macrophages by inducing $CD4^+CD25^+$ T cells to produce interleukin-10 (IL-10) early during infection. Moreover, either a lack of IL-10 production by T cells or a lack of macrophage responsiveness to this cytokine resulted in an increased ability of mice to control B. abortus infection, while inducing elevated production of pro-inflammatory cytokines, and severe pathology in liver and spleen of infected mice. In spite of the significant advances in understanding intracellular survival of B. abortus at the cellular level, little is known about the chronic intracellular niche of B. abortus in vivo. This study demonstrated that B. abortus is able to survive and replicate preferentially in alternatively activated macrophages (AAM), which increase in numbers during chronic infection. The underlying mechanism to this enhanced survival in AAM is a shift in metabolism induced by peroxisome proliferator activated receptor gamma (PPARγ), which increases the availability of intracellular glucose. The ability to take up glucose was crucial for increased replication of B. abortus in AAM, and for persistence. Taken together our results suggest that early IL-10 production by $CD25^+CD4^+$ T cells modulates macrophage function in order to promote persistent infection. Additionally, B. abortus persistence was also determined by a shift in intracellular nutrient availability induced by PPARγ in AAM.

Keywords: Brucellosis, persistence, macrophage, metabolism

INTRODUCTION

Brucellosis is a zoonotic bacterial disease caused by bacteria of the genus *Brucella*, which are able to establish long-term infections in their host (Xavier *et al.*, 2009; Atluri *et al.*, 2011). Human brucellosis, caused most commonly by *B. melitensis* and *B. abortus*, is considered one of the most important zoonotic diseases worldwide, with more than 500,000 new human cases reported annually (Pappas *et al.*, 2006). The disease is characterized by a long incubation period that leads to a chronic, sometimes lifelong, debilitating infection with serious clinical manifestations such as fever, arthritis, hepatomegaly, and splenomegaly (Corbel, 1997; Atluri *et al.*, 2011).

In vivo, *Brucella* is found in association with phagocytic cells, most prominently macrophages, in which a subset of bacteria is able to evade killing in phagolysosomes and replicate successively within an endoplasmic reticulum-associated compartment and a modified autophagosome (Gorvel and Moreno 2002; Starr et al., 2008). The furtive aspect of this pathogen is also exemplified by its ability to evade initial innate immune recognition through toll-like receptors (TLRs) (Andersen-Nissen *et al.*, 2005) as well as by modifications of virulence factors such as lipopolysaccharide - LPS (Lapaque *et al.*, 2006) and flagellin (Terwagne *et al.*, 2013), resulting in a mild pro-inflammatory response that leads to bacterial persistence (Atluri *et al.*, 2011). In spite of the important role of TLR evasion in *Brucella* pathogenesis, little is known about subsequent host-pathogen interactions that lead to establishment of chronic infection.

Several pathogens are able to modulate the immune response through induction of regulatory cytokines, such as interleukin-10 (IL-10) (Anderson *et al.*, 2007; Jankovic *et al.*, 2007; Saraiva and O'garra, 2010). Like other chronic pathogens, *Brucella* is able to induce IL-10 in infected cells *in vitro* and during early *in vivo* infection, suggesting that the IL-10 pathway could play an important role in enabling bacterial persistence (Fernandes and Baldwin, 1995; Fernandes *et al.*, 1996; Fernández-Lago *et al.*, 1996). However, the real impact of IL-10 during *in vivo* infection as well as the cell types producing IL-10 or responding to this cytokine during brucellosis is not clear.

Years of research have demonstrated that immune cells can adopt different functional states according to the immune environment around them, and macrophages are no exception (Gordon and Martinez, 2010; Van Dyken and Locksley, 2013). Indeed, an environment rich in Th1 cytokines such as interferon gamma (IFNg) leads to development of classically activated macrophage (CAM) population, characterized by production of nitric oxide (NO) and inflammatory cytokines such as tumor necrosis factor alpha (TNFa) and interleukin 6 (IL-6) (Mosser and Edwards, 2008). Conversely, an environment rich in Th2 cytokines such as interleukin-4 (IL-4) and interleukin-13 (IL-13) promotes the development of alternatively activated macrophages (AAM), which play important roles in allergic inflammation, helminth infection and tissue repair (Reyes and Terrazas, 2007; Shirey *et al.*, 2008; Lawrence and Natoli, 2011).

Interestingly, in addition to their critical influence in establishment of the immune response, CAM and AAM also play important roles in host physiology and metabolism (Chawla, 2010). For instance, development of the AAM phenotype is dependent on peroxisome proliferator activated receptors - PPARs; (Odegaard *et al.*, 2007), which act downstream of STAT6 signaling to regulate macrophage metabolism.

In this context, it is important to note that a key aspect of *Brucella* pathogenesis is its interaction with macrophages. Indeed, research focusing on the *in vitro* *Brucella*/macrophage interaction has been critical for the understanding of how *B. abortus* survives intracellularly (Gorvel and Moreno 2002; Atluri *et al.*, 2011). However, several factors required for

chronic persistence *in vivo* do not appear to mediate intracellular replication in cultured macrophages (Hong *et al.*, 2000; Fretin *et al.*, 2005), suggesting that the different macrophage populations, as well as their metabolic state, may be determinant factors for chronic *Brucella* spp. persistence *in vivo*.

CHAPTER I: LITERATURE REVIEW

1 - Brucellosis

Brucellosis is a zoonotic disease caused by Gram-negative bacteria of the genus *Brucella*, which are facultative intracelllular coccobacilli belonging to the α2-Proteobacteria family (Garrity, 2001). Currently, the genus *Brucella* is divided into six classical species, according to zoonotic potential and host preference: *B. melitensis*, *B. abortus*, *B. suis*, *B. canis*, and *B. ovis* (Osterman and Moriyon, 2006). *B. melitensis*, *B. suis*, and *B. abortus* are considered the most pathogenic species for humans and have small ruminants, pigs and cattle respectively as their preferred hosts (Godfroid *et al.*, 2005). Importantly, two recently identified *Brucella* species isolated from marine mammals, *B. ceti* and *B. pinnipedialis*, can also cause human brucellosis (Foster *et al.*, 2007). Moreover, *B. canis*, a dog pathogen, has a comparatively low zoonotic potential, while *B. neotomae* and *B. ovis*, that infect desert rats and sheep, respectively, are not associated with human disease (Godfroid *et al.*, 2005; Xavier *et al.*, 2010).

When infecting domestic animals, *Brucella* spp. targets reproductive organs, such as placenta and mammary glands in females and epididymis in males, resulting in late trimester abortion and infertility (Xavier *et al.*, 2009; Carvalho Júnior *et al.*, 2012). *Brucella* spp. transmission within the reservoir hosts can occur via ingestion or contact with a highly colonized placenta (Atluri *et al.*, 2011). Alternatively, the transmission between natural hosts can occur through ingestion of contaminated milk, or through contact with semen and/or genital secretions during mating (Xavier *et al.*, 2010; Atluri *et al.*, 2011).

The World Health Organization (WHO) estimates that 500,000 new cases of human brucellosis occur annually, making it one of the most frequently diagnosed zoonoses worldwide (Pappas *et al.*, 2006). Although brucellosis has been eradicated or efficiently controlled in most developed countries, many areas of the world still have a high prevalence of the disease, including Central and South America, and countries of the Caucasus and Central Asia (Pappas *et al.*, 2006). The economic impact of brucellosis in developing countries is doubled and extremely significant. The human disease causes high morbidity, resource consumption for patient treatment, and inability of infected people to work and provide to their family Additionally, the animal disease affects the livestock, which provides a livelihood to many farmers. Together, these facts have led the WHO to classify the disease a neglected zoonosis (Atluri *et al.*, 2011).

In humans, clinical manifestations of *Brucella* infection usually appear between 5 to 60 days after exposure (Young, 1995). During the acute phase of the disease, affected patients present clinical signs such as fever, fatigue, anorexia, mialgia, and joint pain. Frequently, the absence of specific clinical symptoms during initial stage of infection may result in lack of a correct diagnosis, which in turn leads to the development of chronic disease (Young, 1995). Chronic brucellosis, a more severe form of the disease, can be associated with osteo-articular signs and/or colonization of the brain, spleen, liver, genitourinary tract and endocardium (Xavier *et al.*, 2010; Dean *et al.*, 2012). Treatment of chronic brucellosis is notoriously difficult, since antimicrobial drugs may not reach the infection foci, such as granulomas and abcesses, caused by the bacteria. As a result, the patient tends to suffer for a long period of months or years with recurrent episodes of fever and weakness (Franco *et al.*, 2007). Importantly, live attenuated vaccines are available for animal brucellosis prevention, however these vaccines are not considered safe for human use (Franco *et al.*, 2007).

2 –Effects of *Brucella* infection on the immune response

2.1 – The furtive aspect of Brucella spp.

In the host, the preferential target cells for *Brucella* spp. include macrophages, dendritic cells, and placental trophoblasts (Atluri *et al.*, 2011), in which the bacterium can persist and replicate (Xavier *et al.*, 2010). Occasionally, *Brucella* spp. can also target B cells (Goenka *et al.*, 2012). Intracellular *Brucella* survival involves a temporary fusion of the *Brucella*-containing vacuole (BCV) with the lysosome, and subsequent exclusion of the lysosomal proteins (Starr *et al.*, 2008). Interestingly enough, after this process, the BCV becomes associated with the rough endoplasmatic reticulum, creating the compartment in which intracellular replication of *Brucella* occurs (Anderson and Cheville, 1986; Pizarro-Cerda *et al.*, 1998; Celli *et al.*, 2003). Once inside the ER-associated compartment, *Brucella* spp. becomes practically invisible to the immune system (Xavier *et al.*, 2010), fact demonstrated by low production of cytokines and antibodies during the chronic phase of infection (Rodriguez-Zapata *et al.*, 2010; Martirosyan *et al.*, 2011). Therefore, the initial immune response becomes key factor for the control of *Brucella* spp. infection.

The initial detection of pathogenic bacteria by host cells is mediated primarily by innate immunity. This arm of the immune response uses a surveillance system which relies on a pattern of pathogen recognition receptors (PRRs), including membrane-associated toll-like receptors (TLRs) (Iwasaki and Medzhitov, 2004) and cytosolic nucelotide binding and oligomerization domain-like receptors (NLRs) (Franchi *et al.*, 2008). Both TLRs and NLRs function as molecular bar code readers that enable the host to distinguish bacteria from other types of infectious agents by recognizing characteristic combinations of conserved pathogen-associated molecular patterns (PAMPs) (Hoebe *et al.*, 2004). For instance, TLR3, TLR7, and TLR8 recognize nucleic acids and, therefore, are specialized in viral recognition; while TLR1, TLR2, TLR4, TLR5, and TLR6 recognize structures only present in bacteria (Iwasaki and Medzhitov, 2004).

Previous studies have suggested TLR2, TLR4, TLR6, and TLR9 as the PRRs responsible for sensing different *Brucella* components, leading to secretion of pro-inflammatory cytokines during early stages of infection *in vivo* (Weiss *et al.*, 2005; Copin *et al.*, 2007; Macedo *et al.*, 2008; De Almeida *et al.*, 2013). However, the inflammatory response elicited during *in vivo Brucella* infection is considerably milder than the one induced by other proteobacterial pathogens such as *Salomonella*, fact that reflects the ability of *Brucella* spp. to evade the initial detection by the innate immune system (Barquero-Calvo *et al.*, 2007; Martirosyan *et al.*, 2011). Indeed, *Brucella* organisms are devoid of many classical structures involved in virulence/immune recognition such as pili, fimbria, capsules and plasmids (Martirosyan *et al.*, 2011). Moreover, *Brucella* spp. have the ability to modify the lipid A fraction of their LPS through the incorporation of a much longer fatty acid residue (C_{28}) when compared with enterobacterial LPS (C_{12}-C_{16}), and this modification greatly reduces the endotoxic properties of *Brucella* LPS by lowering its TLR4 agonist activity (Lapaque *et al.*, 2006). Interestingly, *Brucella* spp. flagelin do not possess the structural domain necessary for recognition of this PAMP by TLR5 (Andersen-Nissen *et al.*, 2005). As a result, *Brucella* flagelin can be considered an inefficient inductor of TLR5 mediated inflammatory responses (Terwagne *et al.*, 2013). Finally, *B. abortus* produces a protein named Btp1, which contains a Toll/IL-1 (TIR) receptor domain, and is able to inhibit TLR2 mediated pro-inflammatory responses (Salcedo *et al.*, 2008). Therefore, by producing LPS and flagellin with reduced TLR agonist activity and by modulating TLR2 dependent signaling, *Brucella* spp. is able to hide two key molecular features that would otherwise allow the innate immune system to identify them as Gram-negative bacteria (Atluri *et al.*, 2011). The failure to detect this molecular signatures through TLR4 and TLR5 decreases the host's ability to mount an appropriate antibacterial

response resulting in impaired bacterial clearance (Tsolis *et al.*, 2008).

2.2 – The immune response during Brucella infection

The immune response to *Brucella* spp. has been characterized most extensively in the murine model. During the initial stage of *Brucella* infection in mice, the host response developed resembles the T helper 1 (Th1) type, with production of interferon gamma (IFN-γ) by Th and natural killers (NK) cells, as well as production of interleukin 12 (IL-12) and tumoral necrotis factor alpha (TNF-α) by infected macrophages (Zhan and Cheers, 1995; Zhan *et al.*, 1996; Copin *et al.*, 2007; Rolán and Tsolis, 2008). Moreover, in the murine model, both $CD4^+$ and $CD8^+$ T cells contribute to control of the infection, and this is thought to occur via production of IFN-γ (Araya *et al.*, 1989; Fernandes *et al.*, 1996). Indeed, induction of a Th1 immune response during brucellosis seems to be critical, since mice deficient for IFN-γ production or mice lacking interferon regulatory factor-1 (IRF-1) are unable to control systemic bacterial replication and succumb to an exacerbated *B. abortus* infection (Murphy *et al.*, 2001; Ko *et al.*, 2002). Additionally, IL-12 and TNF-α depletion result in increased colony forming units (CFU) counts in spleen from mice infected with *B. abortus*; however the phenotype observed is not as severe as the one described for absense of IFN-γ (Zhan and Cheers, 1995; Zhan *et al.*, 1996).

In humans, the initial immune response to *Brucella* spp. is also characterized by elevated levels of pro-inflammatory cytokines linked to Th1 response, such as IL-1β, IL-6, IL-12p40, TNF-α, and IFN-γ (Rafiei *et al.*, 2006; Rodriguez-Zapata *et al.*, 2010). Additionally, previous studies have demonstrated that mutations in genes encoding the cytokines IFN-γ, IL-6, TNF-α, and IL-10 contribute to increased susceptibility to human brucellosis (Budak *et al.*, 2007; Karaoglan *et al.*, 2009). However, during chronic human brucellosis, the initial Th1 response is dampened and acquires features of Th2 responses, such as an increase in IL-13 producing T cells (Rafiei *et al.*, 2006).

In spite of its well established furtive behavior, *Brucella* spp. do rely on an important virulence factor for intracellular survival, the type IV secretion system (T4SS) encoded by the genes *virB1-virB12* (O'callaghan *et al.*, 1999; Delrue *et al.*, 2001; Den Hartigh *et al.*, 2008). The critical role of *Brucella* T4SS is demonstrated by the inability of T4SS deficient mutants to establish *in vivo* persistence, both in the murine (Hong *et al.*, 2000a; Den Hartigh *et al.*, 2004; Den Hartigh *et al.*, 2008), as well as in the caprine infection models (Zygmunt *et al.*, 2006). Interestingly, previous studies have demonstrated that the T4SS is required not only for establishment of long-term infection, but also for the induction of Th1 immune response in infected mice (Roux *et al.*, 2007). This function was confirmed by the fact that a functional T4SS is necessary for B cell maturation, activation of $CD4^+$ T cells and for initial secretion of IL-12 and IFN-γ (Rolan and Tsolis, 2007; Rolán and Tsolis, 2008). Moreover, *B. abortus* detection by NLRs, leading to ASC-inflammasome mediated production of IL-1β and IL-18, was also shown to be dependent on the type IV secretion system (Gomes *et al.*, 2013).

3 – Role of interleukin 10 (IL-10) during infection

Interleukin 10 (IL-10) is considered an immunoregulatory cytokine which can be produced by different cell types, including B cells, T cells, macrophages, and keratinocytes (Saraiva and O'garra, 2010). The main cell type responsible for IL-10 production in defined situations is dependent on the kind of stimulus, type of affected tissue, and time point in an immune process (Couper *et al.*, 2008). Therefore, IL-10 is able to function at different stages of an immune response, affirming its crucial role as a regulator of both Th1 and Th2 cell responses (Moore *et al.*, 2001; Saraiva and O'garra, 2010).

Due to its anti-inflammatory functions, IL-10 production has been associated with the control of different auto-immune processes, such as Irritable Bowel Disease and rheumatological disorders (Kuhn *et al.*, 1993; Carter *et al.*, 2012). Interestingly, in the context of infectious diseases, IL-10 production usually results in control of the underlying pathology which can be detrimental to the host, without necessarily affecting pathogen survival (Saraiva and O'garra, 2010).

Initially, the anti-inflammatory role of IL-10 was demonstrated through its ability to regulate both T cell and NK cell function (Fiorentino *et al.*, 1989; Couper *et al.*, 2008). However, current research indicates that these effects are indirect and mediated through direct IL-10 induced regulation of monocytes and macrophage functions (Couper *et al.*, 2008). Indeed, IL-10 influences three important monocyte/macrophage functions: secretion of inflammatory mediators, antigen presentation and phagocytosis (Sabat *et al.*, 2010). In these cells, IL-10 inhibits expression of MHC class II and the co-stimulatory molecules B7-1 and B7-2, in addition to limiting the production of pro-inflammatory cytokines such as IL-6, IL-12, IL-18 and TNF-α, as well as chemokines such as MCP-1, RANTES, IL-8, and MIP-2 (Moore *et al.*, 2001; Couper *et al.*, 2008). Consequently, IL-10 plays an important role in innate immunity, modulating macrophage and dendritic cells effector functions and subsequent T cell activation (Moore *et al.*, 2001; Saraiva and O'garra, 2010).

Macrophages are considered important immune system effector cells, hence are one of the main sources of IL-10 during infection (Siewe *et al.*, 2006; Couper *et al.*, 2008). Macrophage activation takes place through recognition of PAMPs by PRRs, which in turn stimulates the expression of pro-inflammatory cytokines (Iwasaki and Medzhitov, 2004). Therefore, IL-10 production by this cell type is thought to occur through the same mechanism (Siewe *et al.*, 2006). Indeed, previous studies have suggested that TLR2 agonists are specialized in induction of IL-10 expression by antigen presenting cells (APC) (Dillon *et al.*, 2004; Netea *et al.*, 2004). For instance, the TLR2 signaling pathway is crucial for IL-10 production by macrophages stimulated with *Mycobacterium tuberculosis* or *Yersinia pestis* lipopeptides (Sing *et al.*, 2002; Jang *et al.*, 2004). Additionally, significant IL-10 production can occur in response to TLR4 and TLR9 agonists (Boonstra *et al.*, 2006).

If considering IL-10 production by T cells, it was first believed that IL-10 was a product of Th2 clones following protein or antigen stimulation (Fiorentino *et al.*, 1989). However, it is now known that IL-10 is not just produced by Th2 cells, but can also be secreted by most if not all $CD4^+$ T-cell subsets, including Th1 and Th17 (Saraiva and O'garra, 2010). In the context of infectious diseases, regulatory T cells (Tregs) serve as a major source of immunoregulatory IL-10, and may come in several forms depending on their developmental origin (Saraiva and O'garra, 2010; Redford *et al.*, 2011). Naturally occuring T regs are mostly $CD25^+$ and are generated in the thymus, but also peripherally in response to tolerogenic stimuli (Sabat *et al.*, 2010). Thymic and inducible Tregs also express the transcription factor FoxP3 ($FoxP3^+$ Tegs) and can suppress effector responses through the soluble factors transforming growth factor β (TGF-β) and IL-10 (Saraiva and O'garra, 2010; Redford *et al.*, 2011). Moreover, several populations of antigen-driven $FOXP3^-$ IL-10 producing T cells with regulatory activity that are distinct from naturally occuring Treg cells have been described (Vieira *et al.*, 2004; Saraiva and O'garra, 2010), and are possibly originated along a Th1 cell pathway (Gabrysova *et al.*, 2009). Indeed, $FoxP3^-$ IL-10 producing Th1 cells have been shown to play a role in immunomodulation during *Leishmania* (Anderson *et al.*, 2007) and *Toxoplasma* (Jankovic *et al.*, 2007) infections.

3.1 –IL-10 during Brucella spp. infection.

Previous studies have demonstrated that polymorfisms in IL-10 encoding genes are

associated with increased susceptibility to human brucellosis (Budak *et al.*, 2007; Karaoglan *et al.*, 2009). The role of IL-10 during *Brucella* spp. infection has also been studied in the mouse model. Fernández-Lago *et al*. (1996) have shown that CD-1 mice intravenoysly infected with *Brucella abortus* present increased IL-10 levels in spleen during the first week post-infection. Moreover, *in vivo* IL-10 neutralization in Balb/C mice intraperitoneally infected with a low ($5x10^3$ CFU) and high ($5x10^6$ CFU) dose of *Brucella abortus* resulted in decreased bacterial survival and increased IFNγ production during early infection (Fernandes and Baldwin, 1995; Fernandes *et al.*, 1996). However, this phenotype was not observed in *Brucella* infected C57BL/6 mice, despite the fact that splenocytes obtained from this mouse strain had an increased ability to produce IL-10 in response to *Brucella abortus* infection *in vitro* (Fernandes *et al.*, 1996). Interestingly, anti-*Brucella* effector functions of IFNγ activated macrophages were dampened by IL-10 during *in vitro* infection (Fernandes and Baldwin, 1995; Fernandes *et al.*, 1996). These previous studies suggest an important role of IL-10 in modulating the initial immune response to *Brucella abortus*, resulting in decreased pathogen survival in some mouse strains, probably due to regulation of macrophage functions.

Goenka et al. (2011) have suggested that B cells play an important role in enabeling *Brucella* persistence in the host, since B cell deficient mice present a decreased ability to control *B. abortus* infection when compared with control animals. In this study, spleens from *Brucella* infected B cell deficient mice showed decreased frequency of IL-10 producing cells, indicating that the B cell mediated *Brucella* persistence could be, at least partially, due to B cell dependent immune modulation through IL-10 production (Goenka *et al.*, 2011). However, this phenotype was only observed around 21 days post-infection, while previous studies have demonstrated that IL-10 levels were increased in *Brucella* infected mice as soon as the first week of infection (Fernandes and Baldwin, 1995; Fernández-Lago *et al.*, 1996). Additionally, spleens from B cell deficient and control mice showed no significant differences in IL-10 gene expression at 3 days post- *B. abortus* infection (Rolán *et al.*, 2009). Taken together, these studies suggest that other cells types could take part in IL-10 production and immune regulation during initial stages of *Brucella* infection.

4 - Macrophage plasticity during infection

Antigen presenting cells such as macrophages play a key role as first line of defense during infectious processes and as a major link between innate and adaptive immune responses (Benoit *et al.*, 2008). However, in spite of being considered important immune effector cells, macrophages have another significant function – the removal of celular debris in order to clear the interstitial space from foreign bodies and to maintain tissue homeostasis (Mosser and Edwards, 2008). Thus, macrophages are considered a dynamic and heterogenous cell population due to their wide range of functions and the diverse mechanisms which drive their differentiation, tissue distribution and stimuli response (Mosser, 2003; Gordon and Martinez, 2010).

As one of the immune system sentinel cells, macrophages are able to detect both endogenous and pathogen-induced danger signals through TLRs, NLRs or interleukin-1 receptor (IL-1R), resulting in cell activation and increase in its pathogen killing capacity (Mosser and Edwards, 2008). However, the recognition of danger signals does not always result in changes that will induce macrophage immune effector functions (Benoit *et al.*, 2008; Mosser and Edwards, 2008). In reality, activation of both innate and adaptive immune responses may result in macrophages that are more susceptible to pathogens and less efficient in production of pro-inflammatory cytokines (Mosser, 2003; Mosser and Edwards, 2008). Therefore, due to their vast plasticity, macrophages have been divided into at least three subpopulations: classically activated

macrophages (CAM, M1); alternatively activated macrophages (AAM, M2, M2a); and regulatory macrophages (M2c), according with their function during inflammation (Benoit *et al.*, 2008; Mosser and Edwards, 2008; Gordon and Martinez, 2010).

The term classically activated macrophages is used to describe cells that present evident effector characteristics in response to activation of Th1 or cellular immune response (Mosser and Edwards, 2008). Thus, CAM differentiation occurs when Th1 cytokines such as IFN-γ and TNF-α are present, resulting in cells with increased bactericidal capacity due to nitric oxid (NO) production as well as secretion of proinflammatory cytokines such as IL-1β, IL-6 and IL-12 (Benoit *et al.*, 2008; Mosser and Edwards, 2008). Normally, the presence of CAM is essential for the control of intracellular pathogens during acute phase of infection, as suggested by the increased susceptibility of IFNγ and TNFα deficient mice to infection by the intracellular pathogenic bacteria *Listeria monocytogenes* (Rothe *et al.*, 1993) as well as by the M1 polarization of macrophages during acute *Mycobacterium tuberculosis* and *Salmonella typhi* infection (Ehrt *et al.*, 2001; Benoit *et al.*, 2008). However, an excessive or prolonged CAM program can be deleterious to the host, via development of severe pathology in affected organs as a consequence of overhelming production of proinflammatory cytokines (Benoit *et al.*, 2008).

As previously described for CAM, the AAM population can also arise in response to innate and/or adaptive immunological stimuli (Mosser and Edwards, 2008). However, while Th1 cytokines are necessary for CAM development, AAM differentiaion usually occurs in the presence of Th2 cytokines, such as interleukin 4 (IL-4) and interleukin 13 (IL-13) (Loke *et al.*, 2007). IL-4 is mostly produced by basophils, mast cells, and $CD4^+$ T cells (Brandt *et al.*, 2000), and is usually present during fungal and parasitic diseases (Kreider *et al.*, 2007). Nevertheless, IL-4 production can also occur during bacterial infection, exemplified by the detection of this cytokine during *Mycobacterium tuberculosis* (Harris *et al.*, 2007), *Francisella tularensis* (Shirey *et al.*, 2008), and *Yersinia enterocolítica* (Tumitan *et al.*, 2007) infections. When present during an inflammatory process, IL-4 leads to the development of macrophages with decreased bactericidal capacity, which in turn promotes pathogen persistence. Therefore, it is believed that AAM play an important role in chronic bacterial diseases (Benoit *et al.*, 2008). Moreover, IL-4 is able to convert resident macrophages incells programmed to promote fibrosis and pathology resolution (Mosser and Edwards, 2008). Hence, AAM show increase arginase (Arg1) activity, an enzyme responsible for the conversion of arginine to ornitine, an important precursor of polyamines and collagen used for the production of extracellular matrix (Kreider *et al.*, 2007). Additionally, studies have demonstrared that AAM are able to produce significant amounts of the chitinase Ym1 as well as the resistin-like protein Fizz1 (Raes *et al.*, 2002) and upregulate the expression of galactose-type C-type lectin CD301 (mMGL1) (Raes *et al.*, 2005). Consequently, increased Arg1, Ym1, Fizz1 and CD301 gene expression and protein levels can be used as biomarkers for the identification of this macrophage subpopulation (Raes *et al.*, 2005; Mosser and Edwards, 2008).

The third macrophage subpopulation described is known as regulatory macrophages or M2c, due to their ability to modulate the inflammatory response through secretion of the anti-inflammatory cytokine IL-10 (Benoit *et al.*, 2008; Mosser and Edwards, 2008). This subpopulation was first identified after *in vitro* macrophage stimulation with TLR agonists in the presence of immune complex (Gerber and Mosser, 2001). Currently it is known that regulatory macrophage differentiation can occur in response to a wide range of stimuli, including prostaglandin, apoptotic cells, and presence of IL-10 or G protein-coupled receptor ligands (Hasko *et al.*, 2007). In the context of infectious diseases, regulatory macrophages can arrise during different stages of the process, usually having the

primary function to regulate the immune response and to limit detrimental inflammation (Mosser, 2003). Indeed, IL-10 production by this macrophage subpopulation has been linked to increased persistence of bacterial pathogens such as *Mycobacterium leprae* (Sieling and Modlin, 1994), *Mycobacterium tuberculosis* (O'leary *et al.*, 2011) and *Coxiella burnetti* (Ghigo *et al.*, 2001), most likely due to their ability to modulate the Th1 immune response necessary for the control of intracellular pathogens.

5 - Role of PPARγ in macrophage activation and metabolism

5.1 – Metabolic changes in macrophages

IFNγ and TLR macrophage activation leads to upregulation of the inducible form of nitric oxide synthase (iNOS) (Everts *et al.*, 2012) and production of reactive oxygen species (ROS) (West *et al.*, 2011). Therefore, ROS and nitric oxide (NO) production are key functional features of the inflammatory and antibactericidal CAM macrophage, and the metabolic alterations that occur are integral to this process (O'neill and Hardie, 2013). Interestingly, NO competes with oxygen to inhibit cytochrome c oxidase, the terminal electron acceptor of the respiratory chain. This fact prevents the reoxidation of NADH, which in turn limits flux through the tricarboxylic acid (TCA) cycle. Moreover, increased generation of ROS by mitochondria also contributes to reduced macrophage reliance on the TCA cycle and the respiratory chain for energy and ATP production. However, M1 macrophages still need to maintain ATP levels for biosynthesis, as well as to maintain mitocondrial membrane potential and to prevent apoptosis (O'neill and Hardie, 2013). Therefore, decreased TCA flux in CAM leads to ATP production through anaerobic glycolysis and lactate production. Consequently, these cells show elevated expression of the glucose transporter GLUT1 as well as marked switch from expression of the liver isoform of the enzime 6-phosphofructo-2-kinase (encoded by *PFKFB1*) to the PFKFB3 isoform (Rodriguez-Prados *et al.*, 2010). This leads to increased glucose uptake and consumption, as well as accumulation of fructose-2,6-bisphosphate which, in turn, increases glycolytic flux (O'neill and Hardie, 2013).

The opposite is true when macrophages are activated by IL-4 and IL-13, which promote the AAM phenotype. This macrophage subpopulation shows a profund increase in the entire program of fatty-acid metabolism, including uptake and oxidation of fatty acids and mitocondrial biogenesis, as well as much lower rates of glycolysis (Vats *et al.*, 2006; Rodriguez-Prados *et al.*, 2010). This shows that while AAM macrophages preferentially utilize glucose, the alternative program of macrophage activation switches over to fatty acid oxidation for energy homeostasis (Vats *et al.*, 2006). Since AAM macrophages are involved in chronic processes and tissue repair, it is possible that the more energy efficient oxidative metabolism is better suited to the long-term roles of this subpopulation (O'neill and Hardie, 2013).

Interestingly, the control of the genetic program for long-term activation is dependent on STAT6 phosphorylation (Martinez *et al.*, 2008; O'neill and Hardie, 2013). As consequence, phosphorylated STAT6 dimerizes and translocates to the nucleus where it induces expression of its target genes, including markers (*Arg1, Ym1, Fizz1, Cd301*) and regulators of macrophage metabolism and alternative activation (i.e.:*Pparγ, Pparδ* and *PGC-1β*) (Bensinger and Tontonoz, 2008). The role of the AAM metabolism regulators will be discussed below.

5.2 – The role of PPARγ

Peroxisome proliferator-activated receptors are ligand-controlled transcription factors of the nuclear family capable of regulating gene expression by transactivation or transrepression (Gautier *et al.*, 2012). The PPAR family has been shown to modulate various cellular functions, including adipocyte differentiation, fatty-acid

oxidation and glucose metabolism (Bensinger and Tontonoz, 2008). Interestingly, the PPAR family also plays an important role in the inhibition of inflammatory gene expression (Bensinger and Tontonoz, 2008).

One of the receptors in the PPAR family, PPARγ, is a nuclear receptor activated by fatty acids, which has recently been linked to the polarization of macrophage phenotype (Odegaard *et al.*, 2007). Therefore, even though PPARγ is best known for its influence in adipocyte development and insulin-resistance (Bensinger and Tontonoz, 2008), it can also have an widespread influence on macrophage biology (Zhang and Chawla, 2004; Tontonoz and Spiegelman, 2008). Interestingly, studies using PPARγ –deficient cells have demonstrated that, in the absence of PPARγ signaling, macrophages neither appropriately suppress infammatory cytokine production nor acquire an oxidative metabolic program that is associated with the AAM macrophage phenotype (Odegaard *et al.*, 2007; Bensinger and Tontonoz, 2008).

Previous studies have demonstrated the role of PPARγ signalling pathway in medating increased fatty-acid oxidation in AAM macrophages through upregulation of the PPARγ coativator 1β (PGC1β), in a IL-4 and STAT-6 dependent manner (Vats *et al.*, 2006; Bensinger and Tontonoz, 2008). PGC1β is a transcriptional co-activator that promotes oxidative metabolism, notably by inducing expression of genes involved in fatty-acid oxidation (Wu *et al.*, 1999). Indeed, over-expression of PGC1β in macrophages promotes the M2 phenotype. Moreover, macrophage PGC1β – specific knockdown limits the shift to oxidative phosphorylation and the function of AAM macrophage, and greatly boosts the TLR4 activating effects of LPS (Vats *et al.*, 2006).

An important repressive function of PPARγ is to inhibit inflammatory gene expression by several mechanisms, including direct interactions with AP-1 and NF-κB (Chung *et al.*, 2000) and nucleocytoplasmatic redistribution of the p65 subunit of NF-κB (Kelly *et al.*, 2004), among others. Indeed, in LPS and IFNγ activated murine macrophages, PPARγ activation repressed the induction of pro-inflammatory genes, including *Nos2*, *Cox2* and *Il12* (Ricote *et al.*, 1998; Welch *et al.*, 2003).

In the context of infectious diseases, PPARγ induction in macrophages has been implicated in increased persistence of the intracellular pathogens such as *Listeria monocytogenes* (Abdullah, Z. *et al.*, 2012) and *Mycobacterium tuberculosis* (Mahajan, S. *et al.*, 2012), ostensibly through modulation of pathogen-induced proinflammatory responses. However, the implications of PPARγ mediated metabolic changes leading to nutrient availability in macrophages during infectious diseases have yet to be determined.

CHAPTER II: CD4$^+$ T CELL-DERIVED IL-10 PROMOTES *BRUCELLA ABORTUS* PERSISTENCE VIA MODULATION OF MACROPHAGE FUNCTION*

Introduction

Persistent bacterial infections have a significant impact on public health (Svetic *et al.*, 1993). While evasion of host immune responses is a prerequisite for these chronic infections, the underlying mechanisms are not fully understood. Human brucellosis, caused by the intracellular gram-negative coccobacilli *Brucella* spp., is considered one of the most important zoonotic diseases worldwide, with more than 500,000 new human cases reported annually (Pappas *et al.*, 2006). The disease is characterized by a long incubation period that leads to a chronic, sometimes lifelong, debilitating infection with serious clinical manifestations such as fever, arthritis, hepatomegaly, and splenomegaly (Corbel, 1997; Atluri *et al.*, 2011). Human and animal brucellosis share many similarities, such as persistence in tissues of the mononuclear phagocyte system, including spleen, liver, lymph nodes, and bone marrow (Atluri *et al.*, 2011). Therefore, the use of animal models such as mice has been an important tool to better characterize the immune response to *Brucella* infection that leads to long-term bacterial persistence and chronic disease.

There is general agreement that the initial interferon gamma (IFN-γ) mediated Th1 immune response is crucial for the control of *Brucella* infection, since absence of IFN-γ results in decreased control of bacterial growth (Fernandes and Baldwin, 1995; Fernandes *et al.*, 1996) and IFN-γ-deficient C57BL/6 mice succumb to overwhelming disease (Murphy *et al.*, 2001). However, the inflammatory response induced by *Brucella* spp. *in vivo* is much milder than that observed with pyogenic infections such as salmonellosis, suggesting the stealth of *Brucella* as a possible reason for the absence of early proinflammatory responses (Barquero-Calvo *et al.*, 2007; Martirosyan *et al.*, 2011). Recent studies have shown that *Brucella* spp. use both passive and active mechanisms to evade initial innate immune recognition through toll-like receptors (TLRs) (Andersen-Nissen *et al.*, 2005). Although avoidance of TLR recognition is a key factor in the lack of initial inflammation during *Brucella* infection, how subsequent interactions of *Brucella* with the host immune system result in chronic disease is poorly understood.

Interleukin-10 (IL-10) is an immunoregulatory cytokine produced by most T cell subsets, B cells, neutrophils, macrophages, and some dendritic cell subsets (Saraiva and O'garra, 2010). It is suggested that by acting on antigen-presenting cells such as macrophages, IL-10 can inhibit the development of Th1 type responses (Sabat *et al.*, 2010). In the context of infectious diseases, it is believed that the host uses IL-10 to control over-exuberant immune responses to pathogenic microorganisms in order to limit tissue damage (Saraiva and O'garra, 2010). Interestingly, studies using chronic pathogens such as *Leishmania major* (Belkaid *et al.*, 2001), human cytomegalovirus (Chang and Barry, 2010), or *Mycobacterium tuberculosis* (reviewed in (Redford *et al.*, 2011)) have demonstrated that the absence of IL-10 leads to a better clearance of these pathogens, with variable degrees of immunopathology. These studies suggest that pathogens have developed mechanisms to take advantage of the host immune-regulation in order to persist for longer periods and establish chronic infection.

Similar to other chronic pathogens, *B. abortus* infection induces IL-10 production (Fernandes and Baldwin, 1995; Fernandes *et al.*, 1996; Fernández-Lago *et al.*, 1996). Moreover, IL-10 gene polymorphisms have been associated with increased susceptibility to human brucellosis (Budak *et al.*, 2007). However, questions regarding the impact of IL-10 in *B. abortus* persistence and

* Article accepted for publication in PLOS Pathogens

establishment of chronic infection, as well as the cell types responsible for this cytokine production remain to be answered. Therefore, we used IL-10 deficient mice to determine the role of IL-10 in modulating the initial immune response to *Brucella* infection. Furthermore, using cell-specific knock-out mice, we elucidated the immunological mechanisms underlying IL-10 induced immune-regulation during brucellosis.

Material and Methods

Bacterial strains, media and culture conditions: Bacterial strains used in this study were the virulent strain *Brucella abortus* 2308 and its isogenic mutant strain MX2 which has an insertion of pKSoriT-*bla-kan*-P*sojA-mCherry* plasmid (Copin *et al.*, 2012). For strain MX2, positive clones were kanamycin resistant and fluorescent, as previously described (Copin *et al.*, 2012). Strains were cultured on tryptic soy agar (Difco/Becton-Dickinson, Sparks, MD) or tryptic soy broth at 37°C on a rotary shaker. Bacterial inocula for mouse infection were cultured on tryptic soy agar plus 5% blood for 3 days (Alton *et al.*, 1975). For cultures of strain MX2, kanamycin (Km) was added to the culture medium at 100µg/mL. All work with *B. abortus* cells was performed at biosafety level 3.

Bone marrow derived macrophage infection: Bone marrow-derived macrophages were differentiated from bone marrow precursors from femora and tibiae of female, 6 to 8 weeks old, C57BL/6J and IL-$10^{-/-}$ mice obtained from The Jackson Laboratory (Bar Harbor) following a previously published procedure (Rolan and Tsolis, 2007). For BMDM experiments, 24-well microtiter plates were seeded with macrophages at concentration of 5 x10^5 cells/well in 0.5 mL of RPMI media (Invitrogen, Grand Island, NY) supplemented with 10% FBS and 10 mM L-glutamine (RPMI supl) incubated for 48 h at 37°C in 5% CO_2. Preparation of the inoculum and BMDM infection was performed as previously described (Rolan and Tsolis, 2007). Briefly, for inoculum preparation, *B. abortus* 2308 was grown for 24 h and then diluted in RPMI supl, and about 5×10^7 bacteria in 0.5 mL of RPMI supl were added to each well of BMDM, reaching multiplicity of infection (MOI) of 100. Microtiter plates were centrifuged at 210 × **g** for 5 min at room temperature in order to synchronize infection. Cells were incubated for 20 min at 37°C in 5% CO_2, free bacteria were removed by three washes with phosphate-buffered saline (PBS), and the zero-time-point sample was taken as described below. After the PBS wash, RMPI supl plus 50 mg gentamicin per mL was added to the wells, and the cells were incubated at 37°C in 5% CO_2. For cytokine production assays, supernatants from each well were sampled at 0, 8, 24, or 48 h after infection, depending on the experiment performed. In order to determine bacterial survival, the medium was aspirated at the time points described above, and the BMDM were lysed with 0.5 mL of 0.5% Tween 20, followed by rinsing of each well with 0.5 mL of PBS. Viable bacteria were quantified by serial dilution in sterile PBS and plating on TSA. For gene expression assays, BMDM were resuspended in 0.5 mL of TRI-reagent (Molecular Research Center, Cincinnati) at the time-points described above and kept at -80°C until further use. When necessary, 1 ng/mL of mouse rIL-10 (eBioscience, San Diego, CA) or 1 ng/mL of mouse rIFN-γ (BD Bioscience, San Jose, CA) was added to the wells and kept throughout the experiments. All experiments were performed independently in triplicate at least three times and the standard error for each time point calculated.

RAW-Blue macrophages experiments: RAW-Blue cells (Invivogen, San Diego, CA) were derived from RAW-264.7 macrophages with chromosomal integration of a SEAP reporter construct inducible by NF-κB and AP-1. RAW-Blue cells were maintained in Zeocin (Invivogen, San Diego, CA) selective medium. For RAW-Blue experiments, 24-well microtiter plates were seeded with macrophages at concentration of 2 x10^5 cells/well in 0.5 mL of DMEM media (Invitrogen, Grand Island, NY) supplemented with 10% FBS and 10

mM L-glutamine (DMEM supl). Preparation of the inoculum and RAW-Blue infection was performed as previously described (Rolan and Tsolis, 2007), using MOI=100. For NF-κB activation assays, supernatant from each well was sampled at 8h and 24h after infection and secretion of the substrate SEAP was detected and measured in a spectrophotometer at 650 nm with QUANTI-Blue (Invivogen, San Diego, CA) according to manufacturer's instructions. When necessary, 1 ng/mL of mouse rIL-10 (eBioscience, San Diego, CA), 1 ng/mL of mouse rIFN-γ (BD Bioscience, San Jose, CA),1 µg/mL of anti-mouse IL-10R antibody (R&D Systems, Minneapolis, MN) or anti-mouse IgG isotype antibody control (R&D Systems, Minneapolis, MN) were added to the wells and kept throughout the experiments. All experiments were performed independently in triplicate at least three times and the standard error for each time point calculated.

Ethics Statement: Experiments with mice were carried out in strict accordance with the recommendations in the Guide for Care and Use of Laboratory Animals of the National Institute of Health and were approved by the Institutional Animal Care and Use Committees at the University of California at Davis (protocol number: 16468).

Animal experiments: Female C57BL/6J wild-type mice, B6.129P2-*Il10*^{tm1Cgn}*/J;* (IL-10$^{-/-}$) mice (Goenka *et al.*, 2011) and *Il-10* GFP reporter mice (Kamanaka *et al.*, 2006), aged 6-8 weeks, were obtained from The Jackson Laboratory (Bar Harbor). Female and male *Il10*$^{flox/flox}$*Cd4cre*$^{+/-}$ (IL-10flox/CD4Cre), and *Il10R*$^{flox/flox}$*Lysmcre*$^{+/-}$ (IL-10Rflox/LysMCre) aged 6-8 weeks, were reported previously (Pasquali *et al.*, 2010; Pils *et al.*, 2010). Female and male *IL10*$^{flox/flox}$*LysMCre*$^{+/-}$ (IL-10flox/LysMCre) were generated at UC Davis. For the strains IL-10 flox/CD4Cre, IL-10Rflox/LysMCre and IL-10flox/LysMCre, littermate *Il10*$^{flox/flox}$*Cd4cre*$^{-/-}$, *Il10R*$^{flox/flox}$*Lysmcre*$^{-/-}$, and *IL10*$^{flox/flox}$*LysMCre*$^{-/-}$ mice were used as control, respectively. Mice were held in microisolator cages with sterile bedding and irradiated feed in a biosafety level 3 laboratory. Groups of 3 to 5 mice were inoculated intraperitoneally (i.p.) with 0.2 mL of phosphate-buffered saline (PBS) containing 5 x 10^5 CFU of *B. abortus* 2308 as previously described (Rolán and Tsolis, 2008). At 3, 9, 15, 21 and/or 42 days after infection, depending on the experiment performed, the mice were euthanized by CO_2 asphyxiation and their serum, livers and spleens were collected aseptically at necropsy. The livers and spleens were homogenized in 2 mL of PBS, and serial dilutions of the homogenate were plated on TSA for enumeration of CFU. Samples of liver and spleen tissue were also collected for gene expression and histopathology analysis as described below.

ELISA: The presence of IL-10, IL-6 and TNF-α in BMDM supernatant and in serum samples from C57BL/6, IL-10flox/CD4Cre, IL-10flox/LysMCre and littermate control mice infected with *B. abortus* 2308 was determined by indirect enzyme-linked immunosorbent assay (ELISA) (eBioscience, San Diego, CA) according to the manufacturer's instructions. The ELISA test was read at 450 nm with an ELISA microplate reader (MR5000; Dynatech). The sensitivity of the ELISA used was 7.8 pg/mL. Data points are the averages of duplicate dilutions, with each measurement being performed twice.

RT-PCR and real time PCR analysis: Eukaryotic gene expression was determined by real-time PCR as previously described (Rolan and Tsolis, 2007). Briefly, eukaryotic RNA was isolated using TRI reagent (Molecular Research Center, Cincinnati) according to the manufacturer's instructions. A Reverse transcriptase reaction was performed to prepare complementary DNA (cDNA) using TaqMan reverse transcription reagents (Applied Biosystems, Carlsbad). A volume of 4 µL of cDNA was used as template for each real-time PCR reaction in a total reaction volume of 25 µL. Real-time PCR was performed using SYBR-Green (Applied Biosystems) along with the primers listed in supplementary Table 1. Data were analyzed using the comparative Ct method (Applied Biosystems, Carlsbad). Transcript

levels of *Il10, Il6, Ifng* and *Tnfa* were normalized to mRNA levels of the housekeeping gene *βactin*.

Histopathology: Formalin fixed spleen and liver tissue sections were stained with hematoxylin and eosin, and two veterinary pathologists (MX and TS) performed a blinded evaluation using criteria described in supplementary Table 2. Representative images were obtained using an Olympus BX41 microscope and the brightness adjusted (Adobe Photoshop CS2).

Flow cytometry: Flow cytometric analysis of IL-10 producing cells was performed in splenocytes from IL-10 GFP reporter mice infected for 3 and 9 days with *B. abortus* 2308. Briefly, after passing the spleen cells through a 100-µm cell strainer and treating the samples with ACK buffer (0.15 M NH_4Cl, 1.0 mM $KHCO_3$, 0.1 mM Na_2EDTA [pH 7.2]) to lyse red blood cells, splenocytes were washed with PBS (Gibco) containing 1% bovine serum albumin (fluorescence-activated cell sorter [FACS] buffer). After cell counting, 4 x 10^6 cells/mouse were re-suspended in PBS and stained with Aqua Live/Dead cell discriminator (Invitrogen, Grand Island, NY) according to the manufacturer's protocol. After Live/Dead staining, splenocytes were resuspended in 50 µL of FACS buffer and cells were stained with a cocktail of anti-B220 Brilliant Violet 421 (Biolegend, San Diego, CA), anti-CD3 PE (BD Pharmingen, San Jose, CA), anti-CD11b APC.Cy7 (Biolegend, San Diego, CA), anti-F4/80 Pe.Cy7 (Biolegend, San Diego, CA), anti-Cd11c APC (Biolegend, San Diego, CA). To determine the T cell subset responsible for IL-10 production, cells were stained with a cocktail of anti-CD3 APC.Cy7 (eBioscience, San Diego, CA), anti-CD8 AF700 (BD Pharmigen, San Jose, CA), anti-TCRγδ PE (BD Pharmigen, San Jose, CA), anti-CD4 eFluor 450 (eBioscience, San Diego, CA), anti-CD25 Pe.Cy7 (eBioscience, San Diego, CA). The cells were washed with FACS buffer and fixed with 4% formaldehyde for 30 min at 4°C, and resuspended in FACS buffer prior to analysis. Flow cytometry analysis was performed using an LSRII apparatus (Becton Dickinson, San Diego, CA), and data were collected for 5 x 10^5 cells/mouse. Resulting data were analyzed using Flowjo software (Treestar, inc. Ashland, OR). Gates were based on Fluorescence-Minus-One (FMO) controls.

Immunofluorescence microscopy: Immunofluorescence of *Brucella* infected BMDM was performed as previously described (Starr *et al.*, 2008). Briefly, *B. abortus* MX2 infected BMDM were grown on 12-mm glass coverslips in 24-well plates were washed three times with PBS, fixed with 3% paraformaldehyde, pH 7.4, at 37°C for 20 min, washed three times with PBS and then incubated for 10 min in 50 mm NH_4Cl in PBS in order to quench free aldehyde groups. Samples were blocked and permeabilized in 10% goat serum and 0.1% saponin in PBS for 30 min at room temperature. Cells were labeled by inverting coverslips onto drops of primary antibodies diluted in 10% horse serum and 0.1% saponin in PBS and incubating for 45 min at room temperature. The primary antibody used was rat anti-mouse LAMP-1 (BD Pharmigen, San Jose, CA). Bound antibodies were detected by incubation with 1:500 dilution of Alexa Fluor 488 donkey anti-rat (Invitrogen, Grand Island, NY) for 45 min at room temperature. Cells were washed twice with 0.1% saponin in PBS, once in PBS, once in H_2O and then mounted in Mowiol 4-88 mounting medium (Calbiochem). Samples were observed on a Carl Zeiss LSM 510 confocal laserscanning microscope for image acquisition (Carl Zeiss Micro Imaging). Confocal images of 1024 × 1024 pixels were acquired as projections of three consecutive slices with a 0.38-µm step and assembled using Adobe Photoshop CS2 (Adobe Systems). For quantification of *Brucella* MX2 and Lamp1+ compartment colocalization, at least 100 bacteria/sample were counted. All experiments were performed independently in quadruplicate at least two times.

Statistical analysis: Fold changes of ratios (bacterial numbers or mRNA levels) and percentages (flow cytometry and fluorescent microscopy) were transformed

logarithmically prior to statistical analysis. An unpaired Student's *t*-test was performed on the transformed data to determine whether differences in fold changes between groups were statistically significant ($P < 0.05$). Significance of differences in histopathology scores was determined by a one-tailed non-parametric test (Mann-Whitney).

Results

Lack of IL-10 production during early B. abortus infection results in lower bacterial survival and increased pathology in vivo

IL-10 has an important role in controlling the immune response induced by different inflammatory processes (Redford *et al.*, 2011). Moreover, *Brucella* infection has been shown to induce IL-10 production by splenocytes *in vitro* (Fernandes and Baldwin, 1995) and during intravenous *in vivo* infection (Fernandes *et al.*, 1996; Fernández-Lago *et al.*, 1996). To determine the time-course of IL-10 production during *B. abortus* infection, C57BL/6 mice were infected intraperitoneally (IP) with 5×10^5 CFU of the virulent *B. abortus* strain 2308 and IL-10 production was determined at 3, 9, 15, and 21 days post-infection (d.p.i.). Infected mice exhibited significantly higher levels of IL-10 in the serum (Fig. 1A), which was associated with increased IL-10 transcript levels in the spleen (Fig. 1B) and liver (Fig. 1C) as early as 3 d.p.i. Importantly, significantly increased levels of IL-10 in serum and infected organs was only detected until 15 d.p.i., suggesting a possible regulatory function for this cytokine during acute *Brucella* infection. To further investigate if IL-10 plays a role in modulating the inflammatory response during acute brucellosis, C57BL/6 wild-type and *Il10*-deficient mice ($IL\text{-}10^{-/-}$) were infected IP with 5×10^5 CFU of *B. abortus* 2308 and responses were evaluated at 9 d.p.i.. Interestingly, $IL\text{-}10^{-/-}$ mice had significantly lower bacterial survival in both the spleen (Fig. 2A) and the liver (Fig. 2B). $IL\text{-}10^{-/-}$ mice also exhibited increased induction of pro-inflammatory cytokines such as IFN-γ, interleukin-6 (IL-6) and tumor necrosis factor alpha (TNF-α) in infected organs (Fig. 2C) and in serum from infected mice (Fig. 2D).

The typical tissue response to *Brucella* infection is granulomatous inflammation (Atluri *et al.*, 2011). However, in the spleen and liver of $IL\text{-}10^{-/-}$ mice *B. abortus* infection resulted in development of an acute inflammatory response characterized by vasculitis and thrombosis, necrosis, and influx of neutrophils (Fig 2E and 2F). Collectively, these data demonstrate a critical role for IL-10 in modulating the initial inflammation and pathology in response to *B. abortus* infection, which in turn benefits the pathogen due to enhanced bacterial survival.

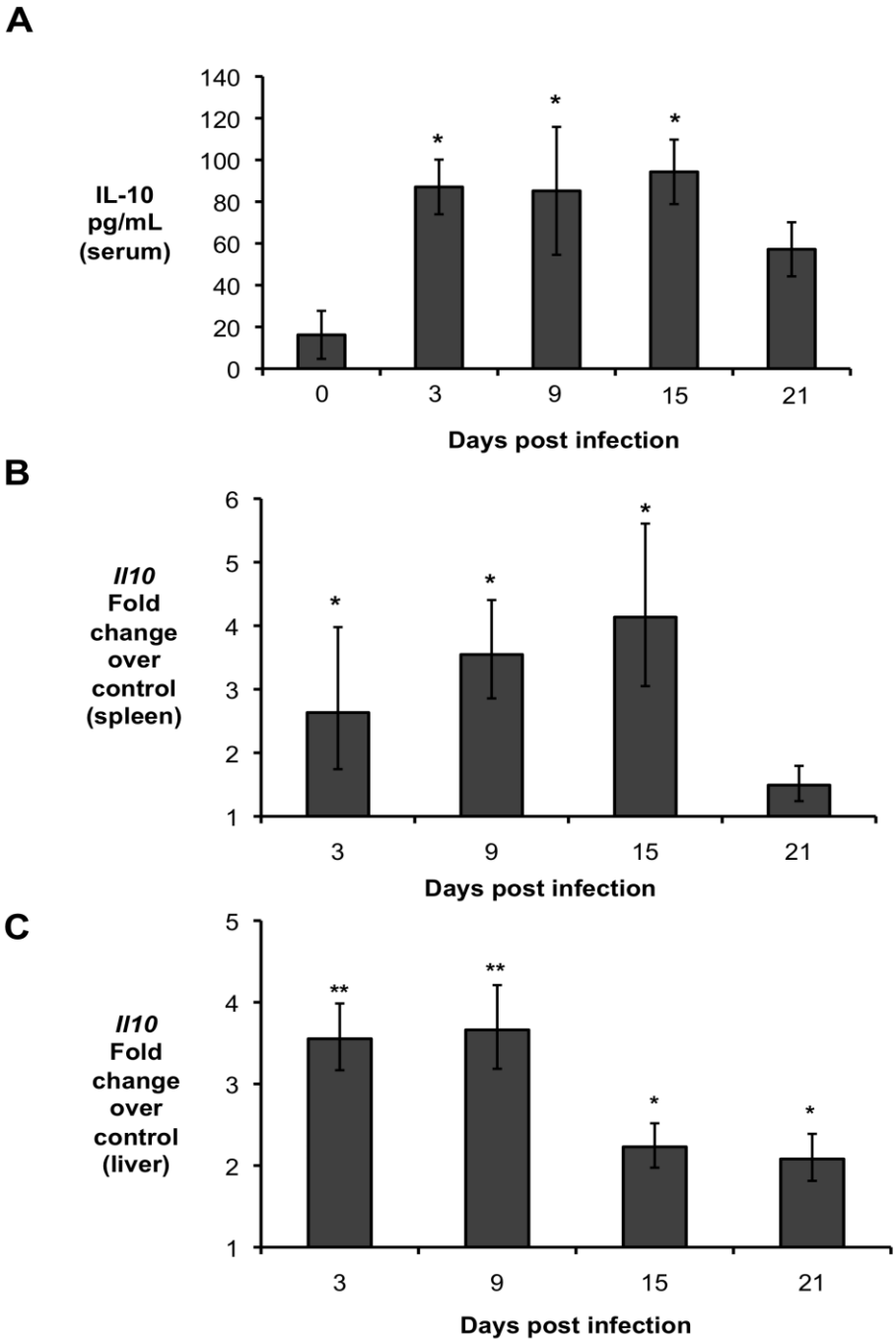

Figure 1. ***Brucella abortus*** **induces IL-10 production by infected organs during early** ***in vivo*** **infection**. (A) IL-10 levels in serum of C57BL/6 infected *with B. abortus* for 3, 9, 15, and 21 days compared to uninfected mice (inoculated with sterile PBS). Real time RT-PCR analysis of IL-10 gene expression in spleen (B) and liver (C) of C57BL/6 mice infected with *B. abortus* 2308 for 3, 9, 15, and 21 days compared to uninfected controls. n=5. (*) represents $P<0.05$ when compared to control. (**) represents $P<0.05$ when compared to days 15 and day 21 for (C) using unpaired t- test statistical analysis.

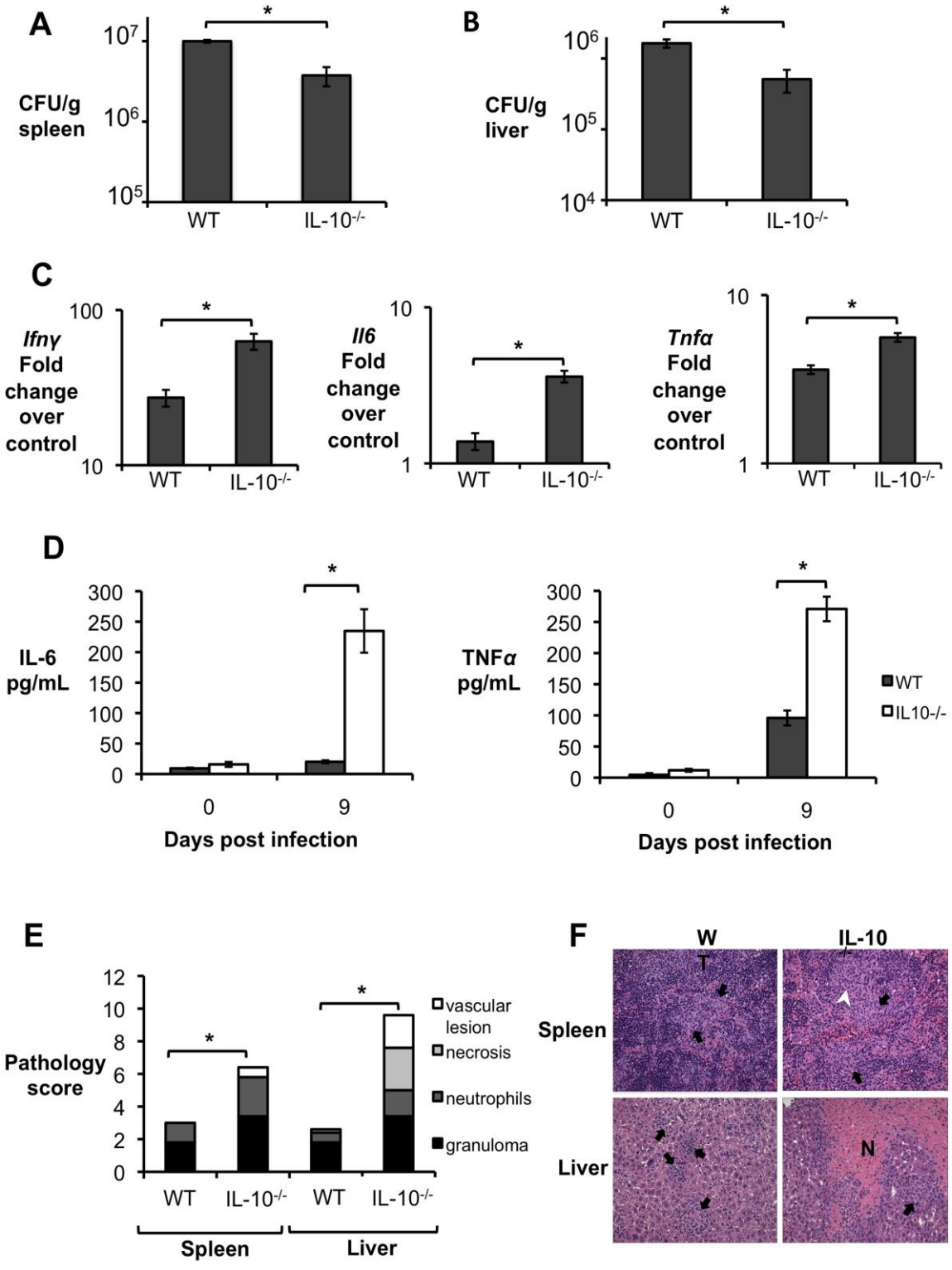

Figure 2. Lack of IL-10 results in lower bacterial survival and increased pathological changes during early *Brucella abortus* infection *in vivo*. (A,B) Colonization of spleen (A) and liver (B) of control or IL-10-/- mice by *B. abortus* at 9 d.p.i. (C) qRT-PCR analysis of IFN-γ, IL-6 and TNF-α gene expression in spleens of C57BL/6 and IL-10 -/- 645 mice infected with *B. abortus* 2308 for 9 days (similar results for liver). (D) IL-6 and TNF-α levels measured by ELISA in serum of C57BL/6 and IL-10 -/- mice infected with *B. abortus* 2308 for 9 days. n=5. Values represent mean ± SEM. *P<0.05 using

unpaired t-test statistical analysis.(E) Histopathology score of spleen and liver from C57BL/6 and IL-10 -/- mice infected with *B. abortus* 2308 for 9 days. (F) Representative pictures from (E). Black arrow shows microgranulomas, white arrowheads shows neutrophilic infiltrate and upper case N shows areas of coagulative necrosis (x20). n=5. Values represent individual mice (black circles) and geometric mean (black dash). *P<0.05 using Mann-Whitney statistical analysis.

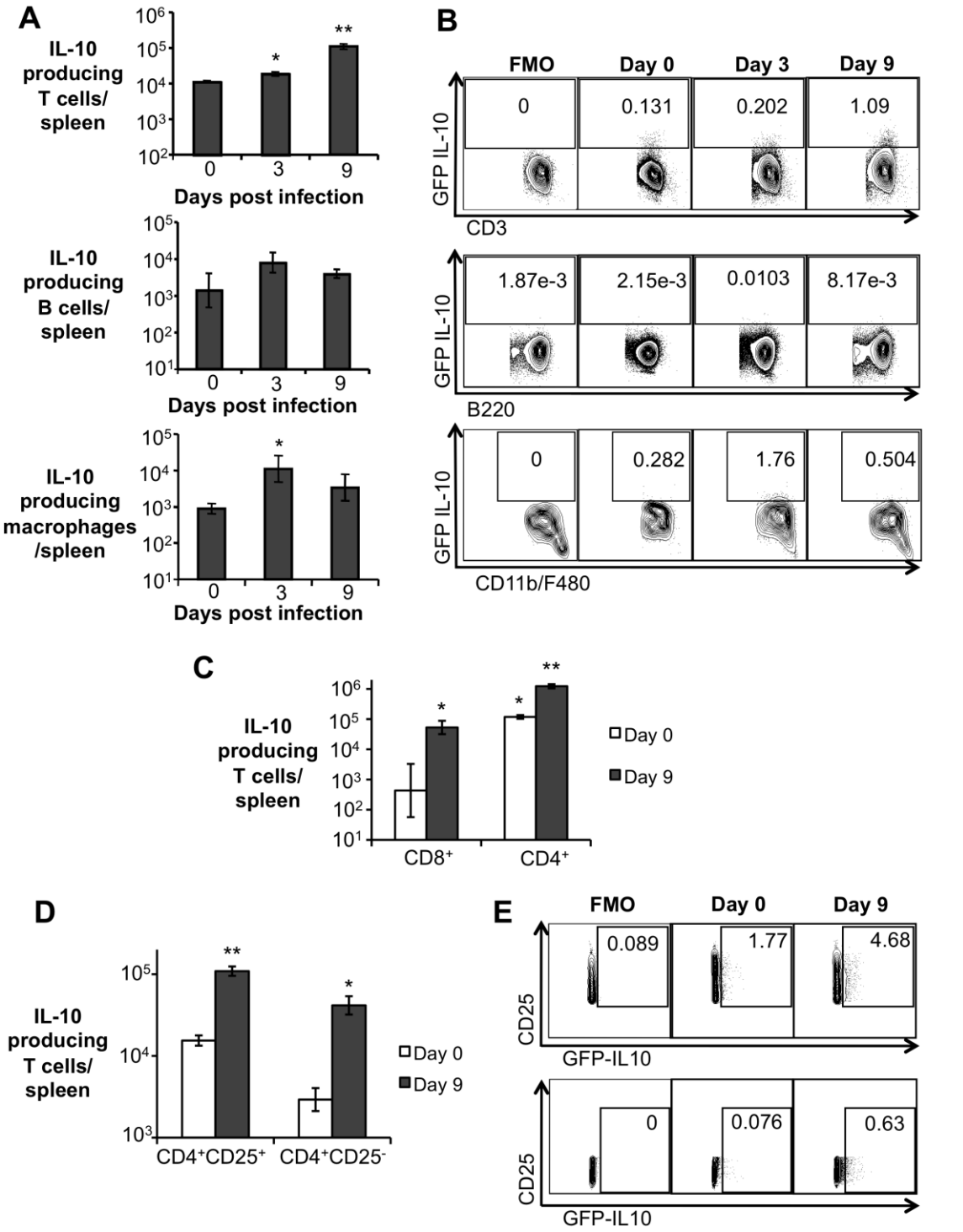

Figure 3. CD4$^+$CD25$^+$ T cells are the main producers of IL-10 during early *Brucella abortus in vivo* infection. (A) Flow cytometry measurement of IL-10 expression in splenic T cells, B cells, and macrophages from C57BL/6 IL-10 GFP-reporter mice infected with *B. abortus* 2308 for 3 and 9 days. (B)

Representative data plot of IL-10 expression in splenic T cells (CD3), B cells (B220), and macrophages (CD11b+F4/80+ 659 cells) from C57BL/6 IL-10 GFP-reporter mice. (C) Flow cytometry measurement of IL-10 expression in splenic CD8+ T cells and $CD4^+$ T cells from C57BL/6 IL-10 GFP-reporter mice infected with *B. abortus* 2308 for 9 days. (D) Flow cytometry measurement of IL-10 expression in splenic CD4+CD25+ T cells and $CD4^+CD25^-$ T cells from C57BL/6 IL-10 GFP-reporter mice infected with *B. abortus* 2308 for 9 days. (E) Representative data plot of IL-10 expression in splenic $CD4^+CD25^+$ (upper panel) and $CD4^+CD25^-$ (lower panel) T cells from C57BL/6 IL-10 GFP-reporter mice. Values represent mean ± SEM. n=4. (*) represents $P<0.05$ relative to uninfected control (day 0), (**) represent $P<0.05$ relative to day 3 infection for (A), relative to $CD8^+$ day 9 infected for (C) and relative to $CD4^+CD25^-$ for (D) using unpaired t-test statistical analysis. FMO = fluorescence minus one.

<u>$CD4^+CD25^+$ T cells are the main IL-10 producers during early B. abortus infection in vivo</u>

IL-10 can be produced by different T cell subsets, as well as by B cells, neutrophils, macrophages, and some DC subsets (Moore *et al.*, 2001). To determine the cell types responsible for IL-10 production during early *B. abortus* infection, *Il10*-GFP reporter mice (Kamanaka *et al.*, 2006) were infected IP with 5×10^5 CFU of *B. abortus* and IL-10 producing cells were identified at 3 and 9 d.p.i. by flow cytometry. A significant increase in the number of IL-10 producing T cells was observed in infected mice at 3 and 9 days post infection, whereas macrophages presented increased production of IL-10 only at 3 d.p.i. Moreover, the number of IL-10 producing B cells, neutrophils, and dendritic cells did not change significantly when compared to uninfected mice (Fig. 3A and 3B, and data not shown). Importantly, even though a significant increase in the number of IL-10 producing $CD8^+$ T cells was observed (Fig. 3C), a tenfold higher number of IL-10 producing T cells was observed in the $CD4^+$ T cell population (Fig. 3C). No IL-10 production by γδ T cells was observed (data not shown).

Various IL-10 producing $CD4^+$ T cells have been described, including the $CD4^+CD25^+$ subset (Shevach, 2002). Interestingly, an expansion of the $CD4^+CD25^+$ T cell population was observed in the spleen of *B. abortus* infected mice at 9 d.p.i. (Fig. 4A and 4B). Moreover, a 5-fold greater number of IL-10 producing $CD4^+CD25^+$ T cells was detected at 9 d.p.i., compared to IL-10 producing $CD4^+CD25^-$ T cells (Fig. 3D and 3E), suggesting that the $CD4^+CD25^+$ T cell subset is the major population responsible for IL-10 production during acute brucellosis in the mouse.

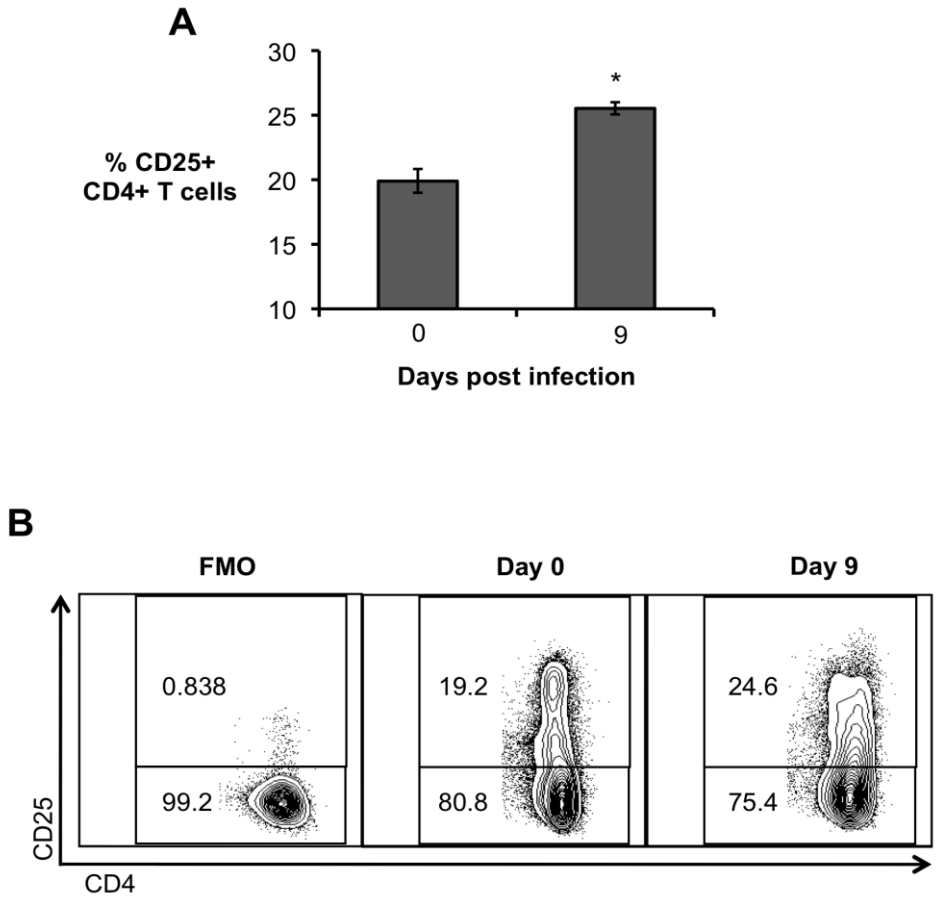

Figure 4. Expansion of $CD4^+CD25^+$ T cells during *Brucella* infection. (A) Flow cytometry quantification of $CD4^+CD25^+$ splenic T cells from C57BL/6 IL-10 GFP-reporter mice infected with *B. abortus* 2308 for 9 days. (B) Representative data plot of CD4 and CD25 expression in splenic T cells from C57BL/6 IL-10 GFP-reporter mice infected with *B. abortus* 2308 for 9 days. Values represent mean ± SEM. *P<0.05. n=4. Values represent mean ± SEM. (*) represents P<0.05 relative to uninfected control using unpaired t-test statistical analysis.FMO = fluorescence minus one.

IL-10 production by T cells is required for B. abortus persistence and for pathology regulation in vivo

Our previous data suggested that T cells and possibly macrophages would be the main cell types producing IL-10 during early *Brucella* infection. Therefore, to further investigate the importance of macrophage derived IL-10 during *Brucella* infection, we generated *Il-10*$^{flox/flox}$*LysMCre*$^{+/-}$ (IL-10flox/LysMCre) mice, which have macrophages and neutrophils that are unable to produce IL-10. IL-10flox/LysMCre mice and littermate *Il-10*$^{flox/flox}$*LysMCre*$^{-/-}$ controls were infected IP with $5x10^5$ CFU of *B. abortus* 2308, and at 3, 9 and 21 d.p.i. disease progression was evaluated. Interestingly, IL-10flox/LysMCre infected mice exhibited decreased levels of IL-10 in the serum (Fig 5A) when compared to control animals only at 3 d.p.i., Moreover, IL-10flox/LysMCre mice exhibited increased ability to control *B. abortus* infection in both spleen (Fig. 5B) and liver (Fig 5C), only at initial stages of infection. This increased host resistance was accompanied by significantly higher levels of the pro-inflammatory cytokines IL-6, TNF-α and IFN-γ in serum (Fig. 5D), spleen (Fig. 5E) and liver (data not shown) as well as increased histopathological lesions in infected organs (Fig. 6A, 6B and 6C) of IL-10flox/LysMCre mice when compared to littermate controls. Collectively, this data suggests that macrophage derived IL-10

plays a limited role in development of the chronic disease caused by *B. abortus* and raises the possibility that T-cells could, indeed, be the main cell type responsible for IL-10 production during early brucellosis.

Therefore, to further investigate the importance of T-cell derived IL-10 during *Brucella* infection, we used *Il-10*$^{flox/flox}$*Cd4Cre*$^{+/-}$(IL-10flox/CD4Cre) mice, which have T cells that are unable to produce IL-10 (Roers *et al.*, 2004). IL-10flox/CD4Cre and littermate *Il-10*$^{flox/flox}$*Cd4Cre*$^{-/-}$ control mice were infected IP with 5x10^5 CFU of *B. abortus* 2308, and at 3, 9,21 and 42 d.p.i., disease progression was evaluated. Remarkably, IL-10flox/CD4Cre infected mice exhibited lower levels of IL-10 in serum (Fig. 7A), and spleen (Fig. 7B) when compared to control animals at 9 d.p.i., providing compelling support for the hypothesis that T-cells are a major source of IL-10 production during early *B. abortus* infection.

Previous results using IL-10$^{-/-}$ and IL-10flox/LysMCre mice (Fig. 2 and 4) suggested that IL-10 was important for initial *B. abortus* persistence in the host. Therefore, we investigated whether the lack of T cell-derived IL-10 would affect bacterial persistence. Indeed, IL-10flox/CD4Cre mice exhibited significantly improved control of *B. abortus* infection in the spleen and liver at 9, 21 and 42 d.p.i. (Fig. 8A and 8B).

Controlling *B. abortus* replication could be beneficial to the host, since the ability to survive for longer periods is a key mechanism for chronic pathogens to thrive. However, loss of IL-10 driven immune modulation has been shown to cause severe and sometimes lethal inflammatory responses in different infectious disease models (Redford *et al.*, 2011). To determine the disease progression, weight changes in IL-10flox/CD4Cre and control mice were followed at 3, 9, 15, 21, 28, 35 and 42 d.p.i. (Fig. 8C). To ensure that any detectable change in weight was the result of *B. abortus* infection, uninfected IL-10flox/CD4Cre and littermate control mice were also used (data not shown).

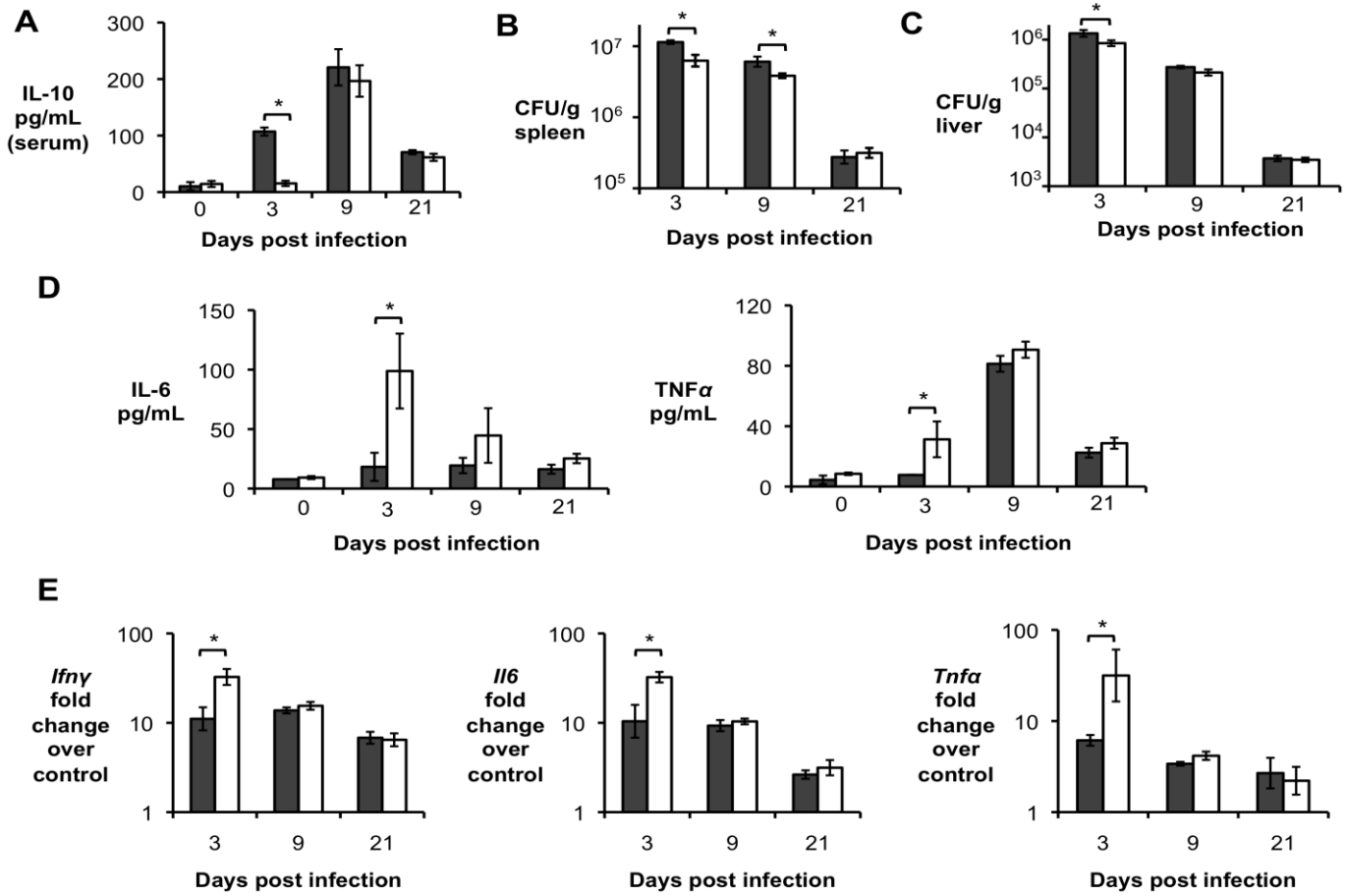

Figure 5. IL-10 production by macrophages and/or neutrophils is not required for *Brucella abortus* long-term persistence *in vivo*. (A) ELISA essay for IL-10 production in serum from littermate control mice (grey bars) compared with IL10flox/LysMCre mice (white bars) at 3, 9 and 21 d.p.i. (B, C). *B. abortus* 2308 CFU counts in spleen (B) and liver (C) from littermate control mice (grey bars) compared with IL10flox/LysMCre mice (white bars) at 3, 9 and 21 d.p.i. (D) ELISA essay for IL-6 and TNF-α production in serum from littermate control mice (grey bars) compared with IL10flox/LysMCre mice (white bars) at 3, 9 and 21 d.p.i. (E) qRT-PCR analysis of pro-inflammatory cytokines in spleens from littermate control mice (grey bars) compared with IL10flox/LysMCre mice (white bars) at 3, 9 and 21 d.p.i.. (*) represents $P<0.05$ using unpaired t-test statistical analysis.

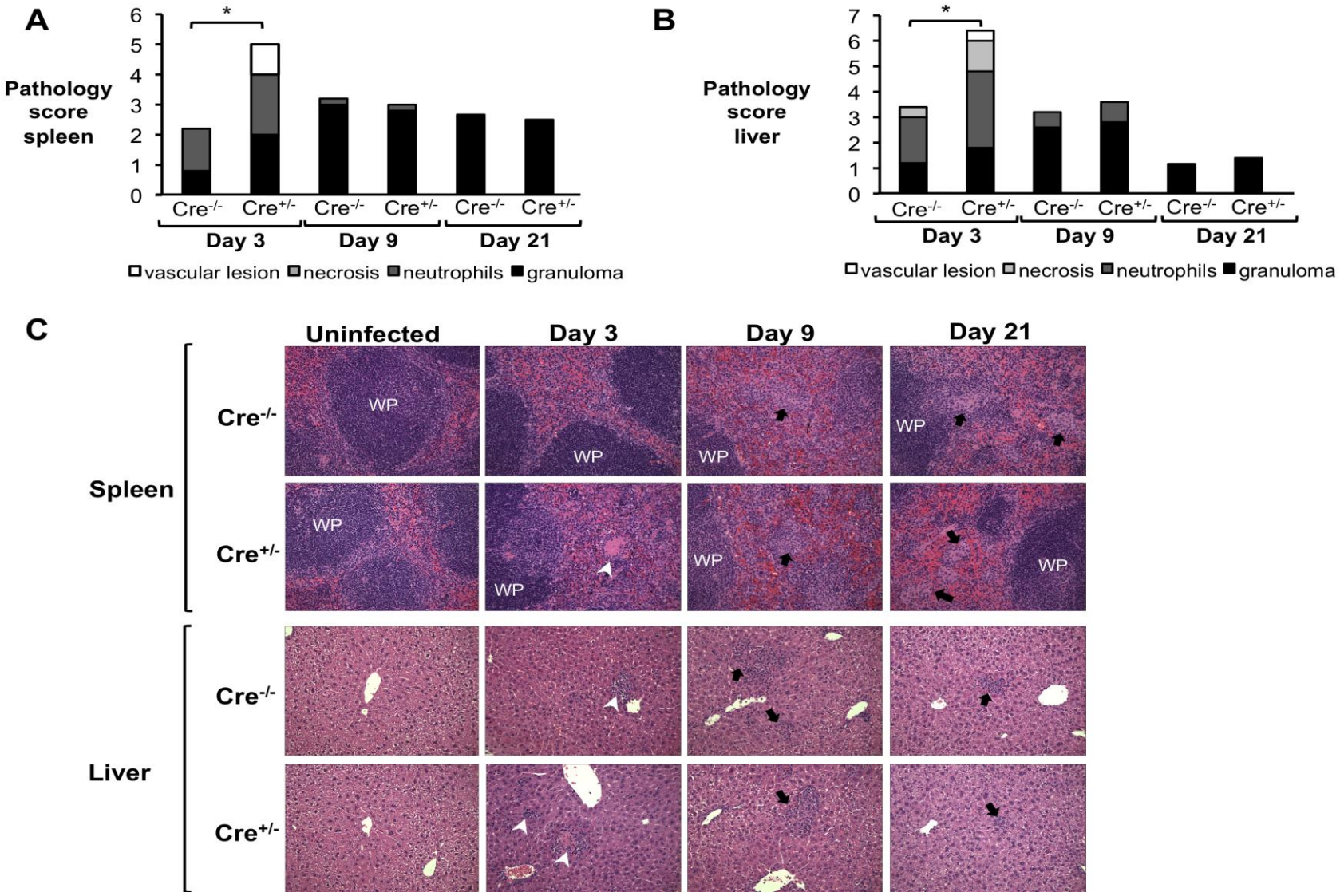
A
Pathology score spleen
6
5
4
3
2
1
0
*
Cre-/-
Cre+/-
Cre-/-
Cre+/-
Cre-/-
Cre+/-
Day 3
Day 9
Day 21
vascular lesion
necrosis
neutrophils
granuloma
B
Pathology score liver
7
6
5
4
3
2
1
0
*
Cre-/-
Cre+/-
Cre-/-
Cre+/-
Cre-/-
Cre+/-
Day 3
Day 9
Day 21
vascular lesion
necrosis
neutrophils
granuloma
C
Uninfected
Day 3
Day 9
Day 21
Spleen
Cre-/-
Cre+/-
Liver
Cre-/-
Cre+/-
WP

Figure 6. Pathology induced by lack of IL-10 production by macrophages and neutrophls during *B. abortus in vivo* infection. (A, B) Histopathology score of spleen (A) and liver (B) from littermate mice (Cre-/-) compared with IL10flox/LysMCre mice (Cre+/-) at 3, 9 and 21 d.p.i. (C) Representative histopathology figures from (A,B) - Black arrows indicate microgranulomas, white arrowheads show neutrophilic infiltrate, and white upper case WP indicates white pulp (x20). n=5. (*) represents $P<0.05$ using Mann-Whitney statistical analysis.

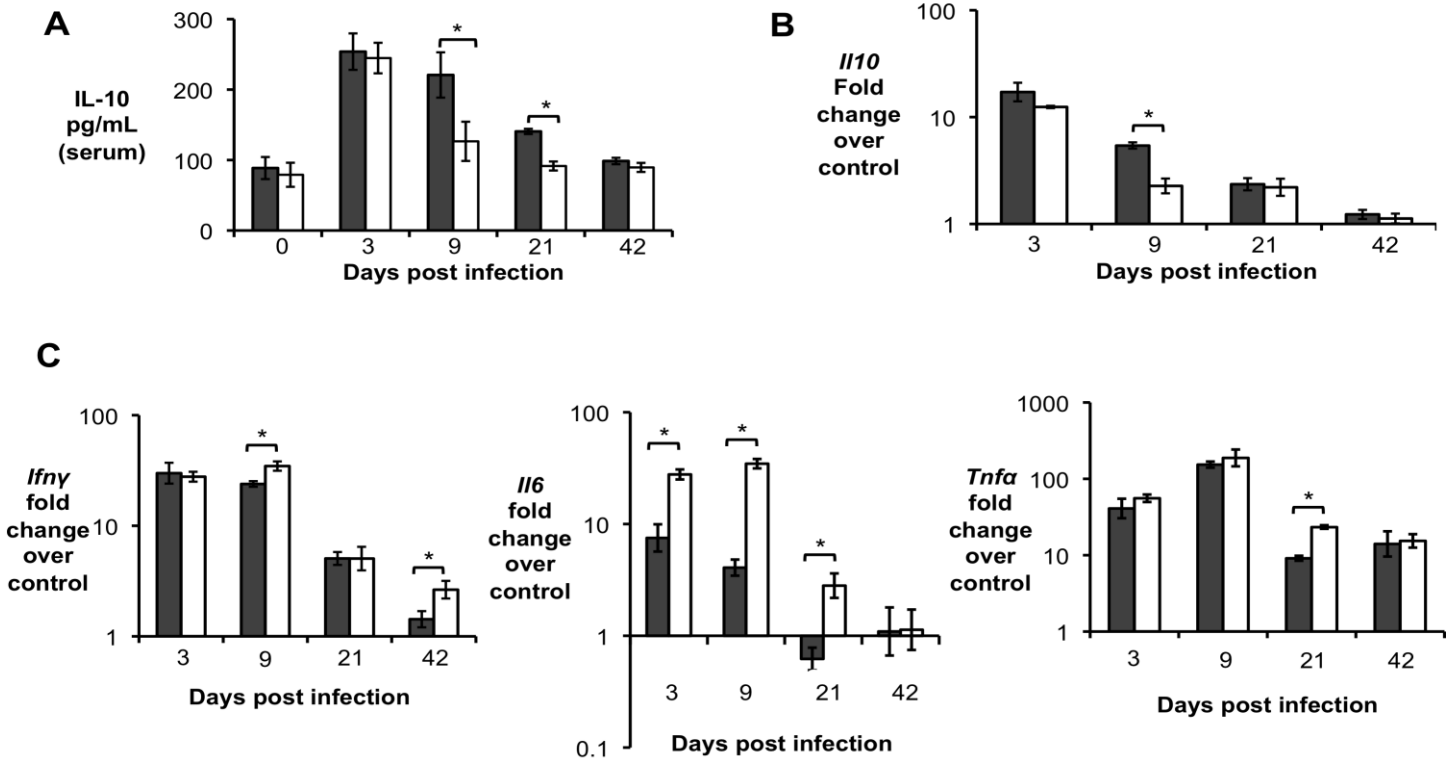

Fig S3

Figure 7. IL-10 production during *B. abortus* infection in mice lacking IL-10 production in T cells. (A) ELISA essay for IL-10 production in serum from littermate control mice (grey bars) compared with IL10flox/CD4Cre mice (white bars) at 3, 9, 21 and 42 d.p.i. (B) qRT-PCR analysis of IL-10 expression in spleen from littermate control (grey bars) compared with IL10flox/CD4Cre mice (white bars) at 3, 9, 21 and 42 d.p.i. (C) qRT-PCR analysis of proinflammatory cytokines in liver from littermate control (grey bars) compared with IL10flox/CD4Cre mice (white bars) at 3, 9, 21and 42 d.p.i. n=5. Values represent mean ± SEM.(*) represents $P<0.05$ relative to uninfected control using unpaired t-test statistical analysis.

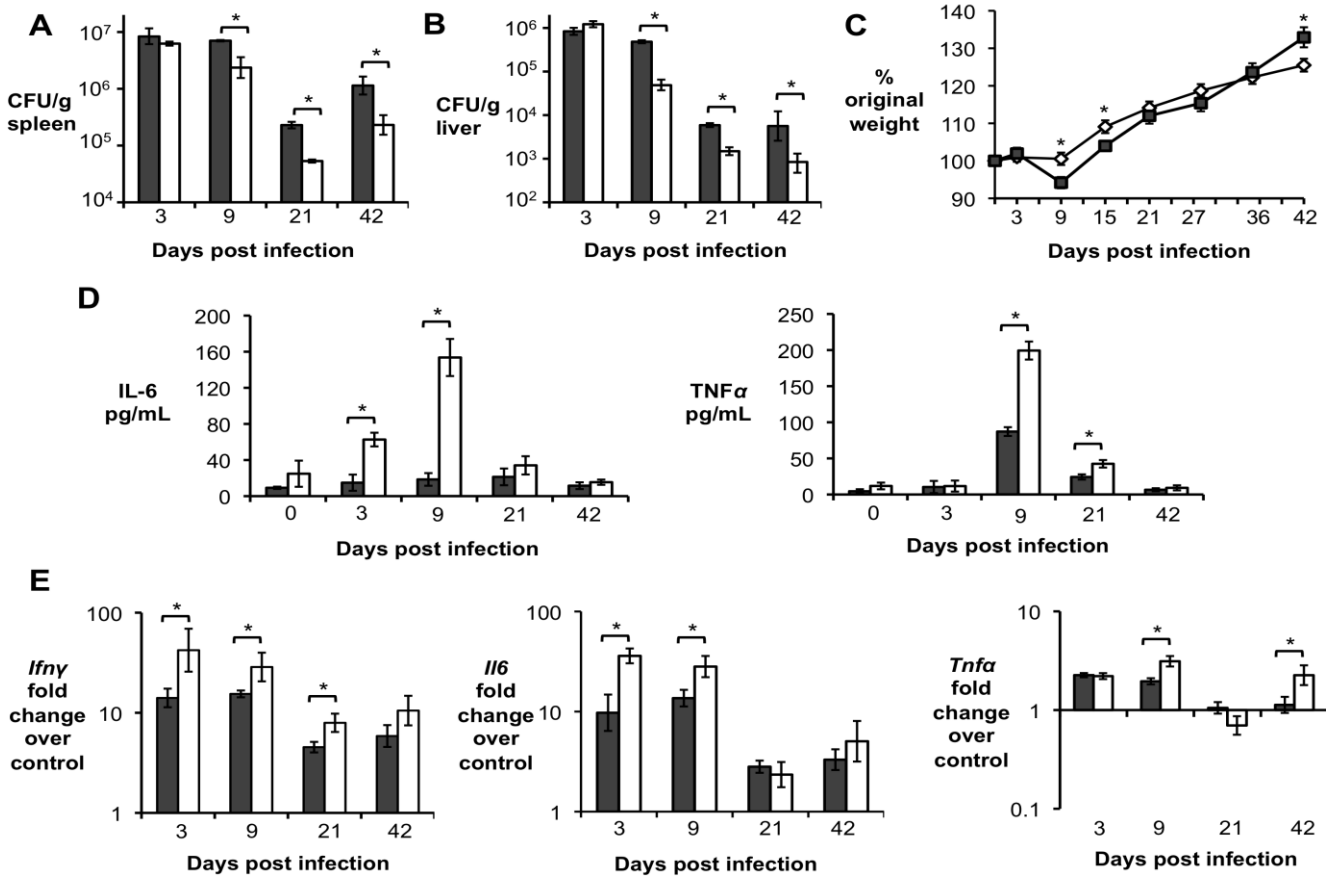

Figure 8. IL-10 production by T cells is required for *Brucella abortus* persistence and for control of inflammatory response *in vivo*. (A, B) *B. abortus* 2308 CFU counts in spleen (A) and liver from littermate control (grey bars) compared with IL10flox/CD4Cre mice (white bars) at 3, 9, 21 and 42 d.p.i. (C) Measurement of mouse weight over time in grams of littermate control mice (grey dots) compared with IL10flox/CD4Cre mice (white dots). (D) ELISA essay for IL-6 and TNF-α production in serum from littermate control mice (grey bars) compared with IL10flox/CD4Cre mice (white bars) at 3, 9, 21 and 42 d.p.i. (E) qRT-PCR analysis of pro-inflammatory cytokines in spleen from littermate control mice (grey bars) compared with IL10flox/CD4Cre mice (white bars) at 3, 9, 21 and 42 d.p.i. n=5. Values represent mean ± SEM. (*) represents P<0.05 using unpaired t-test statistical analysis

IL-10flox/CD4Ce mice exhibited significantly decreased weight gain during early infection and, by 21 days post-infection, they started to behave like control animals. IL-10flox/CD4Cre uninfected mice did not exhibit any slower weight gain and behaved like uninfected control mice (data not shown). Moreover, increased levels of the pro-inflammatory cytokines IFN-γ, IL-6, and TNF-α were observed in serum (Fig. 8D) spleen (Fig. 8E) and liver (Fig. S3C) of IL-10flox/CD4Cre at 3, 9 days and, to a lesser extent, at 21 d.p.i.

To determine if the significantly reduced weight gain and higher induction of pro-inflammatory cytokines were associated with a detrimental inflammatory response, spleen and liver sections from IL-10flox/CD4Cre and control mice were blindly evaluated by veterinary pathologists (MNX and TMS). Interestingly, IL-10flox/CD4Cre mice exhibited increased pathology, characterized by marked influx of neutrophils and histiocytes in the spleen (Fig. 9A and 9C), as well as tissue necrosis and multifocal neutrophilic vasculitis and thrombosis in the liver (Fig. 9B and 9C) at 3 and 9 d.p.i., suggesting an acute inflammatory response. Importantly, a hallmark of *B. abortus* infection is a mild initial pro-inflammatory response, which leads to a chronic infection characterized by formation of granulomas in infected organs (Hunt and Bothwell, 1967; Atluri *et al.*, 2011). However, by 21 d.p.i., IL-10flox/CD4Cre mice exhibited decreased granuloma formation in the spleen (Fig. 9A and 9C) when compared to littermate control mice. Taken together, these data demonstrate that T cell-derived IL-10 production during early *B. abortus* infection is crucial for the development of the chronic disease and morbidity caused by *B. abortus*, and limits the production of the pro-inflammatory response necessary to control the infection. However, the cell types affected by the IL-10 production during *Brucella* infection remained unclear.

Lack of IL-10 results in lower B. abortus survival in infected macrophages due to bacterial inability to escape late endosome

Since *Brucella* spp. are known to invade and survive inside phagocytic cells such as macrophages (Celli, 2006), we hypothesized that macrophages could be the cell type affected by IL-10 during *Brucella* infection. To determine the effect of IL-10 on *B. abortus* survival during macrophage infection *in vitro*, bone marrow derived macrophages (BMDM) from C57BL/6 and IL-$10^{-/-}$ mice were infected with *B. abortus* 2308 (MOI=100) and the bacterial survival was measured at 1, 8, and 24 h post-infection (h.p.i.) (Fig. 10A). *B. abortus* infected wild-type BMDM produced significant amounts of IL-10 (Fig. S1A). *B. abortus* exhibited a significantly decreased ability to survive inside BMDM from IL-$10^{-/-}$ mice at 8 and 24 h.p.i. when compared to BMDM from wild-type mice. Importantly, *B. abortus* infected IL-$10^{-/-}$ BMDM did not exhibit increased cell death, determined by LDH assay (data not shown). Moreover, to ensure that the observed effect resulted from an absence of IL-10 production, recombinant IL-10 (rIL-10) was added to the IL-$10^{-/-}$ BMDM media during infection (Fig. 10A). As expected, the addition of rIL-10 restored *B. abortus* survival inside macrophages. Results similar to those described above (Fig. 10A) were also observed in IFNγ-activated BMDM (data not shown).

The ability of *Brucella* spp. to persist and replicate within macrophages involves a temporary fusion of *Brucella*-containing vacuole with the late endosome/lysosome during the initial hours post-infection, and subsequent exclusion of the endosomal/lysosomal proteins from the *Brucella*-containing vacuole (Starr, T. *et al.*, 2008). To determine if *B. abortus* inability to persist inside macrophages was due to changes in pathogen's intracellular trafficking, we infected wild-type and IL-$10^{-/-}$ BMDM with *B. abortus* expressing mCherry (MOI=100) and bacterial co-localization with the late endosome marker LAMP1 was determined at 24 h.p.i. by confocal microscopy.

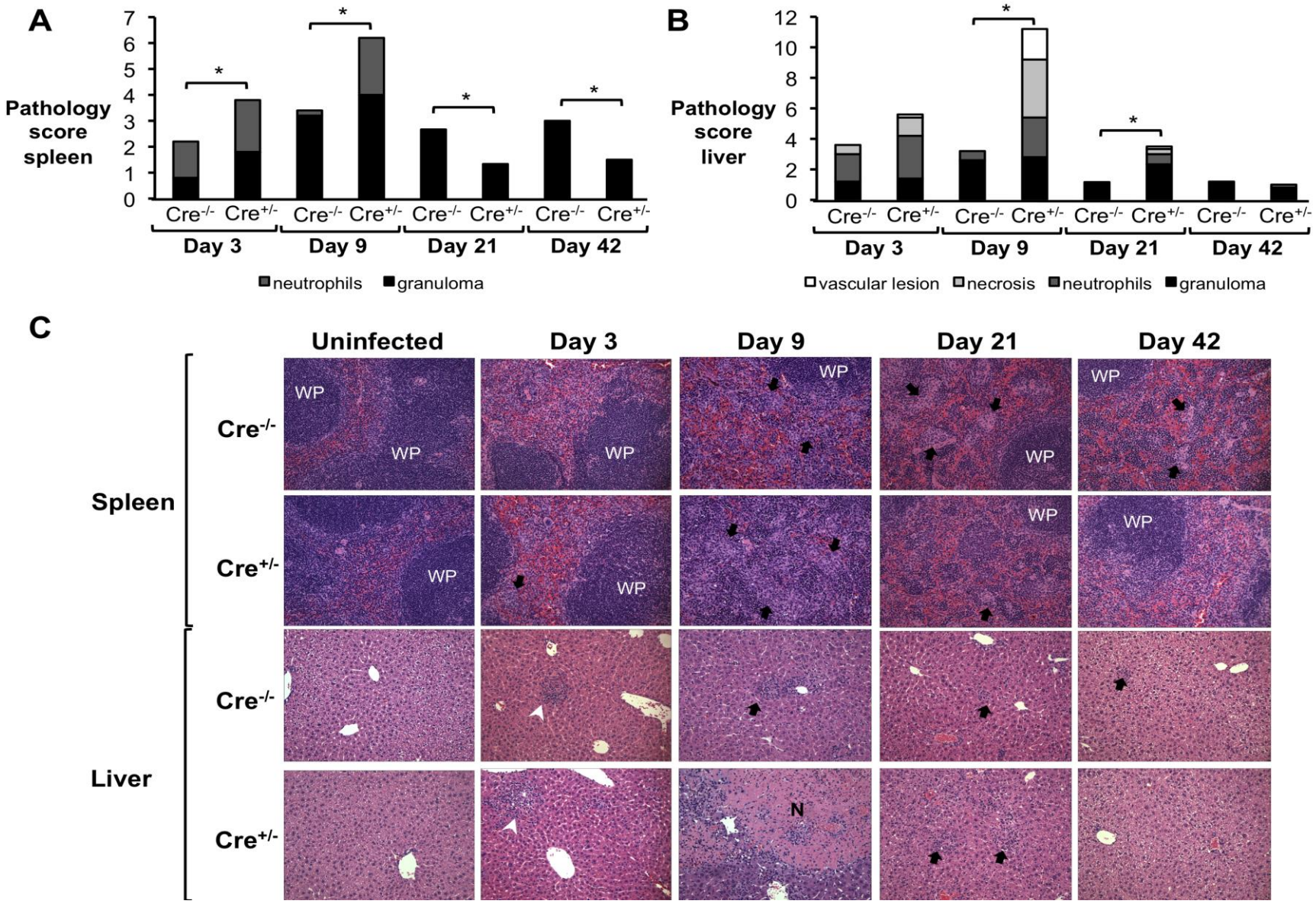
A
Pathology score spleen
0
1
2
3
4
5
6
7
*
*
*
*
Cre-/- Cre+/-
Day 3
Day 9
Day 21
Day 42
neutrophils
granuloma
B
Pathology score liver
0
2
4
6
8
10
12
*
*
Cre-/- Cre+/-
Day 3
Day 9
Day 21
Day 42
vascular lesion
necrosis
neutrophils
granuloma
C
Uninfected
Day 3
Day 9
Day 21
Day 42
Spleen
Liver
Cre-/-
Cre+/-
WP
N

Figure 9. IL-10 production by T cells is required for control of *Brucella abortus* induced pathology *in vivo*. (A, B) Histopathology score of spleen (A) and liver (B) from littermate mice ($Cre^{-/-}$) compared with IL10flox/CD4Cre mice ($Cre^{+/-}$) at 3, 9, 21 and 42 d.p.i. (C) Representative histopathology figures from (A,B) - Black arrows indicate microgranulomas, white arrowheads show neutrophilic infiltrate, and white upper case WP indicates white pulp (x20). n=5. (*) represents $P<0.05$ using Mann-Whitney statistical analysis.

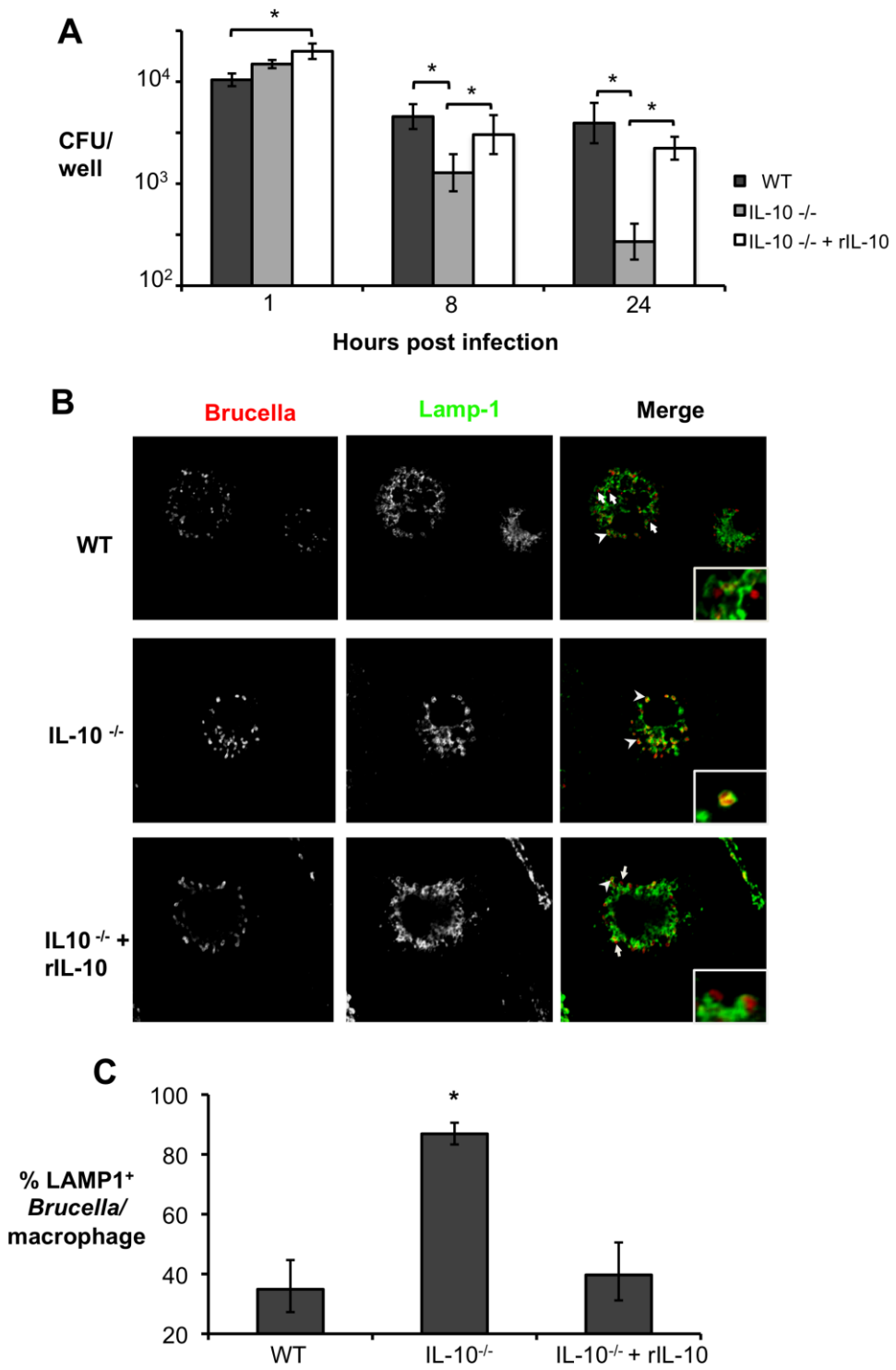

Figure 10. Lack of endogenous IL-10 results in lower *Brucella abortus* survival inside macrophages due to bacterial inability to escape the late endosome. (A) Survival of *B. abortus* over time in BMDM from C57BL/6 WT control mice and IL-10 deficient mice with (IL-10 - /- + rIL-10) or without (IL-10 -/-) rIL-10 added to the culture. (B) Confocal microscopy of BMDM from C57BL/6 WT control mice and IL-10 deficient mice with (IL-10 -/- + rIL-10) or without (IL-10 -/-) added rIL-10, infected with mCherry-expressing *B. abortus* 2308 for 24h. Colocalization of the bacteria (red) with the late endosomal marker LAMP-1 (green) is shown by arrowheads, while arrows indicate bacteria that were able to escape the

endosomal compartment. Intracellular survival of *B. abortus* in each treatment group is shown in Panel (A). (C) Quantification of % of colocalization of mCherry-expressing *B. abortus* and LAMP1 in infected macrophages shown in (B). Representative results of two independent experiments are shown. n=4. Values represent mean ± SEM. *P<0.05 using unpaired t-test statistical analysis.

Interestingly, while the majority of *B. abortus* was found to lack LAMP1 in wild type BMDM, the opposite was found in BMDM derived from IL-$10^{-/-}$ mice, in which over 80% of bacteria were co-localized with LAMP1 (Fig. 10B and 10C). This phenotype was IL-10-dependent, since addition of rIL-10 to the IL-$10^{-/-}$ BMDM restored the ability of the pathogen to escape the late endosome (Fig. 10B and 10C). Results similar to those described (Fig. 10B and Fig. 10C) were also observed in IFNγ activated BMDM (data not shown).

Lack of IL-10 results in higher levels of NF-κB activation and pro-inflammatory cytokine production in B. abortus infected macrophages

It has been demonstrated that IL-10 can inhibit a protective immune response, possibly by blocking NF-κB activation (Wang *et al.*, 1995) and downstream production of pro-inflammatory cytokines by antigen-presenting cells such as macrophages (Fiorentino *et al.*, 1991; Redford *et al.*, 2011). To investigate if IL-10 production would have an effect on NF-κB activation in *Brucella* infected macrophages, we used an NF-κB reporter RAW murine macrophage cell line (RAW-Blue cells). RAW-Blue cells were infected with *B. abortus* 2308 (MOI=100) in the presence of IL-10 receptor blocking antibody (IL-10R Ab) or rIL-10, and NF-κB activation was measured at 8 and 24 h.p.i. *Brucella* infected RAW-Blue macrophages produced significant amounts of IL-10 (Fig. S1B). Blockage of IL-10R resulted in decreased *B. abortus* intracellular survival inside RAW-Blue macrophages when compared to untreated controls at 24 h.p.i., as previously observed in IL-$10^{-/-}$ BMDM (data not shown). *B. abortus* infection did not result in significant NF-κB activation by any of the treatment groups at 8 h.p.i. (Fig. 11A). The use of IL-10R Ab to block the response of *B. abortus* infected RAW-Blue macrophages to IL-10 resulted in a significant increase in NF-κB activation at 24 h.p.i. when compared to untreated infected macrophages. Conversely, addition of exogenous rIL-10 resulted in a significant inhibition of NF-κB activation in *B. abortus* infected cells (Fig. 11A). The results above described were also observed in IFNγ activated RAW blue cells (data not shown).

To confirm that IL-10 affects pro-inflammatory cytokine production by infected macrophages, bone marrow-derived macrophages (BMDM) from C57BL/6 and IL-$10^{-/-}$ mice were infected with *B. abortus* 2308 (MOI=100) and cytokine expression was measured at 24 h.p.i. by ELISA and quantitative real-time PCR. Significantly, an absence of IL-10 resulted in higher expression levels of the pro-inflammatory cytokines IL-6 and TNFα by infected macrophages (Fig. 11B and 11C). Moreover, the phenotype observed was shown to be IL-10 dependent, since the addition of rIL-10 to IL-$10^{-/-}$ infected BMDM restored IL-6 and TNF-α expression to wild-type levels. Results similar to those described in Fig. 11B and Fig. 11C were also observed in IFN-γ activated BMDM (data not shown). Our results demonstrate that IL-10 production during *B. abortus* infection *in vitro* affects macrophage function by modulating NF-κB activation and the production of pro-inflammatory cytokines by infected cells.

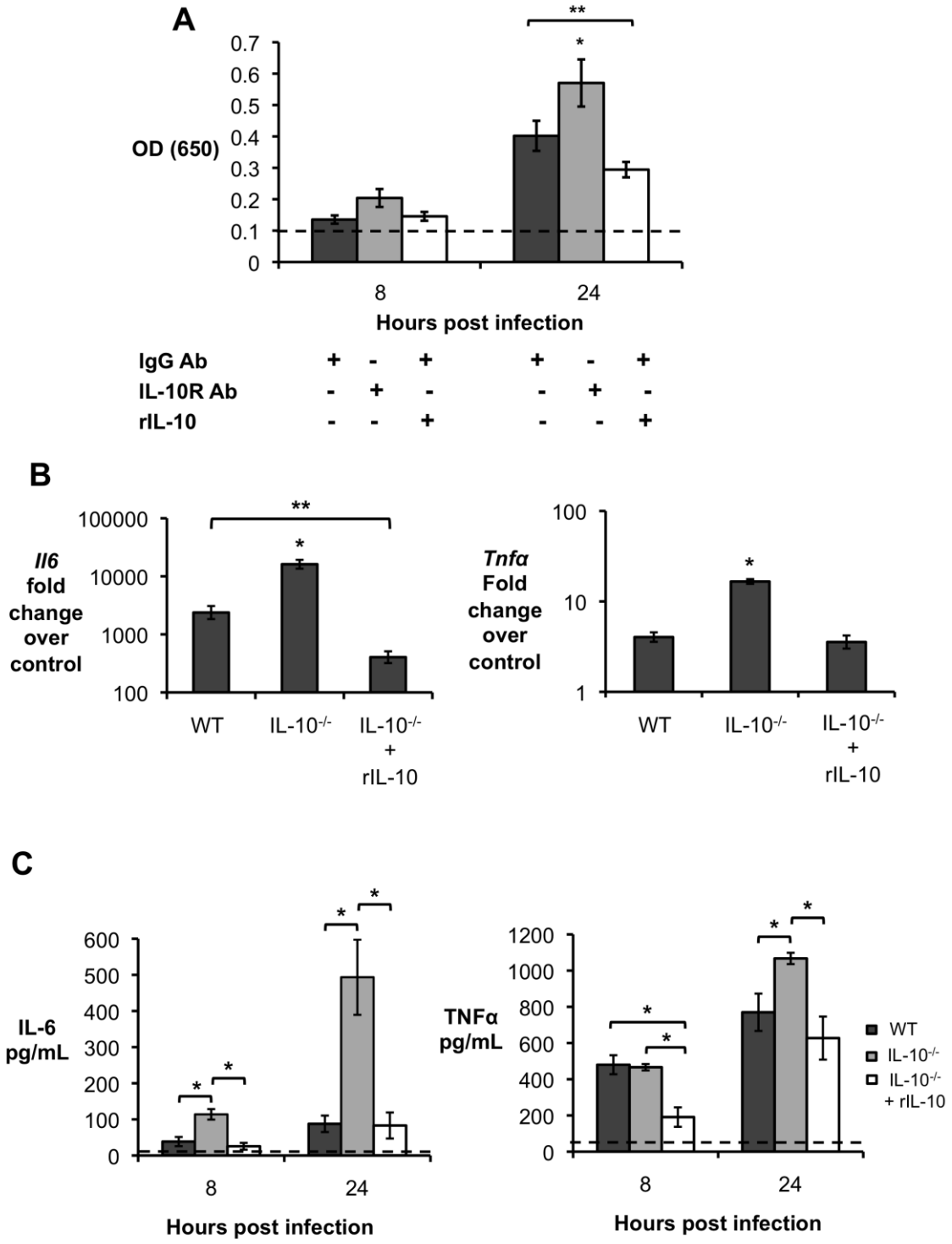

Figure 11. Lack of endogenous IL-10 results in higher NF-kB activation and production of pro-inflammatory cytokines by macrophages infected with *B. abortus*. (A) NF-kB activation measured in RAW-Blue macrophages infected with *B. abortus* 2308 for 8h and 24h in the presence of IL-10 receptor blocking antibody (IL-10R Ab), isotype control (IgG Ab) or exogenous IL-10 (rIL-10). (B) qRT-PCR analysis of IL-6, and TNF-α expression by BMDM from wild type mice (C57BL/6) and IL-10 deficient mice (IL-10-/-) in the presence or absence of recombinant IL-10. (C) ELISA essay for IL-6 and TNF-α production in supernatant from wild type mice (C57BL/6) and IL-10 deficient mice (IL-10-/-) in the presence or absence of recombinant IL-10. Results shown are representative of two independent experiments. n=5. Values represent mean ± SEM. *P<0.05 using unpaired t-test statistical analysis.

Inability of macrophages to respond to IL-10 results in severe acute pathology and decreased B. abortus survival in vivo

To further investigate the possibility that macrophages are the cell type responding to the IL-10 produced during *B. abortus* infection, we used *Il-10R*$^{flox/flox}$*LysMCre*$^{+/-}$ (IL-10Rflox/LysMCre) mice, which are unable to express the IL-10 receptor 1 chain (IL-10R1) specifically in monocytes/macrophages and/or neutrophils (Pils *et al.*, 2010). IL-10Rflox/LysMCre and *Il-10R*$^{flox/flox}$*LysMCre*$^{-/-}$ control mice were infected intraperitoneally with $5x10^5$ CFU of *B. abortus* 2308 for 3, 9, 21 and 42 days and bacterial survival in infected organs was evaluated. Our results from *in vitro* infection suggested that IL-10 affects the ability of *B. abortus* to survive inside macrophages. Remarkably, IL-10Rflox/LysMCre mice showed lower CFU counts in both spleen (Fig. 12A) and liver (Fig. 12B) at 9, 21 and 42 d.p.i. when compared to littermate control mice. This data provided strong support for the idea that macrophage responsiveness to IL-10 is necessary for optimal initial *B. abortus* colonization of the host as well as long-term persistence.

The results shown above (Fig. 8) demonstrated that a lack of IL-10 production by T cells during *B. abortus in vivo* infection resulted in increased pro-inflammatory responses and evident clinical signs of disease in mice. Moreover, our *in vitro* results suggested that blockage of IL-10R played a role in the control of NF-κB activation and pro-inflammatory cytokine production by *B. abortus*-infected macrophages. Therefore, we sought to determine the effect of macrophage responsiveness to IL-10 in the early host response to *B. abortus* infection. *B. abortus*-infected IL-10R/LysMCre mice exhibited decreased weight gain at 9, 15, and 21 d.p.i. when compared to wild-type infected mice (Fig. 12C). Furthermore, levels of IFN-γ, IL-6 and TNF-α were significantly increased in serum (Fig. 12D) spleens (Fig. 12E) and livers (Fig. S2) of IL-10R/LysMCre at 3, 9 d.p.i. and, to a lesser extent, at 21 d.p.i.

To determine if macrophage non-responsiveness to IL-10 would result in detrimental pathologic changes, spleen and liver sections from infected IL-10Rflox/LysMCre and control mice were blindly evaluated by veterinary pathologists (MNX and TMS). As expected, IL-10Rflox/LysMCre showed severe acute lesions characterized by influx of neutrophils and histiocytes, as well as tissue necrosis and multifocal neutrophilic vasculitis and thrombosis in the spleen at 9 d.p.i. (Fig. 13A and 13C) and in the liver (Fig. 13B and 13C) at 9 and 21 d.p.i. However, at 21 and 42 days post-infection, IL-10Rflox/LysMCre mice exhibited decreased granuloma formation in spleen (Fig. 13A and 13C) when compared to littermate control mice, suggesting that macrophage responsiveness to IL-10 is important for development of chronic pathological lesions in spleens of infected animals. These data provide the direct support for the idea that induction of IL-10 during *B. abortus in vivo* infection plays a key role in modulation of macrophage function, which, in turn, provides the ideal initial immunological environment for bacterial colonization and development of chronic infection.

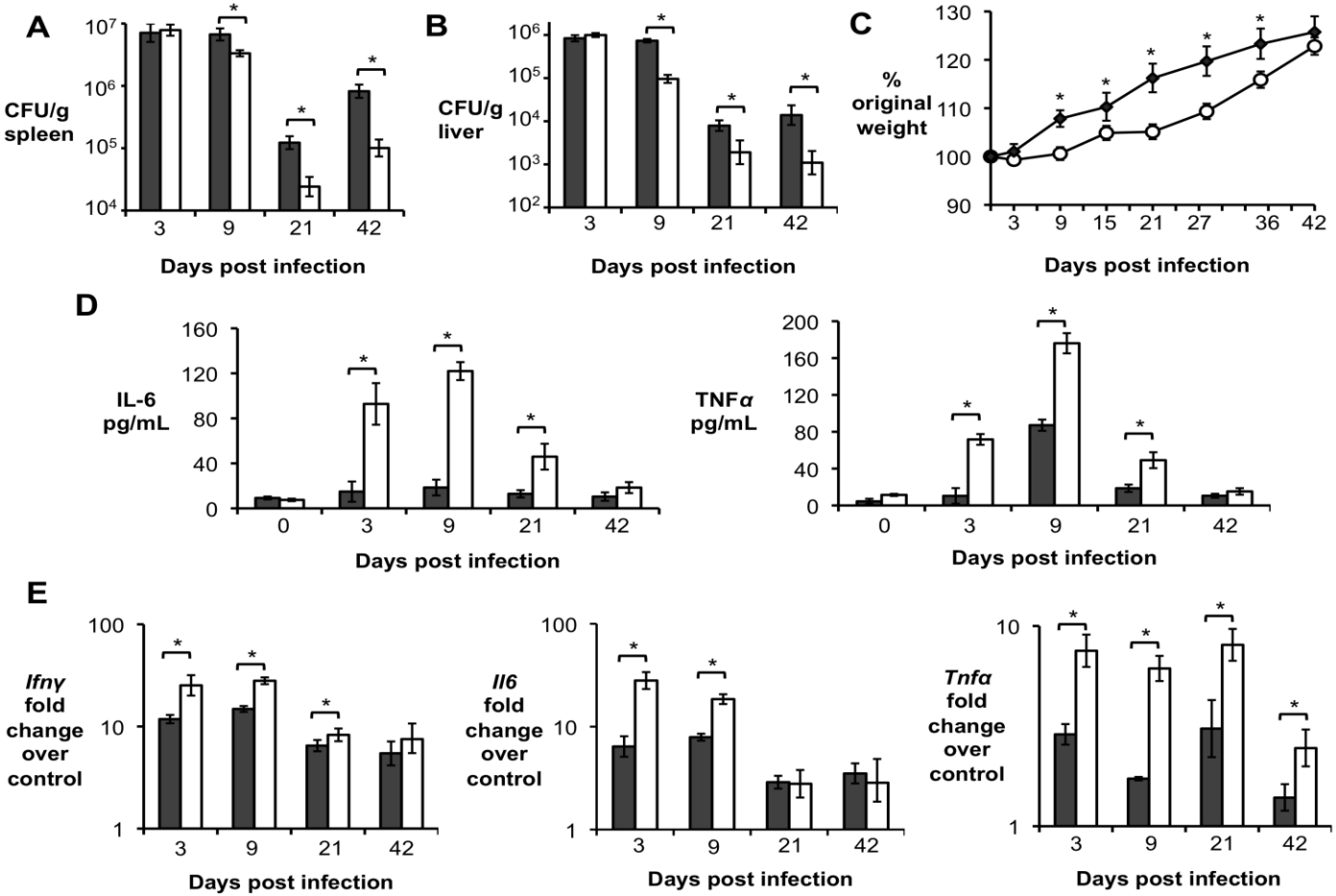

Figure 12. Inability of macrophages to respond to IL-10 results in decreased persistence of *B. abortus in vivo*. (A,B) *B. abortus* CFU counts in spleen (A) and liver (B) from littermate control mice (grey bars) compared with IL10Rflox/LysMCre (white bars) at 3, 9, 21 and 42 d.p.i. (C) Measurement of mouse weight over time in grams of littermate control mice (grey losangle) compared with IL10Rflox/LysMCre (white dots). (D) ELISA essay for IL-6 and TNF-α production in serum from littermate control mice (grey bars) compared with IL10Rflox/LysMCre mice (white bars) at 3, 9, 21 and 42 d.p.i. (E) RT-PCR analysis of pro-inflammatory cytokines in spleen from littermate control mice (grey bars) compared with IL10Rflox/LysMCre mice (white bars) at 3, 9, 21 and 42 d.p.i. n=5. Values represent mean ± SEM. (*) represents $P<0.05$ using unpaired t-test statistical analysis.

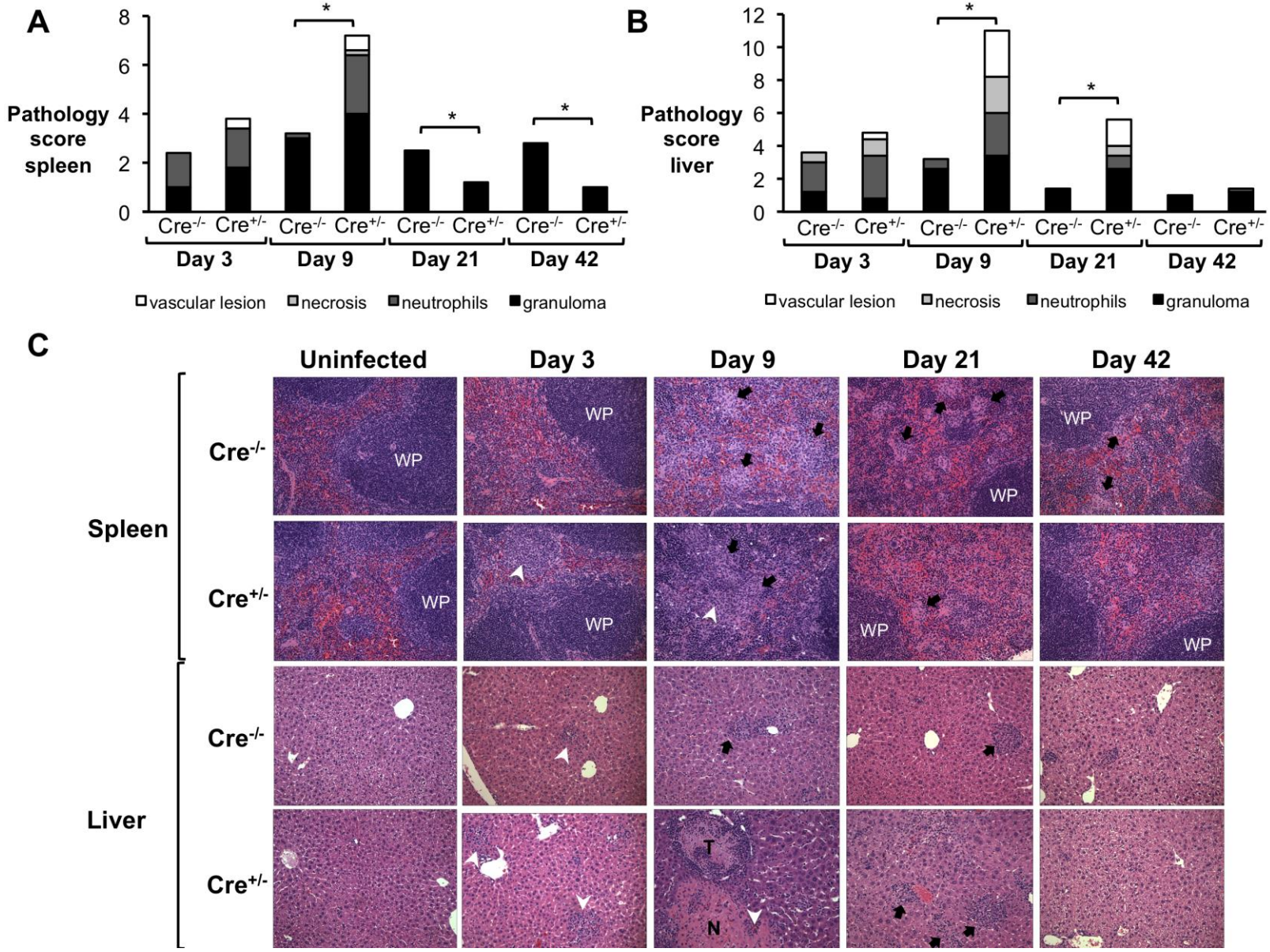
A
Pathology score spleen
0
2
4
6
8
*
*
*
Cre-/- Cre+/- Cre-/- Cre+/- Cre-/- Cre+/- Cre-/- Cre+/-
Day 3
Day 9
Day 21
Day 42
vascular lesion
necrosis
neutrophils
granuloma
B
Pathology score liver
0
2
4
6
8
10
12
*
*
Cre-/- Cre+/- Cre-/- Cre+/- Cre-/- Cre+/- Cre-/- Cre+/-
Day 3
Day 9
Day 21
Day 42
vascular lesion
necrosis
neutrophils
granuloma
C
Uninfected
Day 3
Day 9
Day 21
Day 42
Spleen
Cre-/-
Cre+/-
Liver
Cre-/-
Cre+/-
WP
T
N

Figure 13. Inability of macrophages to respond to IL-10 results in severe acute *B. abortus* induced pathology *in vivo*. (A, B) Histopathology score of spleen (A) and liver (B) from littermate mice (Cre-/-) compared with IL10Rflox/LysMCre mice (Cre+/-) at 3, 9, 21 and 42 d.p.i. (C) Representative histopathology figures from (A,B) - Black arrows indicate microgranulomas, white arrowheads show neutrophilic infiltrate and white upper case WP indicates white pulp (x20). n=5. (*) represents $P<0.05$ using Mann-Whitney statistical analysis.

Discussion

The balance between pro-inflammatory and anti-inflammatory cytokine production appears to be crucial for the ability of the host to eradicate an infection, as well as for the clinical presentation and/or pathology resulting from the infection. This balance appears to shift in the case of persistent pathogens such as *Brucella* spp., which are able to evade TLR signaling during the early stages of infection, thereby preventing development of an immune response that is appropriate to clear the infection (Suraud *et al.*, 2007). It is known that during the acute phase of *B. abortus* infection in mice, neutralization of IL-10 reduces bacterial colonization (Fernandes and Baldwin, 1995). Here, we provide support to the idea that during this phase of *B. abortus* infection, early production of IL-10 by T cells is key to promoting persistent intracellular infection.

In a number of infectious disease models, several cell types, including T cell subsets, B cells, neutrophils, macrophages and some DC subsets have been shown to be able to produce IL-10 (Moore *et al.*, 2001). Even though *B. abortus* infected macrophages are capable of producing IL-10 *in vitro*, only B cells have been implicated as a potential source of IL-10 during *in vivo* infection (Goenka *et al.*, 2011). In this study, however, we have demonstrated that macrophages play a limited role in IL10 production during early acute *B. abortus* infection. Additionally, we identified T cells, more specifically $CD4^+CD25^+$ T cells, as the major source of this cytokine during acute brucellosis. Indeed, Svetić and collaborators (Svetic *et al.*, 1993) have suggested a possible role for CD4+ T cells in IL-10 production during acute murine Brucellosis. Interestingly, previous studies have demonstrated elevated numbers of CD4+CD25+ T cells in PBMCs from human patients with acute brucellosis (Skendros *et al.*, 2007) as well as in draining lymph nodes from *B. melitensis* infected sheep (Suraud *et al.*, 2007). Moreover, Pasquali and collaborators demonstrated that depletion of $CD4^+CD25^+$ T cells resulted in increased control of *B. abortus* infection due to elevated activation of effector T cells and higher production of pro-inflammatory cytokines such as IFN-γ by infected mice (Pasquali *et al.*, 2010). Most likely, the effects seen in this latter study were an indirect effect of the decreased IL-10 production by T cells, resulting in elevated macrophage activation in CD25-depleted mice upon *B. abortus* infection. Taken together, these results point to $CD4^+CD25^+$ T cells as important players in modulating the early immune response to *B. abortus in vivo*.

There is a general agreement that macrophages represent a critical niche for *Brucella* persistence in the host (Atluri *et al.*, 2011). Importantly, they have been described as one of the cell types responding to IL-10 production in other infection models (Pils *et al.*, 2010; Saraiva and O'garra, 2010). Here we have demonstrated that macrophages are a main cell type responding to the immunomodulatory functions of IL-10 during both *in vitro* and *in vivo Brucella* infection. Moreover, IL-10 signaling had a significant impact on the ability of *B. abortus*-infected macrophages to produce pro-inflammatory cytokines and to permit intracellular growth of *B. abortus*. Interestingly, O'Leary and collaborators have demonstrated that IL-10 production by immune cells can affect the ability of *M. tuberculosis* to escape the $LAMP1^+$ late endosomal compartment and to establish infection in human macrophages *in vitro* (O'leary *et al.*, 2011). In agreement with this previous study, we have demonstrated that the capacity of macrophages to respond to IL-10 impacts intracellular survival of *Brucella* by decreasing the pathogen's ability to escape the $LAMP1^+$ late endosome, a prerequisite for replication in an endoplasmic reticulum-associated compartment.

It is important to note that the LysM promoter used to drive Cre expression in IL10Rflox mice is expressed in both neutrophils and macrophages (Pils *et al.*, 2010). Although our understanding of the

role of neutrophils during brucellosis is still evolving (Barquero-Calvo *et al.*, 2007; Barquero-Calvo *et al.*, 2013), we and others have described recruitment of these cells to both spleens and livers of *B. abortus*-infected mice during the acute infection phase (Barquero-Calvo *et al.*, 2013), Fig. 9 and Fig. 13). Moreover, the neutrophil recruitment was more evident in the absence of IL-10 (Fig. 2, Fig. 9 and Fig. 13). Therefore, although *Brucella* resistance to neutrophil killing has been well described (Kreutzer *et al.*, 1979), it is possible that the increased cytokine expression and pathology observed in IL10Rflox/LysMCre mice could also be due in part to a failure of neutrophils recruited to the site of infection to respond to IL-10.

It should be pointed out that, although IL-10 contributes to persistence of *B. abortus in vivo,* abrogation of IL-10 production (Fig. 2) or neutralization of IL-10 in vivo (Fernandes and Baldwin, 1995) did not result in eradication of *B. abortus* from tissues, contrary to what has been shown for *Leishmania* (Belkaid *et al.*, 2001). Therefore, factors in addition to IL-10 production must also contribute to chronic persistence of *B. abortus*. Although TGF-b has been shown to be produced by B cells and macrophages in BALB/c mice (Goenka *et al.*, 2011), consistent with this report, we did not observe any increase in circulating TGF-b1, TGF-b2, or TGF-b3 at 21 or 42 days post infection of C57BL/6 mice (data not shown). However, these results do not rule out a role for local activation of TGF-b in promoting chronic infection. An important factor in persistence of *Brucella* is the transient nature of IFNg production in infected mice, which subsides by 21d post infection in mice (Copin *et al.*, 2007), therefore our observed lack of a role of IL-10 later in infection could suggest that its role is to antagonize the activity of IFNg at earlier stages of infection. Finally, the possibility should be considered that during chronic infection, *B. abortus* may reside in a cell type that has inherently low microbicidal activity, as has been found for *M. tuberculosis* (Peyron *et al.*, 2008) and *B. melitensis* (Copin *et al.*, 2012).

At first glance, our data suggest that inhibition of IL-10 signaling would be beneficial to the host, since IL-$10^{-/-}$, IL-10flox/CD4Cre and IL-10Rflox/LysMcre showed increased ability to control *B. abortus* infection at both acute and chronic stages of infection. Moreover, both IL-10flox/CD4Cre and IL-10Rflox/LysMcre exhibited reduced formation of granulomas, a potential niche for *B. abortus* persistence (Atluri *et al.*, 2011), during the chronic stage of infection. However, in spite of the increased bacterial clearance, we demonstrated that lack of IL-10 during *Brucella* infection could potentially be detrimental to the host, since *B. abortus* infected IL-10 deficient mice presented evident signs of acute disease, characterized by changes in weight gain and marked histopathological lesions in both spleen and liver. Indeed, studies on other chronic pathogens such as *Leishmania major* (Belkaid *et al.*, 2001), human cytomegalovirus (Chang and Barry, 2010), and *M. tuberculosis* (reviewed in (Redford *et al.*, 2011)) have demonstrated that even though absence of IL-10 leads to better clearance of these pathogens, it can also result in severe and sometimes lethal pathologic changes. Therefore, although modulation of the IL-10 signaling pathway could be a potential target to avoid the establishment of chronic infection, more studies are needed to elucidate the optimal activation of the immune system necessary to improve clearance of chronic pathogens without a great cost to the host.

CHAPTER III: A PPARγ-MEDIATED INCREASE IN GLUCOSE AVAILABILITY SUSTAINS CHRONIC *BRUCELLA ABORTUS* INFECTION IN ALTERNATIVELY ACTIVATED MACROPHAGES*

Introduction

Brucella abortus is a zoonotic bacterial pathogen that establishes long-term infections in its host. *In vivo*, bacteria are found in association with phagocytic cells, most prominently macrophages, in which a subset of *B. abortus* is able to evade killing in phagolysosomes. Instead, bacteria replicate with an endoplasmic reticulum-associated compartment and interact subsequently with a modified autophagy pathway to promote cell-to cell spread (Gorvel and Moreno 2002; Starr *et al.*, 2008). While studies on the interaction between *B. abortus* and macrophages have yielded critical insights into how *B. abortus* survives intracellularly, a subset of factors required for chronic persistence *in vivo* do not appear to mediate intracellular replication in cultured macrophages (Hong *et al.*, 2000; Fretin *et al.*, 2005), raising the possibility that the niche for chronic bacterial persistence has different characteristics from macrophages cultured *in vitro*.

Recently, it has been recognized that like other immune cells, macrophages can adopt different functional states that are influenced by the immune microenvironment [reviewed by (Gordon and Martinez, 2010; Van Dyken and Locksley, 2013)]. Activation by interferon gamma (IFNγ) leads to the classically activated macrophage (CAM) phenotype, characterized by production of nitric oxide (NO) and inflammatory cytokines such as tumor necrosis factor alpha (TNFα) and interleukin 6 (IL-6). During inflammation, these cells can arise from $Ly6C^{high}$ inflammatory monocytes that leave the bone marrow in a CCR2-dependent manner (Shi and Pamer, 2011). In contrast, the Th2 cytokines interleukin-4 (IL-4) and IL-13 activate signal transducer and activator of transcription 6 (STAT6) to promote development of alternatively activated macrophages (AAM), which play important roles in allergic inflammation, helminth infection and tissue repair (Reyes and Terrazas, 2007; Shirey *et al.*, 2008; Lawrence and Natoli, 2011). These macrophages express low levels of the inflammatory monocyte marker LY6C.

In addition to roles in inflammation and immunity, CAM and AAM play important roles in host physiology and metabolism (reviewed by (Chawla, 2010). Development of the AAM phenotype is dependent on peroxisome proliferator activated receptors (PPARs; (Odegaard *et al.*, 2007), which act downstream of STAT6 signaling to regulate macrophage metabolism. Interestingly, our previous results (Hong *et al.*, 2000) implicated bacterial metabolism as key to chronic *B. abortus* infection. Therefore, we sought to investigate the relative importance of AAM and CAM as niches for persistent infection, and to determine whether the different metabolic programming of these two macrophage populations contributes to chronic infection by *B. abortus*.

Material and Methods

Bacterial strains, media and culture conditions: Bacterial strains used in this study were the virulent strain *Brucella abortus* 2308, its isogenic mutants strain MX2 which has an insertion of pKSoriT-*bla-kan*-P*sojA-mCherry* plasmid (Copin *et al.*, 2012), BA159 (*gluP*) which has a miniTn**5** Km2 transposon insertion interrupting the gluP locus (Hong et al., 2000) and BA159 complemented mutant MX6 (*gluP*::pGLUP1). For construction of strain MX6, the *gluP* gene sequence including its promoter was amplified by PCR using the primers GluP FWD: 5'-GTCGACTTTGTTGGCTTTCAAGTGG-3' and GluP REV: 5'-GGATCCTCGCCATTCTATTCGGTTTC-3'. The resulting *gluP* PCR product was cloned into pCR2.1 using the TOPO TA cloning kit (Invitrogen, Carlsbad) and correct insertion

*Article accepted for publication in Cell Host & Microbe

confirmed by sequencing (SeqWright Fisher Scientific, Houston) and plasmid digestion using enzymes *Sal*I and *Bam*HI. The final construct (pGLUP1) was introduced by electroporation to strain BA159 to reconstitute the intact gene. For strain MX6, positive clones were selected based on ampicillin (Amp) resistance and intact gene chromosomal insertion was further confirmed by PCR. For strain MX2, positive clones were kanamycin (Km) resistant and fluorescent, as previously described (Copin *et al.*, 2012b). Strains were cultured on tryptic soy agar (Difco/Becton-Dickinson, Sparks, MD) or tryptic soy broth at 37°C on a rotary shaker. Bacterial inocula for mouse infection were cultured on tryptic soy agar plus 5% blood for 3 days (Alton *et al.*, 1975). For cultures of strain MX2 and BA159, Km was added to the culture medium at 100µg/mL. All work with *B. abortus* cells was performed at biosafety level 3, and was approved by the Institutional Biosafety Committee at the University of California, Davis.

Animal experiments: Female C57BL/6J wild-type mice, *Ifng*$^{-/-}$ mice, *Ccr2*$^{-/-}$ mice and *Stat6*$^{-/-}$ mice, aged 6-8 weeks, were obtained from The Jackson Laboratory (Bar Harbor). Female and Male C57BL/6 *Pparg*$^{fl/fl}$*LysM*$^{cre/-}$ (Mac-PPARγ KO) and littermate *Pparg*$^{fl/fl}$*LysM*$^{-/-}$ (Control) mice were generated at UC Davis by mating *Pparg*$^{fl/fl}$ mice with LysM$^{cre/cre}$ mice (The Jackson Laboratory, Bar Harbor). Mice were held in microisolator cages with sterile bedding and irradiated feed in a biosafety level 3 laboratory. Groups of 4 to 6 mice were inoculated intraperitoneally (i.p.) with 0.2 mL of phosphate-buffered saline (PBS) containing 5 x 10^5 CFU of *B. abortus* 2308 or a 1:1 mixture of *B. abortus* 2308 and *gluP* mutant as previously described (Rolán and Tsolis, 2008). At 0, 3, 9, 15, 21, 30 and/or 60 days after infection, according to the experiment performed, the mice were euthanized by CO_2 asphyxiation and their spleens were collected aseptically at necropsy. The spleens were homogenized in 2 mL of PBS, and serial dilutions of the homogenate were plated on TSA and/or TSA+ kanamycin for enumeration of CFU. Spleens samples were also collected for gene expression, flow cytometry and immunohistochemistry analysis as described below. All animal experiments were approved by University of California Laboratory Animal Care and Use Committee and were conducted in accordance with institutional guidelines.

Bone marrow derived macrophage infection: Bone marrow-derived macrophages were differentiated from bone marrow precursors from femora and tibiae of female, 6 to 8 weeks old, C57BL/6J mice or Mac-PPARγ KO (*Pparg*$^{-/-}$) and littermate Control (WT) mice following a previously published procedure (Rolan and Tsolis, 2007). For BMDM experiments, 24-well microtiter plates were seeded with macrophages at concentration of 5 x10^5 cells/well in 0.5 mL of RPMI media (Invitrogen, Grand Island, NY) supplemented with 10% FBS and 10 mM L-glutamine (RPMI supl) incubated for 48 h at 37°C in 5% CO_2. Preparation of the inoculum and BMDM infection was performed as previously described (Rolan and Tsolis, 2007). Briefly, for inoculum preparation, *B. abortus* 2308 or *B. abortus* BA159 (*gluP*) or MX6 were grown for 24 h and then diluted in RPMI supl, and about 5 × 10^7 bacteria in 0.5 mL of RPMI supl were added to each well of BMDM, reaching multiplicity of infection (MOI) of 100. Microtiter plates were centrifuged at 210 × *g* for 5 min at room temperature in order to synchronize infection. Cells were incubated for 20 min at 37°C in 5% CO_2, free bacteria were removed by three washes with phosphate-buffered saline (PBS), and the zero-time-point sample was taken as described below. After the PBS wash, RMPI supl plus 50 mg gentamicin per mL was added to the wells, and the cells were incubated at 37°C in 5% CO_2. In order to determine bacterial survival, the medium was aspirated at 0, 8, 24, and 48 h after infection according to the experiment performed, and the BMDM were lysed with 0.5 mL of 0.5% Tween 20, followed by rising of each well with 0.5 mL of PBS. Viable bacteria were quantified by serial dilution in sterile PBS and plating on TSA.

For gene expression assays, BMDM were resuspended in 0.5 mL of TRI-reagent (Molecular Research Center, Cincinnati) at the time-points described above and kept at -80°C until further use. When necessary, 10 ng/mL of mouse rIFN-γ (BD Bioscience, San Jose, CA) or 10 ng/mL of mouse rIL-4 (BD Bioscience, San Jose, CA), or 3 μM of GW9662 (Cayman Ann Harbor, MI), or 5 μM of Rosiglitazone (Cayman, Ann Harbor, MI), or 50μM of Etomoxir (Sigma-Aldrich, St Louis, MO) were added to the wells overnight prior to experiment and kept throughout the experiments. All experiments were performed independently in duplicate at least four times and the standard error for each time point calculated.

CD11b^{+} *cell isolation:* Macrophages (CD11b^{+} cells) were isolated from the spleens of *B. abortus* infected C57BL/6J, congenic *Ccr2*$^{-/-}$, *Ifng*$^{-/-}$ and *Stat6*$^{-/-}$ mice with a MACS CD11b MicroBeads magnetic cell sorting kit from Miltenyi Biotech (Auburn, CA) by following the manufacturer's instructions, as previously described (Rolán *et al.*, 2009b). Briefly, single cell suspension was prepared by gently teasing apart the spleens, followed passage of splenocytes through a 70-μm cell strainer and treatment with ACK buffer (Lonza, Walkersville, MD) to lyse red blood cells. Cells were washed with PBS-BSA, counted, and incubated with CD11b MicroBeads. Cells were applied to a magnetic column, washed, eluted, and counted. For gene expression assays, total splenic CD11b^{+} cells per mouse were resuspended in 0.5 mL of TRI-reagent (Molecular Research Center, Cincinnati) and kept at -80°C until further use. For *B. abortus* recovery essay, viable bacteria in CD11b^{-} and CD11b^{+} splenocytes fractions was determined by 10-fold serial dilution in sterile PBS and plating on TSA. The results were normalized to CFU per 10^{6} cells.

Treatment with PPARγ agonist/antagonist in vivo: Female C57BL/6J mice were inoculated intraperitoneally (i.p.), daily, for 7 days prior to *B. abortus* infection, with 5mg/kg/day of the PPARγ agonist Rosiglitazone (Cayman, Ann Harbor, MI) diluted in 0.2 mL of sterile PBS solution. For the treatment with PPARγ antagonist GW9662 (Cayman, Ann Arbor, MI), female C57BL/6J mice were inoculated intraperitoneally (i.p.), daily, from day 18 till day 30 post *B. abortus* infection, with 3mg/kg/day of PPARγ antagonist GW9662 (Cayman, Ann Arbor, MI) diluted in 0.2 mL of sterile PBS solution.

RT-PCR and real time PCR analysis: Eukaryotic gene expression was determined by real-time PCR as previously described (Rolan and Tsolis, 2007). Briefly, eukaryotic RNA was isolated using TRI reagent (Molecular Research Center, Cincinnati) according with the manufacturer's instructions. A Reverse transcriptase reaction was performed to prepare complementary DNA (cDNA) using TaqMan reverse transcription reagents (Applied Biosystems, Carlsbad). A volume of 4 μL of cDNA was used as template for each real-time PCR reaction in a total reaction volume of 25 μL. Real-time PCR was performed using SYBR-Green (Applied Biosystems) along with the primers listed in Table S1. Data were analyzed using the comparative Ct method (Applied Biosystems, Carlsbad). Transcript levels of *IL-6, Nos2, Ym1, Fizz1, Tnfa, Pparg, Hifa, Pfkfb3, Glut1, Pgc1b, Acadm* and *Acadl* were normalized to mRNA levels of the housekeeping gene *act2b*, encoding b-actin.

Flow cytometry: Flow cytometry analysis for detection of CAM, AAM and/or *B. abortus* intracellular localization was performed in splenocytes and/or CD11b^{+} splenic cells of C57BL/6J mice infected with *B. abortus* 2308 for 9 or 30 days. Briefly, after passing the spleen cells through a 100-μm cell strainer and treating the samples with ACK buffer (Lonza, Walkersville, MD) to lyse red blood cells, splenocytes were washed with PBS (Gibco) containing 1% bovine serum albumin (fluorescence-activated cell sorter [FACS] buffer). After cell counting, 4 x 10^{6} cells/mouse were re-suspended in PBS and stained with Aqua Live/Dead cell discriminator (Invitrogen, Grand Island, NY) according to the manufacturer's protocol. After Live/Dead staining,

splenocytes were resuspended in 50 µL of FACS buffer and cells were stained with cocktail of anti-B220 PE (BD Pharmigen, San Jose, CA), anti-CD3 PE (BD Pharmingen, San Jose, CA), anti-NK1.1 PE (BD Pharmigen, San Jose, CA), anti-CD11b FITC (BD Pharmingen, San Jose, CA), anti-F4/80 Pe.Cy7 (Biolegend, San Diego, CA), anti-Ly6C Pacific Blue (Biolegend, San Diego, CA), anti-Ly6G PerCP Cy5.5 (Biolegend, San Diego, CA) and anti-CD301 AF647 (AbD serotec, Raleigh, NC). The cells were washed with FACS buffer and fixed with 4% formaldehyde for 30 min at 4°C. To determine intracellular *B. abortus* localization in $CD11b^+$ splenocytes, cells were stained with cocktail of anti-CD11c PE (BD Pharmigen, San Jose, CA), anti-CD11b FITC (BD Pharmingen, San Jose, CA), anti-F4/80 Pe.Cy7 (Biolegend, San Diego, CA), anti-Ly6C Pacific Blue (Biolegend, San Diego, CA), anti-Ly6G PerCP Cy5.5 (Biolegend, San Diego, CA) and anti-CD301 AF647 (AbD serotec, Raleigh, NC), followed by cell fixation and permeabilization using Cytofix/Cytoperm (BD Pharmigen, San Jose, CA) at 4°C for 30 min. For intracellular *B. abortus* labeling, $Cd11b^+$ splenocytes were ressuspended in 50µL of Perm/Wash buffer (BD Pharmigen, San Jose, CA) and stained with APC.Cy7 (AbD serotec, Raleigh, NC) conjugated goat anti-*B. abortus* antibody followed by two washes with Perm/Wash buffer. For all experiments, cells were ressuspended in FACS buffer prior to analysis. Flow cytometry analysis was performed using an LSRII apparatus (Becton Dickinson, San Diego, CA), and data were collected for 5 x 10^5 cells/mouse. Resulting data were analyzed using Flowjo software (Treestar, inc. Ashland, OR). Gates were based on Fluorescence-Minus-One (FMO) controls.

Lactate measurement: For determination of extracellular lactate levels, C57BL/6J BMDM were grown in 24-well plates using RPMI media (Invitrogen, Grand Island, NY) supplemented with 2% FBS and 10 mM L-glutamine (RPMI supl) and infected as described above. At 24h post-infection, supernatants were collected and lactate measurement was performed by using a Lactate Colorimetry Assay Kit (Biovision, Milpitas, CA) according to the manufacturer's instructions.

Glucose measurement: For determination of intracellular glucose levels, C57BL/6J BMDM were grown in 24-well plates and infected as described above. At 24h post-infection, cells were washed three times with cold PBS, and resuspended in 100 µL of glucose assay buffer (Biovision, Milpitas, CA). Further glucose measurement was performed by using a Glucose Assay Kit (Biovision, Milpitas, CA) according to the manufacturer's instructions.

Statistical analysis: Fold changes of ratios (bacterial numbers or mRNA levels) and percentages (flow cytometry and fluorescence microscopy) were transformed logarithmically prior to statistical analysis. An unpaired Student's *t*-test was used on the transformed data to determine whether differences between groups were statistically significant ($P < 0.05$). When more than 2 treatments were used, statistically significant differences between groups were determined by one way ANOVA. All statistical analysis was performed using GraphPad Prism version 6b software (GraphPad Software, La Jolla, CA).

Results

Alternatively activated macrophages are more abundant during chronic B. abortus infection compared to acute infection

To gain insight into the role of different macrophage populations during different phases of *B. abortus* infection, we performed an infection time course experiment. These results showed that early (1-3d) bacterial numbers increased, then subsequently declined over the next 21 days, and we designated this as the acute phase of infection. Between 30 and 60 days post infection, bacterial numbers remained constant, and this was designated the chronic infection phase (Fig. 14A). During the acute phase of infection, a short-lived Th1 response (Fernandes *et al.*, 1996) and an influx of inflammatory macrophages (Copin

et al., 2012) act to control bacterial colonization. However, while *B. abortus* is found within CAM early during infection, the intracellular niche for *B. abortus* during the persistence phase is unknown. To shed light on this question, we compared expression of markers of AAM (Fig. 14 and Fig S5) and CAM (Fig. S5) in the spleen, a site of systemic *B. abortus* persistence, during acute and chronic infection. While markers of classical macrophage activation, such as *Nos2* (encoding inducible nitric oxide synthase), *Il6* (encoding interleukin-6), and *Tnfa* (encoding tumor necrosis factor alpha), were elevated in splenic macrophages ($CD11b^+$ cells) during the acute phase of infection, expression of these markers declined during persistent infection (Fig S5A). Further, while the total number of macrophages in the spleen was increased in both acute and chronic infection compared to uninfected mice (Fig. 14B), a significantly greater proportion of these macrophages had an inflammatory phenotype during acute infection, as evidenced by their $Ly6C^{high}$ phenotype (Figs. 14C and 14E), and low expression of AAM markers *Ym1* and *Fizz1* (Fig. S5B and S5C). $Ly6C^{high}$ monocytes contributed to control of *B. abortus* infection during the acute phase, since mice deficient for the C-C chemokine receptor 2 (*Ccr2*$^{-/-}$ mice), which are deficient for egress of $Ly6C^{high}$ monocytes from the bone marrow, were colonized ~3 fold more highly during the acute phase (9d) of infection (Fig. S14D). Macrophages from *B. abortus*-infected *Ccr2*$^{-/-}$ mice also had reduced levels of inflammatory markers and increased expression of AAM markers (Fig. S14E), suggesting that increased numbers of AAM in the *Ccr2*$^{-/-}$ mice may contribute to the increased *B. abortus* colonization observed in these mice.

In contrast to acute *B. abortus* infection, during the chronic infection phase (30d), flow cytometric analysis of splenic macrophages ($CD3^-B220^-NK1.1^-Ly6G^-CD11b^+F4/80^+$ cells) revealed an increase in cells with a $Ly6C^{low}$ phenotype that were positive for the AAM marker CD301 (Fig. 14D-F). In addition, higher expression levels of the AAM markers *Ym1* and *Fizz1* (encoding proteins secreted by AAM) were observed, suggesting an increased abundance of AAM at this time point (Fig. S5B). Immunohistochemical analysis of Ym1 and Fizz1 expression in splenic tissue confirmed that while these AAM markers were expressed at low levels in uninfected and acutely infected spleen tissue, the abundance of both markers was elevated during chronic infection, at day 30 (Fig. S5C). Together these lines of evidence provided support for the idea that AAM are more abundant in the spleen during the chronic infection phase of brucellosis, and suggested that AAM may provide a niche for persistence of *B. abortus*.

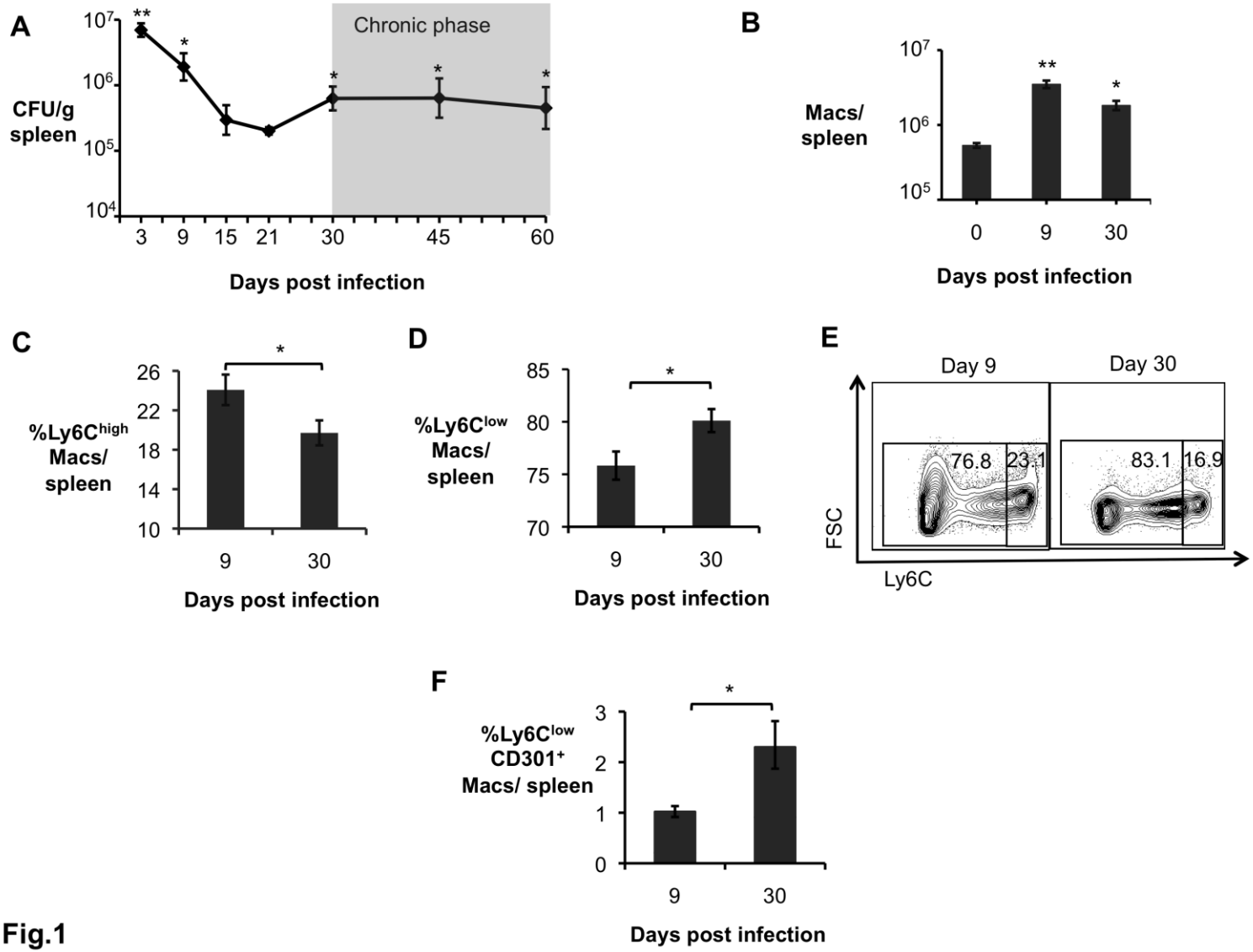
A
Chronic phase
CFU/g spleen
Days post infection
B
Macs/ spleen
Days post infection
C
%Ly6C^high Macs/ spleen
Days post infection
D
%Ly6C^low Macs/ spleen
Days post infection
E
Day 9
Day 30
76.8
23.1
83.1
16.9
FSC
Ly6C
F
%Ly6C^low CD301^+ Macs/ spleen
Days post infection

Fig.1

Figure 14. Alternatively activated macrophages are more abundant during chronic brucellosis. (A) *B. abortus* 2308 CFU counts in spleens from C57BL/6J mice (n=5) at 3, 9, 15, 21, 30, 45 and 60 days post infection (d.p.i). **(B)** Numbers of macrophages ($CD3^-B220^-NK1.1^-Ly6G^-CD11b^+F4/80^+$) determined by flow cytometry in spleens of *B. abortus* infected mice (n=4) at 0, 9 and 30 d.p.i. **(C)** Frequency of $CD3^-B220^-NK1.1^-Ly6G^-CD11b^+F4/80^+Ly6C^{high}$ macrophages (CAM) measured by flow cytometry in spleens of *B. abortus* infected mice (n=4) at 9 and 30 d.p.i.. **(D)** Frequency of $CD3^-B220^-NK1.1^-Ly6G^-CD11b^+F4/80^+Ly6C^{low}$ macrophages determined by flow cytometry in spleens of *B. abortus* infected mice (n=4) at 9 and 30 d.p.i. **(E)** Representative data plot of $Ly6C^{low}$ and $Ly6C^{high}$ populations in spleens of *B. abortus* infected mice at 9 and 30 d.p.i.. **(F)** Frequency of $CD3^-B220^-NK1.1^-Ly6G^-CD11b^+F4/80^+Ly6C^{low}CD301^+$ macrophages (AAM) measured by flow cytometry in spleens of *B. abortus* infected mice (n=4) at 9 and 30 d.p.i.. Values represent mean ± SEM. (*) Represents $P<0.05$ and (**) represents $P<0.01$ using one way ANOVA for (A-B) or unpaired t-test analysis for (C-E).

AAM support increased levels of intracellular B. abortus replication

To determine whether AAM could be a preferred niche for *B. abortus*, we quantified bacterial survival and replication in bone marrow-derived macrophages (BMDM) that were unstimulated, treated with interferon gamma (IFNγ) to produce CAM or treated with interleukin-4 (IL-4) to produce AAM (Fig. 15A). As expected, BMDM responded to IL-4 with increased expression of *Ym1*, *Fizz1* and *Il6*, while CAM expressed higher levels of *Il6* than AAM (data not shown). While the CAM eliminated intracellular *B. abortus* infection, both unstimulated BMDM and AAM were permissive for intracellular replication of *B. abortus* (Fig. 15A). Remarkably, *B. abortus* replicated to tenfold higher numbers in AAM than in untreated control BMDM, demonstrating an increased capacity of these cells to support intracellular infection (Fig. 15A).

To determine whether the AAM also serve as a preferential niche for *B. abortus* during chronic infection, we determined the intracellular localization of *B. abortus* by enrichment of $CD11b^+$ cells and flow cytometry (Fig. 15). During the acute infection, *B. abortus* was recovered from both the $CD11b^+$ and the $CD11b^-$ cell fraction, consistent with a previous report (Copin *et al.*, 2012b). However during chronic infection, *B. abortus* localized predominantly to the $CD11b^+$ fraction (Fig. 15B). Flow cytometric analysis of the $CD11b^+$ fraction revealed that that during acute infection *B. abortus* localized to CD11b+ dendritic cells, as well as to macrophages that were $Ly6C^{high}$ and $Ly6C^{low}$ (Fig. 15C and 15D). In contrast, during chronic infection, *B. abortus* colocalized with macrophages that were $Ly6C^{low}$. Since AAM are described to express low levels of Ly6C as well as the marker CD301, we further analyzed the $Ly6C^{low}$ population for expression of CD301 and found an approximately fivefold higher association of *B. abortus* with $Ly6C^{low}$ $CD301^+$ cells (AAM) than with $Ly6C^{low}$ $CD301^-$ cells (Fig. 15E). Together, these results demonstrated that *B. abortus* preferentially associated with AAM during chronic (but not acute) infection.

Since the results shown above suggested that AAM could be a niche for intracellular persistence of *B. abortus*, we tested whether mice with defects in generation of CAM (*Ifng*$^{-/-}$ mice) or AAM (*Stat6*$^{-/-}$ mice) would be altered in their ability to control *B. abortus* infection (Fig. 16). Consistent with findings of other groups, *Ifng*$^{-/-}$ mice were severely deficient in control of *B. abortus* infection during the acute phase, where bacterial numbers increased rapidly (Fig. 16A). This increased load of *B. abortus* correlated with an increase in the number of $Ly6C^{low}$ $CD301^+$ AAM (Fig. 16B and Fig. 16C). Compared to control (C57BL/6) mice, *Ifng*$^{-/-}$ mice expressed lower levels of the CAM markers *Il6* and *Nos2* and higher levels of the AAM marker *Ym1* in splenic macrophages during the acute infection phase (Fig. S6D). Moreover, immunohistochemical analysis confirmed increased levels of the AAM markers Ym1 and Fizz1 in spleens of *Ifng*$^{-/-}$ mice during acute infection (days 9 and 21) when compared to control mice (Fig. S6E, data not shown). These results suggested that IFNg-deficiency resulted in an increase in numbers of AAM during the acute phase of *B. abortus* infection. Thus one important role of IFNγ in controlling *B. abortus* during the acute phase of infection may be to direct the differentiation of CAM. The opposite effect was seen in *Stat6*$^{-/-}$ mice, which demonstrated an increased ability to control *B. abortus* persistence during the chronic infection phase (30 dpi; Fig 15D). Increased control of *B. abortus* in these mice correlated with decreased expression of AAM markers and increased CAM marker expression in splenic macrophages, suggesting that a decrease in AAM polarization in the *Stat6*$^{-/-}$ mice contributes to their increased resistance to *B. abortus* infection (Fig 15E).

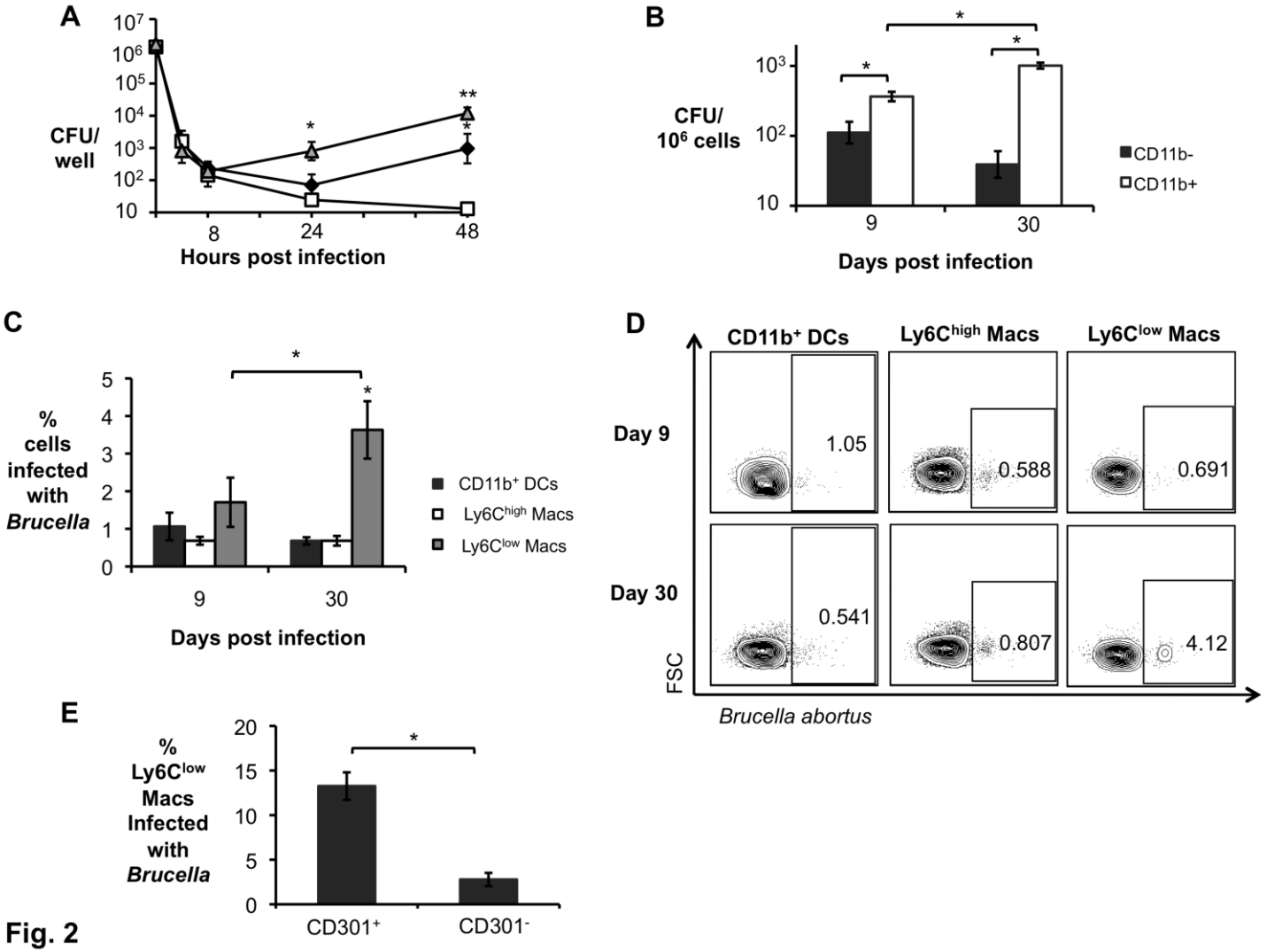
A
CFU/ well
Hours post infection
B
CFU/ 10^6 cells
CD11b-
CD11b+
Days post infection
C
% cells infected with Brucella
CD11b+ DCs
Ly6Chigh Macs
Ly6Clow Macs
Days post infection
D
CD11b+ DCs
Ly6Chigh Macs
Ly6Clow Macs
Day 9
Day 30
1.05
0.588
0.691
0.541
0.807
4.12
FSC
Brucella abortus
E
% Ly6Clow Macs Infected with Brucella
CD301+
CD301-

Fig. 2

Figure 15. Increased *B. abortus* survival in AAM during chronic infection. (A) *B. abortus* survival over time in C57BL/6J BMDM that were not treated (black diamond), or stimulated with 10ng/mL of rIFNγ (CAM, open square) and stimulated with 10ng/mL of rIL-4 (AAM, grey triangle). Data shown are compiled from four independent experiments. **(B)** *B. abortus* 2308 CFU counts in $CD11b^-$ and $CD11b^+$ splenocytes from C57BL/6J mice (n=5) at 9 and 30 days post infection (d.p.i.). **(C)** Frequency *of B. abortus* infected $CD11b^+$ dendritic cells (DCs, $F4/80^-Ly6G^-$ $CD11b^+CD11c^+$), $Ly6C^{high}$ macrophages ($CD11c^-Ly6G^-CD11b^+F4/80^+Ly6C^{high}$) and $Ly6C^{low}$ macrophages ($CD11c^-Ly6G^-CD11b^+F4/80^+Ly6C^{low}$) determined by flow cytometry in $CD11b^+$ splenocytes from infected C57BL/6J mice (n=5) at 9 and 30 d.p.i. **(D)** Representative data plot of populations shown in (C). **(E)** Frequency of *B. abortus* infected $CD301^+$ (AAM) and $CD301^-$ $Ly6C^{low}$ macrophages in $CD11b^+$ splenocytes determined by flow cytometry in $CD11b^+$ splenocytes from C57BL/6J infected mice (n=5) at 30 d.p.i. Values represent mean ± SEM. (*) Represents $P<0.05$ and (**) represents $P<0.01$ using one way ANOVA for (A) or unpaired t-test analysis for (B-C) and (E).

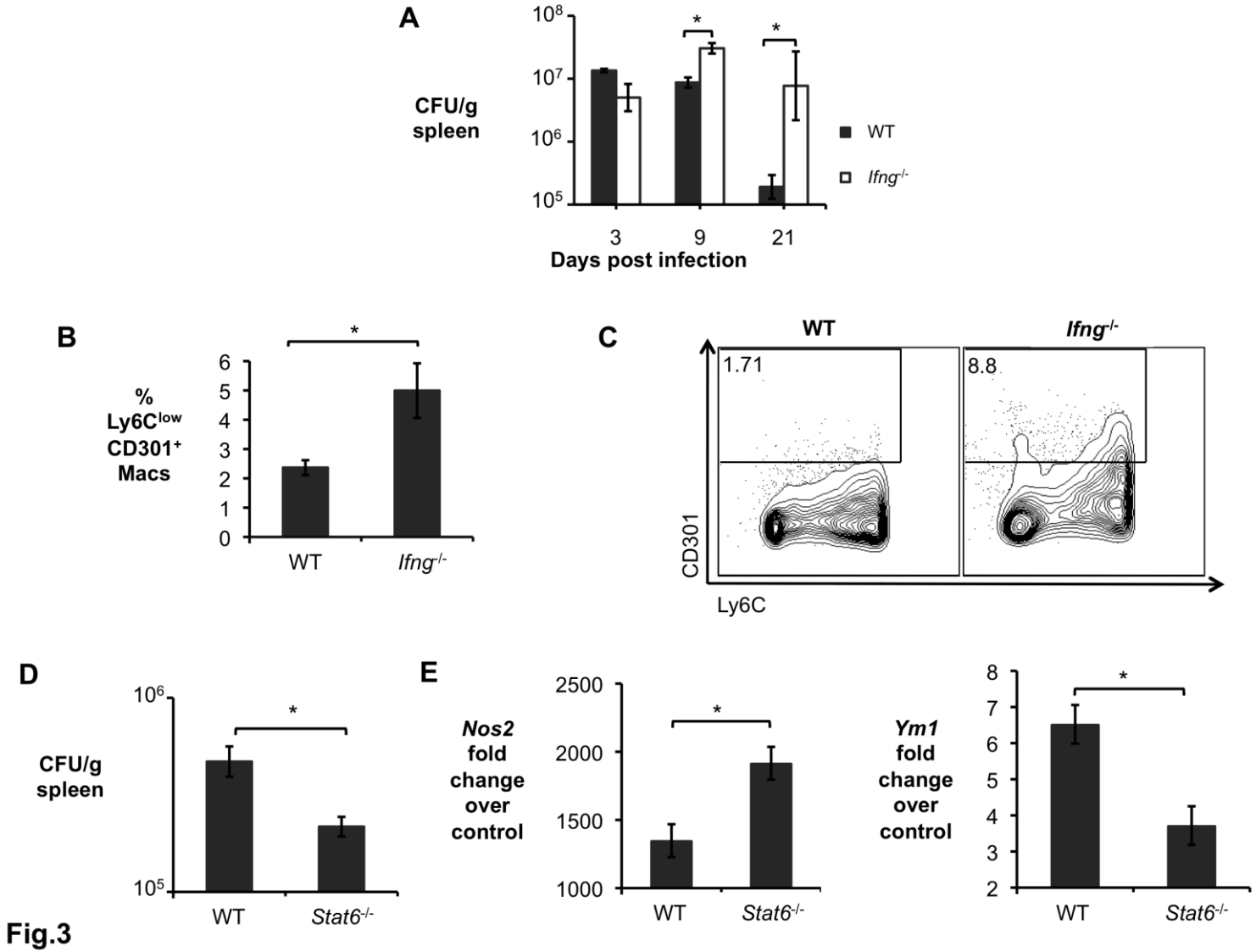
A
CFU/g spleen
10^8
10^7
10^6
10^5
*
*
WT
Ifng-/-
3
9
21
Days post infection
B
% Ly6C^low CD301^+ Macs
*
6
5
4
3
2
1
0
WT
Ifng-/-
C
WT
Ifng-/-
1.71
8.8
CD301
Ly6C
D
CFU/g spleen
10^6
10^5
*
WT
Stat6-/-
E
Nos2 fold change over control
2500
2000
1500
1000
*
WT
Stat6-/-
Ym1 fold change over control
8
7
6
5
4
3
2
*
WT
Stat6-/-

Fig.3

Figure 16. Defects in generation of CAM or AAM affect *B. abortus* survival *in vivo*. (A) *B. abortus* 2308 CFU counts in spleens from C57BL/6J and congenic *Ifng*$^{-/-}$ mice (n=5) at 3, 9, and 21, days post infection (d.p.i). **(B)** Frequency of CD3^{-}B220^{-}NK1.1^{-}Ly6G^{-}CD11b^{+}F4/80^{+}Ly6C^{low}CD301^{+} macrophages (AAM) measured by flow cytometry in spleens of *B. abortus* infected C57BL/6J and congenic *Ifng*$^{-/-}$ mice (n=5) at 9 d.p.i.. **(C)** Representative data plot of populations shown in (B). **(D)** *B. abortus* 2308 CFU counts in spleens of C57BL/6J and congenic *Stat6*$^{-/-}$ mice (n=5) at 30 d.p.i. **(E)** Real time RT-PCR gene expression analysis of CAM gene *Nos2* and AAM gene *Ym1* in CD11b^{+} splenocytes from *B. abortus* infected C57BL/6J and congenic *Stat6*$^{-/-}$ mice (n=5) at 30 d.p.i. Values represent mean ± SEM. (*) Represents P<0.05 using unpaired t-test statistical analysis.

PPARg promotes intracellular B. abortus replication in AAM

A pathway that is crucial to acquisition and maintenance of the AAM phenotype is mediated by peroxisome proliferator-activated receptors (PPARs), a family of nuclear receptors that regulates transcription of genes involved in cellular metabolism (Vats *et al.*, 2006; Odegaard *et al.*, 2007). Since our previous studies of *B. abortus* genes involved in persistent, but not acute infection, implicated metabolic genes in this process (Hong *et al.*, 2000), we tested the hypothesis that PPAR-mediated changes to macrophage metabolism could provide an environment for intracellular persistence of *B. abortus*. To determine whether any of the PPARs could be involved in this process, we analyzed transcripts of the PPARs in splenic $CD11b^+$ cells. Our results showed that transcription of *Pparg*, the gene encoding PPARg, was reduced during acute infection compared to uninfected controls, while during chronic infection (30-60 days), it was elevated (Fig. 17A). Moreover, *Ifng*$^{-/-}$ mice had increased *Pparg* expression in splenic macrophages during acute infection while the opposite was true for chronically infected *Stat6*$^{-/-}$ mice when compared to control animals (data not shown). In *B. abortus*-infected mice, blocking of PPARγ activity by treating the mice with the inhibitor GW9662 specifically prior to chronic infection (days 18 until 30) led to a significant decrease in splenic colonization at 30 days after infection, suggesting that pathways downstream of PPARγ contribute to generating a niche for persistence of *B. abortus* (Fig. 17B). Concomitantly, PPARγ inhibition led to a reduction in the proportion of $Ly6C^{low}$ $CD301^+$ AAM in the spleen at 30 dpi (Fig. 17C), as well as to decreased expression of the AAM marker Ym1 and to increased expression levels of CAM gene *Nos2* and in splenic $CD11b^+$ cells (Fig. S7A). These results suggested that inhibition of PPARY reduced *B. abortus* survival by reducing the abundance of AAM during chronic infection (Fig. 17C). Conversely, treatment of *B. abortus*-infected mice with the PPARγ agonist Rosiglitazone led to a small (twofold) increase in *B. abortus* colonization during the acute (9d) phase and a ~4 fold increase during the chronic (30d) infection phase (Fig. 17D). During the acute infection phase, Rosiglitazone treatment led to an increased percentage of $Ly6C^{low}CD301^+$ macrophages (Fig. 17E), as well as a shift toward expression of AAM markers and a reduction in the CAM marker *Nos2* (Fig. S7B), suggesting that the increase in *B. abortus* infection in Rosiglitazone-treated mice resulted from a relative increase in AAM during the acute phase of infection. Since systemic modulation of PPARγ activity could have effects on cells other than macrophages, we repeated these treatments on *in vitro* polarized AAM. Similar to what we observed *in vivo*, *Pparg* was strongly induced in AAM differentiated *in vitro* (Fig. 17F). Inhibition of PPARγ activity in AAM with GW9662 resulted in a decreased ability to support intracellular replication of *B. abortus*, while activation of PPARγ led to an additional increase in *B. abortus* replication (Fig 17G). Moreover, fluorescence microscopy analysis confirmed that increased *B. abortus* CFU counts in AAM and PPARγ stimulated macrophages were due to increased bacterial numbers within each cell, rather than a higher number of infected cells (Fig S7C). Together, these results suggest that PPARγ-dependent modulation of macrophage physiology promotes intracellular persistence of *B. abortus*.

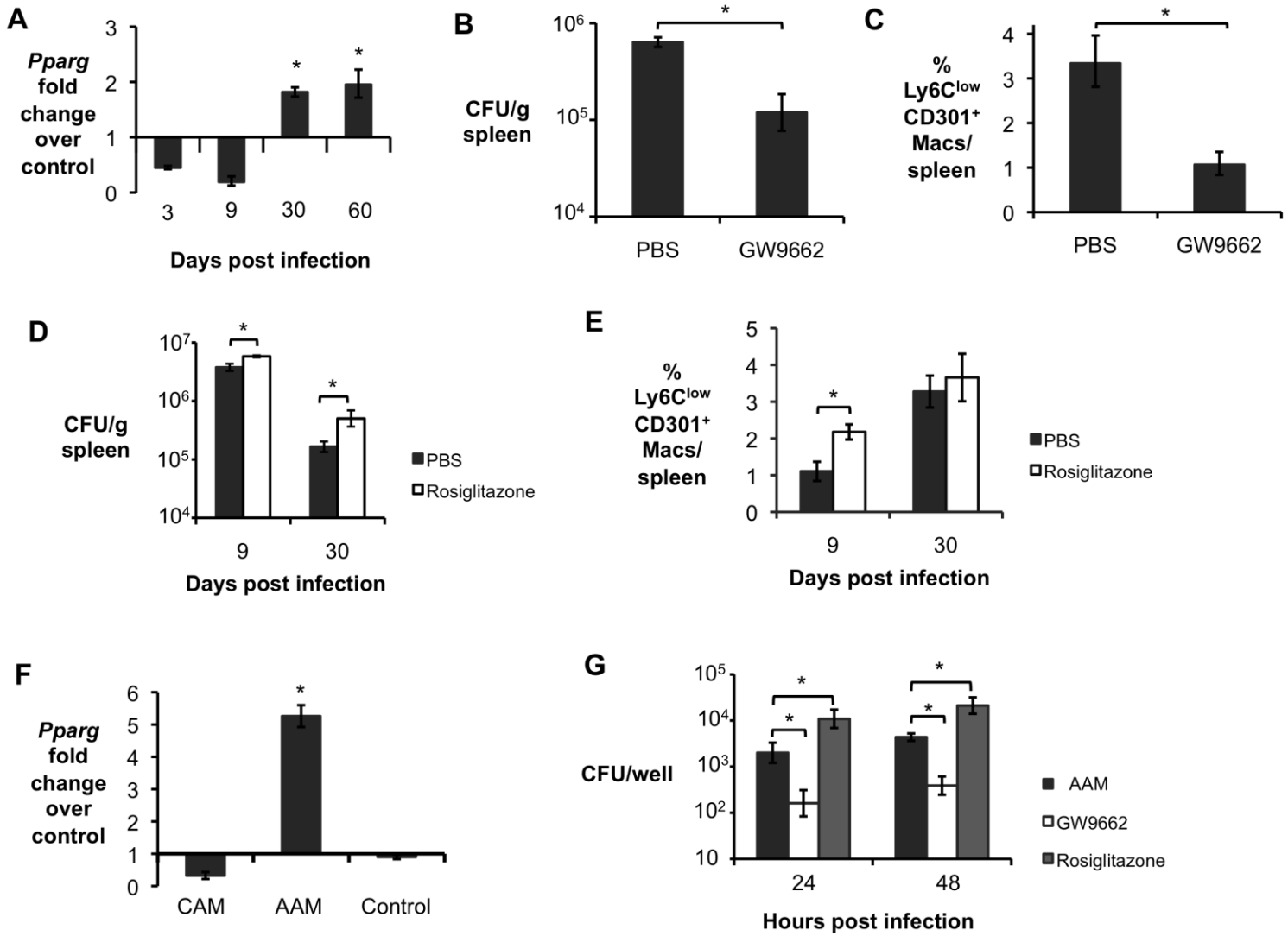
A
Pparg fold change over control
Days post infection
B
CFU/g spleen
PBS
GW9662
C
% Ly6C^low CD301^+ Macs/ spleen
PBS
GW9662
D
CFU/g spleen
PBS
Rosiglitazone
Days post infection
E
% Ly6C^low CD301^+ Macs/ spleen
PBS
Rosiglitazone
Days post infection
F
Pparg fold change over control
CAM
AAM
Control
G
CFU/well
AAM
GW9662
Rosiglitazone
Hours post infection

Fig.4

Figure 17. Increased survival of *B. abortus* during chronic infection is dependent on PPARγ. (A) Real time RT-PCR gene expression analysis of *Pparg* in $CD11b^+$ splenocytes from *B. abortus*-infected C57BL/6J mice (n=5) at 3, 9, 30 and 60 dpi. **(B)** *B. abortus* 2308 CFU counts, measured at 30 d.p.i., in spleens from C57BL/6J mice (n=5) treated daily from 18 to 30 d.p.i. with PPARγ antagonist GW9662 or PBS control. **(C)** Frequency of $CD3^-B220^-NK1.1^-Ly6G^-CD11b^+F4/80^+Ly6C^{low}CD301^+$ macrophages (AAM) measured by flow cytometry at 30 d.p.i. in spleens of C57BL/6J mice (n=5) treated daily from 18 to 30 d.p.i. with PPARγ antagonist GW9662 or PBS control. **(D)** *B. abortus* 2308 CFU counts, measured at 9 and 30 d.p.i., in spleens from C57BL/6J mice (n=5) treated daily for 7 days prior to infection with PPARγ agonist Rosiglitazone or PBS control. **(E)** Frequency of $CD3^-B220^-NK1.1^-Ly6G^-CD11b^+F4/80^+Ly6C^{low}CD301^+$ macrophages (AAM) measured by flow cytometry at 9 and 30 d.p.i. in spleens from C57BL/6J mice (n=5) treated daily for 7 days prior to infection with PPARγ agonist Rosiglitazone or PBS control. **(F)** Real time RT-PCR gene expression analysis of *Pparg* in BMDM from C57BL/6J mice stimulated with rIFN-γ (CAM), rIL-4 (AAM), or non-stimulated (Control) and infected with *B. abortus* for 24h. Data shown are compiled from four independent experiments. **(G)** *B. abortus* 2308 CFU counts in BMDM from C57BL/6J mice, stimulated with rIL-4 (AAM) or with IL-4 + 3μM of PPARγ antagonist GW9662 (GW9662) or with 5μM of PPARγ agonist Rosiglitazone and infected with *B. abortus* for 24 and 48h. Data shown in (F) and (G) are compiled from four independent experiments. Values represent mean ± SEM. (*) Represents $P<0.05$ using one way ANOVA for (A) and (F) or unpaired t-test analysis for (B-E) and (G).

PPARg increases the availability of intracellular glucose in AAM

One of the metabolic changes mediated by PPARγ is a shift from oxidative metabolism of glucose to b-oxidation of fatty acids. Further, PPARγ agonists are used therapeutically to lower blood glucose by increasing cellular glucose uptake (Yki-Järvinen, 2004). Since *B. abortus* is able to utilize glucose for growth (Mccullough and Beal, 1951) we tested the possibility that increased intracellular glucose availability could promote intracellular replication of *B. abortus* in AAM.

We first investigated whether *B. abortus* infection altered the phenotype of macrophages cultured *in vitro*. Infection of non-polarized macrophages with *B. abortus* or the closely related *B. melitensis* led to moderately increased abundance of glycolytic pathway enzymes (Fig. S8A), as well as an increase in expression of the CAM markers *Hifa*, *Pfkfb3* and *Glut1* (Fig. S8B). In contrast, *B. abortus* infection decreased expression of *Pgc1b*, encoding a transcriptional activator and *Acadm* and *Acadl*, encoding enzymes involved in mitochondrial β-oxidation (Fig. S8C). The induction of the glycolytic pathway in *B. abortus*-infected macrophages was confirmed by detection of increased concentrations of extracellular lactate, an end-product of glycolysis (Fig. S8D). The relative induction of the macrophage glycolytic pathway by *B. abortus* was dependent on the macrophage phenotype: infection of CAM (induced by IFNγ) or AAM (induced by IL-4) treated with the PPARγ antagonist GW9662 shifted the metabolism more strongly toward glycolysis and led to a marked reduction in b-oxidation genes expression (Figs. 18A-18C). In contrast, compared to control (untreated) macrophages, the shift toward glycolysis induced by *B. abortus* infection was attenuated in AAM or in cells treated with Rosiglitazone (Figs. 18A -18C). Taken together, these data suggested that while *B. abortus* infection does not induce AAM polarization, infection of AAM results in lower induction of the glycolytic pathway in the infected macrophages.

Compared to untreated control bone marrow-derived macrophages, AAM induced *in vitro* by IL-4 treatment had significantly elevated glucose content, which was lowered to the level of control macrophages by infection with *B. abortus*, raising the possibility that the pathogen may consume this carbon source (Fig. 18D). Increased intracellular glucose in AAM was recapitulated by treatment with Rosiglitazone, and was negated by treatment of AAM with GW9662, suggesting that increased intracellular glucose in AAM is dependent on PPARγ mediated transcriptional changes (Fig. 18D). Interestingly, our previous work identified a glucose transporter of the major facilitator superfamily, GluP, as a *B. abortus* factor required for chronic, but not acute, infection (Essenberg *et al*., 1997; Hong *et al*., 2000).

To directly test the idea that glucose availability could promote intracellular replication of *B. abortus* in AAM, we compared replication of wild type *B. abortus* and the *gluP* mutant. *In vitro*, the *gluP* mutant grew similarly to wild type *B. abortus* in medium (Tryptone/Soytone) lacking glucose, while addition of glucose enhanced replication of wild type *B. abortus*, but not of the *gluP* mutant (Fig. S9A). Enhanced growth in glucose-containing medium was restored by complementation of the *gluP* mutation (Fig. S9A). Remarkably, while there was no difference in the ability of the two *B. abortus* strains to survive in untreated control macrophages, wild type *B. abortus* was recovered in tenfold greater numbers than the *gluP* mutant from AAM (Fig. 19A). Treatment of unpolarized BMDM with Rosiglitazone increased the intracellular replication of wild type *B. abortus*, but had no effect on intracellular replication of the *gluP* mutant, consistent with an inability to utilize increased glucose within the macrophage (Fig. 19B). The growth advantage of wild type *B. abortus* over the *gluP* mutant was eliminated by treatment of AAM with GW9662 (Fig. 19B).

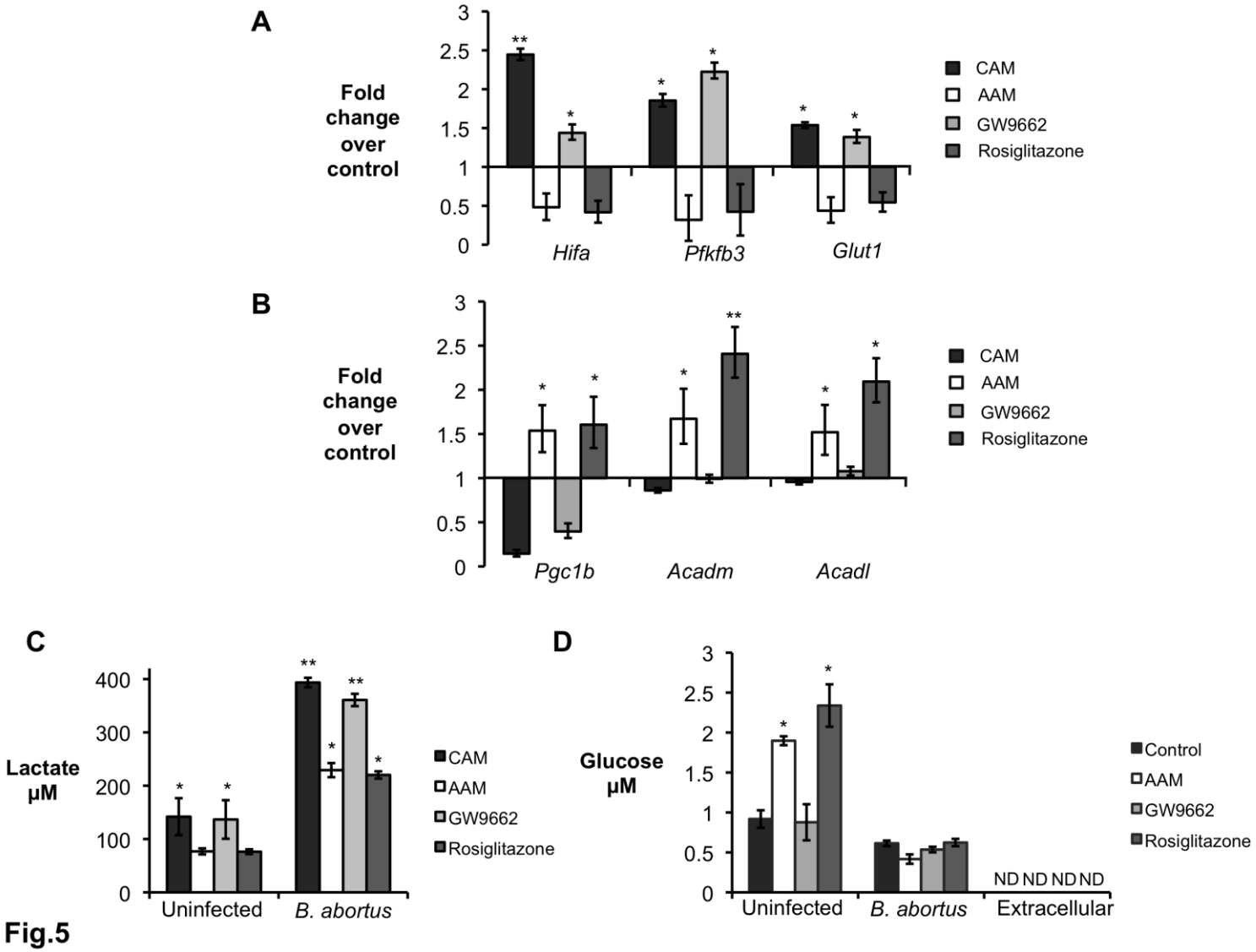
A
Fold change over control
3
2.5
2
1.5
1
0.5
0
Hifa
Pfkfb3
Glut1
CAM
AAM
GW9662
Rosiglitazone
B
Fold change over control
Pgc1b
Acadm
Acadl
CAM
AAM
GW9662
Rosiglitazone
C
Lactate µM
400
300
200
100
0
Uninfected
B. abortus
CAM
AAM
GW9662
Rosiglitazone
D
Glucose µM
Uninfected
B. abortus
Extracellular
ND ND ND ND
Control
AAM
GW9662
Rosiglitazone

Fig.5

Figure 18. *B. abortus* infected AAM exhibit a PPARγ-dependent decrease in glycolytic metabolism. (A) Real time RT-PCR gene expression analysis of glycolytic pathway genes *Hifa* (hypoxia inducible factor α), *Pfkfb3* (phosphofructokinase-3) and *Glut1* (glucose transporter 1) in C57BL/6J BMDM stimulated with rIFNγ (CAM), with rIL-4 (AAM), with IL-4 + GW9662 (GW9662) or with Rosiglitazone and infected with *B. abortus* for 8 hours. Results are expressed as fold change over untreated macrophages infected with *B. abortus*. **(B)** Real time RT-PCR gene expression analysis of fatty acid β-oxidation pathway genes *Pgc1b* (PPARγ coactivator 1 β), *Acadm* (medium-chain acyl-CoA dehydrogenase) and *Acadl* (long-chain acyl-CoA dehydrogenase) in BMDM from C57BL/6J stimulated rIFNγ (CAM), with rIL-4 (AAM), with IL-4 + GW9662 (GW9662) or with Rosiglitazone and infected with *B. abortus* for 8 hours. Results are expressed as fold change over untreated macrophages infected with *B. abortus*. **(C)** Measurement of lactate concentration in supernatant from BMDM from C57BL/6J stimulated with rIFNγ (CAM), with rIL-4 (AAM) or IL-4 + GW9662 (GW9662) or with Rosiglitazone and uninfected or infected with *B. abortus* for 24 hours. **(D)** Measurement of intracellular glucose concentration in BMDM from C57BL/6J unstimulated (control) and stimulated with rIL-4 (AAM), with IL-4 + GW9662 (GW9662), or with Rosiglitazone and uninfected or infected with *B. abortus* for 24 hours. Values represent mean ± SEM and represent combined results of four independent experiments conducted in duplicate. (*) Represents $P<0.05$ and (**) represents $P<0.01$ using one way ANOVA.

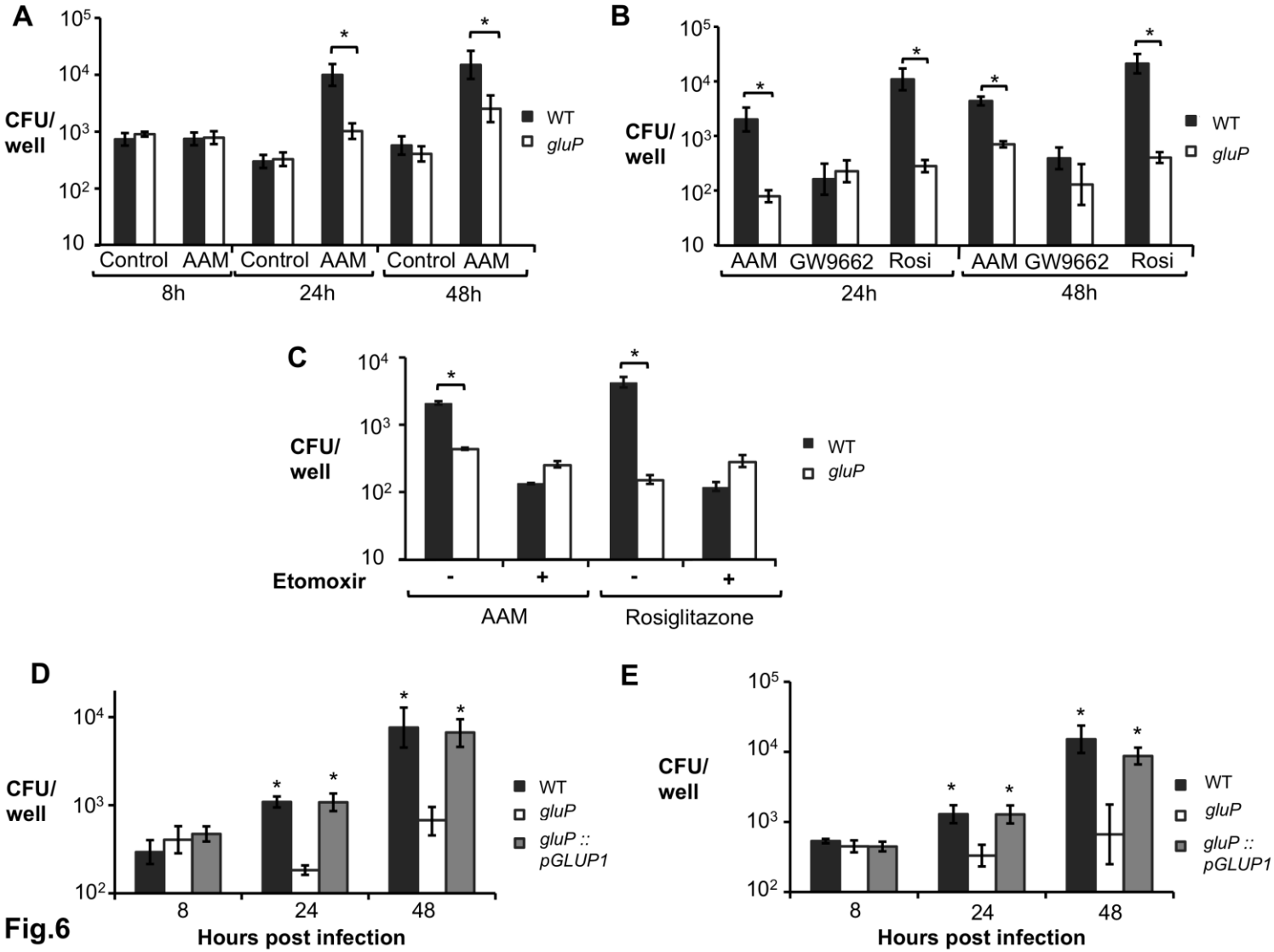
A
CFU/ well
Control AAM Control AAM Control AAM
8h 24h 48h
WT
gluP
B
CFU/ well
AAM GW9662 Rosi AAM GW9662 Rosi
24h 48h
WT
gluP
C
CFU/ well
Etomoxir
- + - +
AAM Rosiglitazone
WT
gluP
D
CFU/ well
8 24 48
Hours post infection
WT
gluP
gluP :: pGLUP1
E
CFU/ well
8 24 48
Hours post infection
WT
gluP
gluP :: pGLUP1

Fig.6

Figure 19. A PPARγ-dependent increase in intracellular glucose availability promotes survival of *B. abortus* in macrophages. (A) Recovery of *B. abortus* from C57BL/6J BMDM that were sham-treated (Control) or treated with rIL-4 (AAM). BMDM were infected with *B. abortus* 2308 WT or isogenic *gluP* mutant for 8, 24 and 48h. **(B)** Recovery of *B. abortus* from C57BL/6J BMDM stimulated with rIL-4 (AAM), with IL-4 + GW9662 (GW9662) or with Rosiglitazone (Rosi) and infected with *B. abortus* 2308 (WT) or isogenic *gluP* mutant for 24 and 48h. **(C)** Recovery of *B. abortus* from BMDM from C57BL/6J treated or not with the β-oxidation inhibitor etomoxir (50 µM) in the presence of rIL-4 (AAM) or Rosiglitazone and infected with *B. abortus* 2308 WT or isogenic *gluP* mutant for 48h. **(D)** Recovery of *B. abortus* from BMDM from C57BL/6J stimulated rIL-4 (AAM) and infected with *B. abortus* 2308 WT or isogenic *gluP* mutant or complemented *gluP* mutant (*gluP*::pGLUP1) for 8, 24 and 48h. **(E)** Recovery of *B. abortus* from BMDM from C57BL/6J stimulated with Rosiglitazone and infected with *B. abortus* 2308 WT or isogenic *gluP* mutant or complemented *gluP* mutant (*gluP*::pGLUP1) for 8, 24 and 48h. Values represent mean ± SEM of data from four independent experiments conducted in duplicate. (*) Represents $P<0.05$ using unpaired t-test for (A-C) or one way ANOVA statistical analysis for (D-E).

The growth advantage of wild type *B. abortus* over the *gluP* mutant was eliminated by treatment of AAM with GW9662 (Fig. 19B). Inhibition of mitochondrial β-oxidation in AAM or Rosiglitazone-treated cells, using the carnitine palmitoyltransferase inhibitor etomoxir, also reduced the ability of *B. abortus* to replicate intracellularly, but had no effect on the *gluP* mutant (Fig. 19C and Fig. S9B). The growth defect of the *gluP* mutant within AAM or Rosiglitazone-treated macrophages was restored by complementation (Fig 19D and 19E), demonstrating that the ability to transport glucose is essential for increased growth in these macrophages. To control for possible off-target effects of the inhibitors on *B. abortus*, we examined replication of wild type and the *gluP* mutant in macrophages from conditionally PPARγ-deficient mice, in which only macrophages lack PPARγ (Figs. S9C and S9D). Similarly to what was observed with the PPARγ inhibitor-treated AAM (Fig. 19B), GluP-dependent replication of *B. abortus* within either IL-4 or Rosiglitazone-treated macrophages was dependent on the function of PPARγ (Figs. S9C and S9D). These results provide evidence that the increased replication of *B. abortus* in AAM is dependent on its ability to utilize the elevated intracellular pool of glucose that is induced by PPARγ.

Persistent infection by B. abortus depends on the ability to transport glucose

The results presented above raised the question, whether the PPARγ-dependent increase in glucose concentration that we observed in cultured macrophages could also promote *B. abortus* infection *in vivo*. To investigate this, we determined the requirement for GluP during acute and chronic infection (Fig. 20A), using a competitive infection assay. During acute infection (9 days) the ratio of wild type *B. abortus* to the *gluP* mutant was not significantly different from the 1:1 ratio in the inoculum (Fig. 20A). However during chronic infection, the *gluP* mutant was outcompeted 20-fold by the wild type. To determine whether this competitive defect was the result of PPARγ activation, we repeated the experiment in mice treated with the PPARγ antagonist GW9662 (Fig. 20B). Inhibition of PPARγ during the chronic infection stage strongly reduced the competitive defect of the *gluP* mutant at 30 dpi. Since the survival defect of the *gluP* mutant was observed only during chronic infection, when PPARγ expression was increased, we next asked whether activation of PPARγ during acute infection would affect the survival of the *gluP* mutant (Fig. 20C). Treatment of mice during acute infection with Rosiglitazone increased the ability of the wild type *B. abortus* to outcompete the gluP mutant at 9d by approximately four-fold, resembling the phenotype only previously seen at later stages of infection (30d). Finally, to control for off-target effects of the inhibitors, we repeated the competitive infection in mice conditionally deficient for *Pparg* expression in macrophages (*Pparg*$^{flox/flox}$ LysM$^{cre/-}$; (Odegaard *et al.*, 2007)). The growth advantage of wild type *B. abortus* over the *gluP* mutant was strongly reduced in the conditionally *Pparg*-deficient mice (Fig. 20D), demonstrating that expression of PPARγ specifically in macrophages is required for *B. abortus* to benefit from acquisition of glucose in AAM during chronic infection. Taken together, these results demonstrate that, *in vivo*, the ability of *B. abortus* to benefit from PPARg-mediated changes in host macrophage metabolism is dependent on the ability of *B. abortus* to take up glucose.

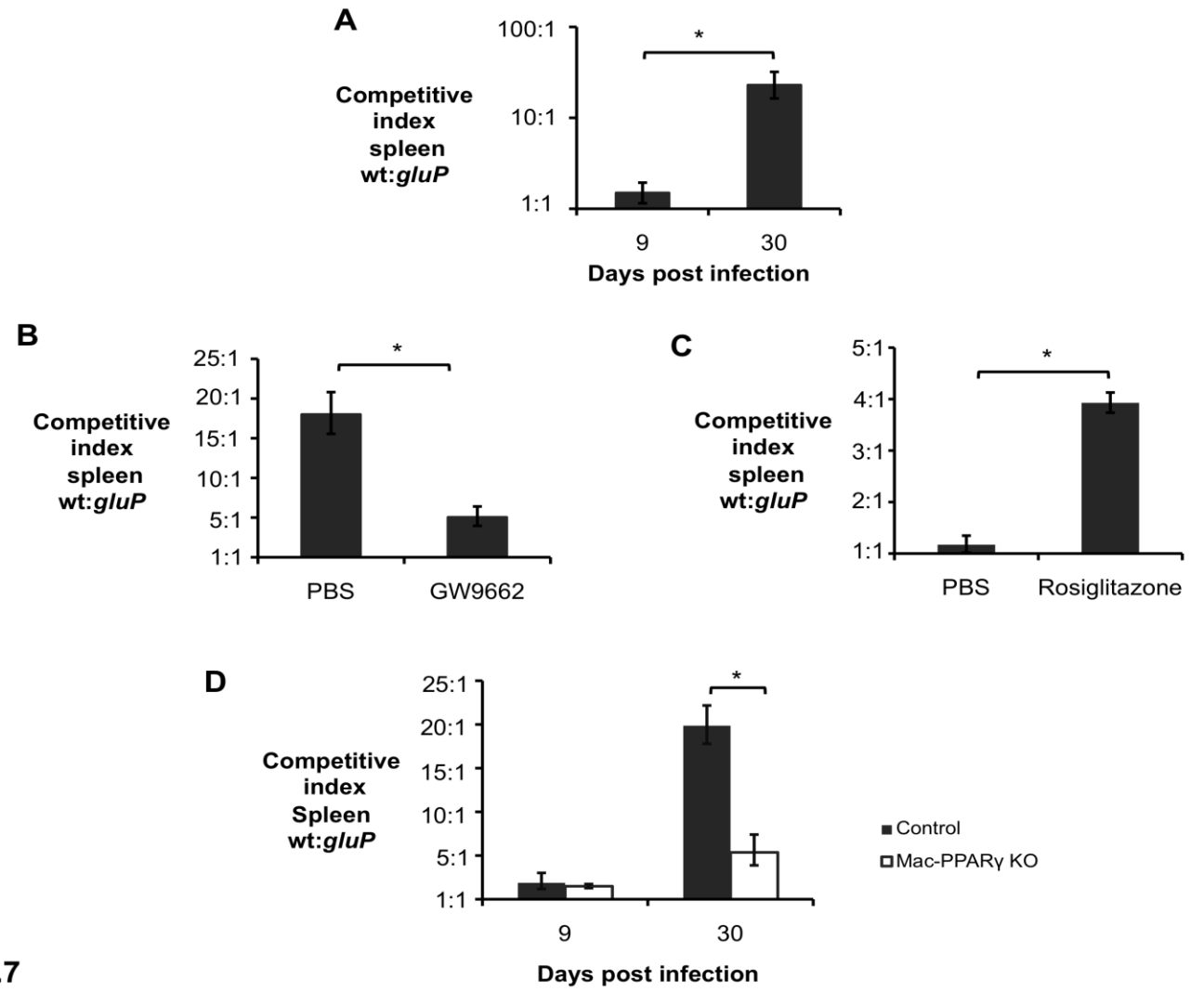
A
Competitive index spleen wt:gluP
100:1
10:1
1:1
*
9
30
Days post infection
B
Competitive index spleen wt:gluP
25:1
20:1
15:1
10:1
5:1
1:1
*
PBS
GW9662
C
Competitive index spleen wt:gluP
5:1
4:1
3:1
2:1
1:1
*
PBS
Rosiglitazone
D
Competitive index Spleen wt:gluP
25:1
20:1
15:1
10:1
5:1
1:1
*
9
30
Days post infection
Control
Mac-PPARγ KO

Fig.7

Figure 20. A PPARγ-dependent increase in intracellular glucose availability in macrophages promotes *B. abortus* persistence *in vivo*. (A) Competitive index (ratio of WT to *gluP* mutant) in spleens of C57BL/6J mice (n=5) infected with a 1:1 mixture of *B. abortus* 2308 WT and isogenic *gluP* mutant for 9 and 30 days. **(B)** Competitive index, measured at 30 days post infection (d.p.i.), in spleens from C57BL/6J mice (n=5) treated daily from 18 to 30 d.p.i. with PPARγ antagonist GW9662 or PBS control and infected with a 1:1 mixture of *B. abortus* 2308 WT and isogenic *gluP* mutant. **(C)** Competitive index, measured at 9 and 30 d.p.i., in spleens from C57BL/6J mice (n=5) treated daily for 7 days prior to infection with PPARγ agonist Rosiglitazone or PBS control and infected with a 1:1 mixture of *B. abortus* 2308 WT and isogenic *gluP* mutant. **(D)** Competitive index, measured at 9 and 30 d.p.i., in spleens from $Pparg^{fl/fl}LysM^{cre/-}$ (Mac-PPARγ KO) or littermates $Pparg^{fl/fl}LysM^{-/-}$ (Control) mice (n=5) infected with a 1:1 mixture of *B. abortus* 2308 WT and isogenic *gluP* mutant. Values represent mean ± SEM. (*) Represents $P<0.05$ using unpaired t-test statistical analysis.

Discussion

Recent studies have shed light on the extensive interactions between immune and metabolic functions of macrophages. For the case of CAM, oxygen is required as a substrate for NADPH oxidase, and therefore these cells meet their energetic needs via anaerobic glycolysis. Since anaerobic glucose utilization is a relatively inefficient way to generate ATP (only 2 ATP/molecule of glucose), a large amount of glucose must be utilized, and the relative intracellular concentration of free glucose is low. In contrast, in AAM, this metabolic program is antagonized by STAT6-dependent induction of PPARγ and PPARδ (Szanto *et al.*, 2010). As a result, AAM shift to aerobic metabolism, in which they gain energy by β-oxidation of fatty acids (Bensinger and Tontonoz, 2008; O'neill and Hardie, 2013). Our results demonstrate that this metabolic shift leads to an increase in intracellular glucose, which becomes available to support growth of intracellular bacteria (Fig. 18). An exhaustive screen of *B. suis* genes required for intracellular infection in human THP-1 cells identified sugar metabolism genes as being required for intracellular infection, and suggested that the replicative niche for *Brucella* within the cell is poor in nutrients (Kohler *et al.*, 2002). Further, at late stages during cellular infection, the bacterial glycolysis pathway was downregulated, which led to the proposition that *Brucella* may use fatty acids or amino acids rather than sugars during this growth phase (Al Dahouk *et al.*, 2008; Barbier *et al.*, 2011). However, the increased growth rate of *B. abortus* within AAM *in vitro* compared to unpolarized or CAM-polarized macrophage populations used for previous studies suggests that AAM may provide additional nutrients, such as glucose, that are less abundant in other macrophage populations.

Like *B. abortus*, other bacteria have been shown to induce PPARγ expression, such as *Mycobacterium tuberculosis* (Mahajan *et al.*, 2012) and *Listeria monocytogenes* (Abdullah *et al.*, 2012). Interestingly, a lack of PPARγ expression in macrophages was shown to render mice more resistant to *L. monocytogenes* infection (Abdullah *et al.*, 2012). While the underlying mechanism in this study was not identified, our work shows for the first time that antagonizing PPARγ activity during *B. abortus* infection helps control the pathogen burden by reducing intracellular glucose availability. Importantly, these observations raise the possibility that PPARγ-induced increases in intracellular glucose availability may be a general mechanism promoting growth of intracellular bacteria.

It should be noted that unlike *Francisella tularensis*, which induces differentiation of AAM to promote its replication (Shirey *et al.*, 2008), *B. abortus* does not directly induce this pathway, since cultivation of *B. abortus* with BMDM *in vitro* did not induce expression of AAM markers (Fig. S8). Rather, as a result of its inherently low TLR4-stimulatory activity for macrophages and dendritic cells (reviewed by (Martirosyan *et al.*, 2011), *B. abortus* induces only a weak and transient Th1 response during the acute infection phase, which is characterized by an influx of inflammatory macrophages (Fig. 14, Fig. S6A) and (Copin *et al.*, 2012). It is likely that this transient IFNγ response is unable to sustain the CAM polarization of these cells, and perhaps together with the constant IL-4 levels throughout infection (Fig. S6B) as well as induction of IL-13 (Fig. S6C) and PPARγ during chronic infection by *B. abortus*, macrophages that have already entered the site of infection may become polarized to the AAM phenotype. Such a scenario would be consistent with our finding of similar increases in macrophage numbers during both acute and chronic infection, but a relative increase in AAM only during the chronic infection phase. These findings in the mouse model are

consistent with reports of transient IFNγ responses and an increase in IL-13 producing T cells in human patients with chronic brucellosis (Rafiei *et al.*, 2006).

Our results fit with previous reports suggesting that during chronic infection, persistent pathogens undergo a shift in their metabolism. For example, it has long been known that *M. tuberculosis* utilizes the glyoxylate shunt during intracellular infection (Wayne and Lin, 1982), and characterization of isocitrate lyase, an enzyme of this pathway needed for the chronic, but not the acute phase of infection (Mckinney *et al.*, 2000), identified this enzyme as a potential therapeutic target. Like tuberculosis, brucellosis is a chronic infection causing significant morbidity that requires protracted treatment with multiple antibiotics. Treatment failures and relapses are common for brucellosis, therefore identification of PPARγ, a well-characterized drug target, as a host factor providing a metabolic advantage to *B. abortus* during chronic infection suggests inhibitors of PPARγ as a potential adjunct to antibiotic therapy for the prevention of relapsing chronic infection.

CONCLUSION

Taken together, our data suggests that the balance between inflammatory and anti-inflammatory cytokines is crutial for the control of Brucellosis. While lack of IL-10 resulted in increased ability to control *B. abortus* infection at both acute and chronic stages of infection, it also resulted in evident signs of acute disease. Therefore, although modulation of the IL-10 signaling pathway could be a potential target to avoid the establishment of chronic infection, more studies are needed to elucidate the optimal activation of the immune system necessary to improve clearance of chronic pathogens without a great cost to the host.

Morevoer, this study demonstrated that another survival strategy of *B. abortus* is to replicate preferentially in alternatively activated macrophages (AAM), which increase in numbers during chronic infection. The underlying mechanism to this enhanced survival in AAM was a shift in metabolism induced by peroxisome proliferator activated receptor gamma (PPARγ), which increased the availability of intracellular glucose. Interestingly, brucellosis is a chronic infection causing significant morbidity that requires protracted treatment with multiple antibiotics. Therefore identification of PPARγ, a well-characterized drug target, as a host factor providing a metabolic advantage to *B. abortus* during chronic infection suggests inhibitors of PPARγ as a potential adjunct to antibiotic therapy for the prevention of relapsing chronic infection.

REFERENCES

ABDULLAH, Z.; GEIGER, S.; NINO-CASTRO, A. et al. Lack of PPARgamma in myeloid cells confers resistance to *Listeria monocytogenes* infection. **PLoS ONE,** v. 7, n. 5, p. e37349, 2012. ISSN 1932-6203. Disponível em: < http://dx.doi.org/10.1371%2Fjournal.pone.0037349 >

AL DAHOUK, S.; JUBIER-MAURIN, V.; SCHOLZ, H. C. et al. Quantitative analysis of the intramacrophagic *Brucella suis* proteome reveals metabolic adaptation to late stage of cellular infection. **Proteomics,** v. 8, n. 18, p. 3862-70, Sep 2008. ISSN 1615-9861 (Electronic) 1615-9853 (Linking). Disponível em: < http://www.ncbi.nlm.nih.gov/pubmed/18704908 >.

ALTON, G. G.; JONES, L. M.; PIETZ, D. E. **Laboratory Techniques in Brucellosis 2nd ed**. Geneva: World Health Organization, 1975.

ANDERSEN-NISSEN, E.; SMITH, K. D.; STROBE, K. L. et al. Evasion of Toll-like receptor 5 by flagellated bacteria. **Proc Natl Acad Sci U S A,** v. 102, n. 26, p. 9247-52, Jun 28 2005. Disponível em: < http://www.ncbi.nlm.nih.gov/entrez/query.fcgi?cmd=Retrieve&db=PubMed&dopt=Citation&list_uids=15956202 >.

ANDERSON, C. F.; OUKKA, M.; KUCHROO, V. J. et al. CD4(+)CD25(-)Foxp3(-) Th1 cells are the source of IL-10-mediated immune suppression in chronic cutaneous leishmaniasis. **The Journal of Experimental Medicine,** v. 204, n. 2, p. 285-297, February 19, 2007 2007. Disponível em: < http://jem.rupress.org/content/204/2/285.abstract >.

ANDERSON, T. D.; CHEVILLE, N. F. Ultrastructural morphometric analysis of *Brucella abortus*-infected trophoblasts in experimental placentitis. Bacterial replication occurs in rough endoplasmic reticulum. **Am J Pathol,** v. 124, n. 2, p. 226-37., 1986. Disponível em: < http://www.ncbi.nlm.nih.gov/htbin-post/Entrez/query?db=m&form=6&dopt=r&uid=3090887 >.

ARAYA, L. N.; ELZER, P. H.; ROWE, G. E. et al. Temporal development of protective cell-mediated and humoral immunity in BALB/c mice infected with *Brucella abortus*. **J Immunol,** v. 143, n. 10, p. 3330-7, Nov 15 1989. ISSN 0022-1767 (Print)
0022-1767 (Linking).

ATLURI, V. L.; XAVIER, M. N.; DE JONG, M. F. et al. Interactions of the Human Pathogenic *Brucella* Species with Their Hosts. **Annual Review of Microbiology,** v. 65, n. 1, p. 523-541, 2011. Disponível em: < http://www.annualreviews.org/doi/abs/10.1146/annurev-micro-090110-102905 >.

BARBIER, T.; NICOLAS, C.; LETESSON, J. J. *Brucella* adaptation and survival at the crossroad of metabolism and virulence. **FEBS Lett,** v. 585, n. 19, p. 2929-34, Oct 3 2011. ISSN 1873-3468 (Electronic)
0014-5793 (Linking). Disponível em: < http://www.ncbi.nlm.nih.gov/pubmed/21864534 >.

BARQUERO-CALVO, E.; CHAVES-OLARTE, E.; WEISS, D. S. et al. *Brucella abortus* uses a stealthy strategy to avoid activation of the innate immune system during the onset of infection. **PLoS ONE,** v. 2, n. 7, p. e631, 2007. Disponível em: < http://www.ncbi.nlm.nih.gov/entrez/query.fcgi?cmd=Retrieve&db=PubMed&dopt=Citation&list_uids=17637846 >.

BARQUERO-CALVO, E.; MARTIROSYAN, A.; ORDOÑEZ-RUEDA, D. et al. Neutrophils Exert a

Suppressive Effect on Th1 Responses to Intracellular Pathogen *Brucella abortus*. **PLoS Pathog,** v. 9, n. 2, p. e1003167, 2013. Disponível em: < http://dx.doi.org/10.1371%2Fjournal.ppat.1003167 >.

BELKAID, Y.; HOFFMANN, K. F.; MENDEZ, S. et al. The role of interleukin (IL)-10 in the persistence of *Leishmania major* in the skin after healing and the therapeutic potential of anti-IL-10 receptor antibody for sterile cure. **J Exp Med,** v. 194, n. 10, p. 1497-506, Nov 19 2001. ISSN 0022-1007 (Print)
0022-1007 (Linking). Disponível em: < http://www.ncbi.nlm.nih.gov/pubmed/11714756 >.

BENOIT, M.; DESNUES, B.; MEGE, J. L. Macrophage polarization in bacterial infections. **J Immunol,** v. 181, n. 6, p. 3733-9, Sep 15 2008. ISSN 1550-6606 (Electronic) 0022-1767 (Linking).

BENSINGER, S. J.; TONTONOZ, P. Integration of metabolism and inflammation by lipid-activated nuclear receptors. **Nature,** v. 454, n. 7203, p. 470-477, 2008. ISSN 0028-0836. Disponível em: < http://dx.doi.org/10.1038/nature07202 >.

BOONSTRA, A.; RAJSBAUM, R.; HOLMAN, M. et al. Macrophages and myeloid dendritic cells, but not plasmacytoid dendritic cells, produce IL-10 in response to MyD88- and TRIF-dependent TLR signals, and TLR-independent signals. **J Immunol,** v. 177, n. 11, p. 7551-8, Dec 1 2006. ISSN 0022-1767 (Print) 0022-1767 (Linking).

BRANDT, E.; WOERLY, G.; YOUNES, A. B. et al. IL-4 production by human polymorphonuclear neutrophils. **J Leukoc Biol,** v. 68, n. 1, p. 125-30, Jul 2000. ISSN 0741-5400 (Print) 0741-5400 (Linking).

BUDAK, F.; GÖRAL, G. H.; HEPER, Y. et al. IL-10 and IL-6 gene polymorphisms as potential host susceptibility factors in *Brucellosis*. **Cytokine,** v. 38, n. 1, p. 32-36, 2007. ISSN 1043-4666. Disponível em: < http://www.sciencedirect.com/science/article/pii/S1043466607000877 >.

CARTER, N. A.; ROSSER, E. C.; MAURI, C. Interleukin-10 produced by B cells is crucial for the suppression of Th17/Th1 responses, induction of T regulatory type 1 cells and reduction of collagen-induced arthritis. **Arthritis Res Ther,** v. 14, n. 1, p. R32, 2012. ISSN 1478-6362 (Electronic) 1478-6354 (Linking).

CARVALHO JÚNIOR, C. A.; MOUSTACAS, V. S.; XAVIER, M. N. et al. Andrological, pathologic, morphometric, and ultrasonographic findings in rams experimentally infected with *Brucella ovis*. **Small Ruminant Research,** v. 102, n. 2, p. 213-222, 2012. ISSN 0921-4488. Disponível em: < http://linkinghub.elsevier.com/retrieve/pii/S0921448811002999?showall=true >.

CELLI, J. Surviving inside a macrophage: the many ways of *Brucella*. **Res Microbiol,** v. 157, n. 2, p. 93-8, Mar 2006. Disponível em: < http://www.ncbi.nlm.nih.gov/entrez/query.fcgi?cmd=Retrieve&db=PubMed&dopt=Citation&list_uids=16364608 >.

CELLI, J.; DE CHASTELLIER, C.; FRANCHINI, D. M. et al. *Brucella* evades macrophage killing via VirB-dependent sustained interactions with the endoplasmic reticulum. **J Exp Med,** v. 198, n. 4, p. 545-56, Aug 18 2003. Disponível em: < http://www.ncbi.nlm.nih.gov/entrez/query.fcgi?cmd=Retrieve&db=PubMed&dopt=Citation&list_uids=12925673 >.

CHANG, W. L. W.; BARRY, P. A. Attenuation of innate immunity by cytomegalovirus IL-10 establishes a long-

term deficit of adaptive antiviral immunity. **Proceedings of the National Academy of Sciences,** v. 107, n. 52, p. 22647-22652, December 28, 2010 2010. Disponível em: < http://www.pnas.org/content/107/52/22647.abstract >.

CHAWLA, A. Control of macrophage activation and function by PPARs. **Circ Res,** v. 106, n. 10, p. 1559-69, May 28 2010. ISSN 1524-4571 (Electronic)
0009-7330 (Linking). Disponível em: < http://www.ncbi.nlm.nih.gov/pubmed/20508200 >.

CHUNG, S. W.; KANG, B. Y.; KIM, S. H. et al. Oxidized low density lipoprotein inhibits interleukin-12 production in lipopolysaccharide-activated mouse macrophages via direct interactions between peroxisome proliferator-activated receptor-gamma and nuclear factor-kappa B. **J Biol Chem,** v. 275, n. 42, p. 32681-7, Oct 20 2000. ISSN 0021-9258 (Print)
0021-9258 (Linking).

COPIN, R.; DE BAETSELIER, P.; CARLIER, Y. et al. MyD88-Dependent Activation of B220-CD11b+LY-6C+ Dendritic Cells during *Brucella melitensis* Infection. **J Immunol,** v. 178, n. 8, p. 5182-5191, Apr 15 2007. Disponível em: < http://www.ncbi.nlm.nih.gov/entrez/query.fcgi?cmd=Retrieve&db=PubMed&dopt=Citation&list_uids=17404301 >.

COPIN, R.; VITRY, M.-A.; HANOT MAMBRES, D. et al. In Situ Microscopy Analysis Reveals Local Innate Immune Response Developed around *Brucella* Infected Cells in Resistant and Susceptible Mice. **PLoS Pathog,** v. 8, n. 3, p. e1002575, 2012. Disponível em: < http://dx.doi.org/10.1371%2Fjournal.ppat.1002575 >.

CORBEL, M. J. Brucellosis: an overview. **Emerg Infect Dis,** v. 3, n. 2, p. 213-21., 1997. Disponível em: < http://www.ncbi.nlm.nih.gov/htbin-post/Entrez/query?db=m&form=6&dopt=r&uid=9204307 >.

COUPER, K. N.; BLOUNT, D. G.; RILEY, E. M. IL-10: the master regulator of immunity to infection. **J Immunol,** v. 180, n. 9, p. 5771-7, May 1 2008. ISSN 0022-1767 (Print) 0022-1767 (Linking).

DE ALMEIDA, L. A.; MACEDO, G. C.; MARINHO, F. A. et al. Toll-Like Receptor 6 Plays an Important Role in Host Innate Resistance to *Brucella abortus* Infection in Mice. **Infect Immun,** v. 81, n. 5, p. 1654-62, May 2013. ISSN 1098-5522 (Electronic) 0019-9567 (Linking).

DEAN, A. S.; CRUMP, L.; GRETER, H. et al. Clinical manifestations of human brucellosis: a systematic review and meta-analysis. **PLoS Negl Trop Dis,** v. 6, n. 12, p. e1929, 2012. ISSN 1935-2735 (Electronic) 1935-2727 (Linking).

DELRUE, R. M.; MARTINEZ-LORENZO, M.; LESTRATE, P. et al. Identification of *Brucella* spp. genes involved in intracellular trafficking. **Cell Microbiol,** v. 3, n. 7, p. 487-97., 2001. Disponível em: < http://www.ncbi.nlm.nih.gov/htbin-post/Entrez/query?db=m&form=6&dopt=r&uid=11437834 >.

DEN HARTIGH, A. B.; ROLAN, H. G.; DE JONG, M. F. et al. VirB3-VirB6 and VirB8-VirB11, but not VirB7, are essential for mediating persistence *Brucella* in the reticuloendothelial system. **J Bacteriol**, May 9 2008. Disponível em: < http://www.ncbi.nlm.nih.gov/entrez/query.fcgi?cmd=Retrieve&db=PubMed&dopt=Citation&list_uids=18469100 >.

DEN HARTIGH, A. B.; SUN, Y. H.; SONDERVAN, D. et al. Differential requirements for VirB1 and VirB2 during *Brucella abortus* infection. **Infect Immun,**

v. 72, n. 9, p. 5143-9, Sep 2004. Disponível em: < http://www.ncbi.nlm.nih.gov/entrez/query.fcgi?cmd=Retrieve&db=PubMed&dopt=Citation&list_uids=15322008 >.

DILLON, S.; AGRAWAL, A.; VAN DYKE, T. et al. A Toll-like receptor 2 ligand stimulates Th2 responses in vivo, via induction of extracellular signal-regulated kinase mitogen-activated protein kinase and c-Fos in dendritic cells. **J Immunol,** v. 172, n. 8, p. 4733-43, Apr 15 2004. ISSN 0022-1767 (Print) 0022-1767 (Linking).

EHRT, S.; SCHNAPPINGER, D.; BEKIRANOV, S. et al. Reprogramming of the macrophage transcriptome in response to interferon-gamma and *Mycobacterium tuberculosis*: signaling roles of nitric oxide synthase-2 and phagocyte oxidase. **J Exp Med,** v. 194, n. 8, p. 1123-40, Oct 15 2001. ISSN 0022-1007 (Print) 0022-1007 (Linking).

ESSENBERG, R. C.; CANDLER, C.; NIDA, S. K. *Brucella abortus* strain 2308 putative glucose and galactose transporter gene: cloning and characterization. **Microbiology,** v. 143 (Pt 5), p. 1549-55, May 1997. ISSN 1350-0872 (Print) 1350-0872 (Linking). Disponível em: < http://www.ncbi.nlm.nih.gov/pubmed/9168605 >.

EVERTS, B.; AMIEL, E.; VAN DER WINDT, G. J. et al. Commitment to glycolysis sustains survival of NO-producing inflammatory dendritic cells. **Blood,** v. 120, n. 7, p. 1422-31, Aug 16 2012. ISSN 1528-0020 (Electronic) 0006-4971 (Linking).

FERNANDES, D. M.; BALDWIN, C. L. Interleukin-10 downregulates protective immunity to *Brucella abortus*. **Infection and Immunity,** v. 63, n. 3, p. 1130-3, March 1, 1995 1995. Disponível em: < http://iai.asm.org/content/63/3/1130.abstract >.

FERNANDES, D. M.; JIANG, X.; JUNG, J. H. et al. Comparison of T cell cytokines in resistant and susceptible mice infected with virulent Brucella abortus strain 2308. **FEMS Immunology & Medical Microbiology,** v. 16, n. 3-4, p. 193-203, 1996. ISSN 1574-695X. Disponível em: < http://dx.doi.org/10.1111/j.1574-695X.1996.tb00136.x >.

FERNÁNDEZ-LAGO, L.; MONTE, M.; CHORDI, A. Endogenous gamma interferon and interleukin-10 in *Brucella abortus* 2308 infection in mice. **FEMS Immunology & Medical Microbiology,** v. 15, n. 2-3, p. 109-114, 1996. ISSN 1574-695X. Disponível em: < http://dx.doi.org/10.1111/j.1574-695X.1996.tb00060.x >.

FIORENTINO, D. F.; BOND, M. W.; MOSMANN, T. R. Two types of mouse T helper cell. IV. Th2 clones secrete a factor that inhibits cytokine production by Th1 clones. **J Exp Med,** v. 170, n. 6, p. 2081-95, Dec 1 1989. ISSN 0022-1007 (Print) 0022-1007 (Linking).

FIORENTINO, D. F.; ZLOTNIK, A.; MOSMANN, T. R. et al. IL-10 inhibits cytokine production by activated macrophages. **The Journal of Immunology,** v. 147, n. 11, p. 3815-22, December 1, 1991 1991. Disponível em: < http://jimmunol.org/content/147/11/3815.abstract >.

FOSTER, G.; OSTERMAN, B. S.; GODFROID, J. et al. *Brucella ceti* sp. nov. and *Brucella pinnipedialis* sp. nov. for *Brucella* strains with cetaceans and seals as their preferred hosts. **Int J Syst Evol Microbiol,** v. 57, n. Pt 11, p. 2688-93, Nov 2007. ISSN 1466-5026 (Print) 1466-5026 (Linking).

FRANCHI, L.; PARK, J. H.; SHAW, M. H. et al. Intracellular NOD-like receptors in innate immunity, infection and disease. **Cell Microbiol,** v. 10, n. 1, p. 1-8, Jan 2008. ISSN 1462-5822 (Electronic) 1462-5814 (Linking).

FRANCO, M. P.; MULDER, M.; GILMAN, R. H. et al. Human brucellosis. **Lancet Infect Dis,** v. 7, n. 12, p. 775-86, Dec 2007. ISSN 1473-3099 (Print) 1473-3099 (Linking).

FRETIN, D.; FAUCONNIER, A.; KÖHLER, S. et al. The sheathed flagellum of *Brucella melitensis* is involved in persistence in a murine model of infection. **Cellular Microbiology,** v. 7, n. 5, p. 687-698, 2005. ISSN 1462-5822. Disponível em: < http://dx.doi.org/10.1111/j.1462-5822.2005.00502.x >.

GABRYSOVA, L.; NICOLSON, K. S.; STREETER, H. B. et al. Negative feedback control of the autoimmune response through antigen-induced differentiation of IL-10-secreting Th1 cells. **J Exp Med,** v. 206, n. 8, p. 1755-67, Aug 3 2009. ISSN 1540-9538 (Electronic) 0022-1007 (Linking).

GARRITY, G. **Bergey's manual of systematic bacteriology**. 2nd. New York: Springer, 2001.

GAUTIER, E. L.; CHOW, A.; SPANBROEK, R. et al. Systemic analysis of PPARgamma in mouse macrophage populations reveals marked diversity in expression with critical roles in resolution of inflammation and airway immunity. **J Immunol,** v. 189, n. 5, p. 2614-24, Sep 1 2012. ISSN 1550-6606 (Electronic) 0022-1767 (Linking).

GERBER, J. S.; MOSSER, D. M. Reversing lipopolysaccharide toxicity by ligating the macrophage Fc gamma receptors. **J Immunol,** v. 166, n. 11, p. 6861-8, Jun 1 2001. ISSN 0022-1767 (Print) 0022-1767 (Linking).

GHIGO, E.; CAPO, C.; RAOULT, D. et al. Interleukin-10 stimulates *Coxiella burnetii* replication in human monocytes through tumor necrosis factor down-modulation: role in microbicidal defect of Q fever. **Infect Immun,** v. 69, n. 4, p. 2345-52, Apr 2001. ISSN 0019-9567 (Print) 0019-9567 (Linking).

GODFROID, J.; CLOECKAERT, A.; LIAUTARD, J. P. et al. From the discovery of the Malta fever's agent to the discovery of a marine mammal reservoir, brucellosis has continuously been a re-emerging zoonosis. **Vet Res,** v. 36, n. 3, p. 313-26, May-Jun 2005. Disponível em: < http://www.ncbi.nlm.nih.gov/entrez/query.fcgi?cmd=Retrieve&db=PubMed&dopt=Citation&list_uids=15845228 >.

GOENKA, R.; GUIRNALDA, P. D.; BLACK, S. J. et al. B Lymphocytes provide an infection niche for intracellular bacterium *Brucella abortus*. **J Infect Dis,** v. 206, n. 1, p. 91-8, Jul 1 2012. ISSN 1537-6613 (Electronic)
0022-1899 (Linking).

GOENKA, R.; PARENT, M. A.; ELZER, P. H. et al. B Cell-deficient Mice Display Markedly Enhanced Resistance to the Intracellular Bacterium *Brucella abortus*. **Journal of Infectious Diseases,** v. 203, n. 8, p. 1136-1146, April 15, 2011 2011. Disponível em: < http://jid.oxfordjournals.org/content/203/8/1136.abstract >.

GOMES, M. T.; CAMPOS, P. C.; OLIVEIRA, F. S. et al. Critical role of ASC inflammasomes and bacterial type IV secretion system in caspase-1 activation and host innate resistance to *Brucella abortus* infection. **J Immunol,** v. 190, n. 7, p. 3629-38, Apr 1 2013. ISSN 1550-6606 (Electronic) 0022-1767 (Linking).

GORDON, S.; MARTINEZ, F. O. Alternative Activation of Macrophages: Mechanism and Functions. **Immunity,** v. 32, n. 5, p. 593-604, 2010. ISSN 1074-7613. Disponível em: < http://www.sciencedirect.com/science/article/pii/S1074761310001731 >.

GORVEL, J. P.; MORENO, E. *Brucella* intracellular life: from invasion to intracellular replication. **Vet Microbiol,** v. 90, n. 1-4, p. 281-97., 2002. Disponível em: < http://www.ncbi.nlm.nih.gov/htbin-post/Entrez/query?db=m&form=6&dopt=r&uid=12414149 >.

HARRIS, J.; DE HARO, S. A.; MASTER, S. S. et al. T helper 2 cytokines inhibit autophagic control of intracellular Mycobacterium tuberculosis. **Immunity,** v. 27, n. 3, p. 505-17, Sep 2007. ISSN 1074-7613 (Print)
1074-7613 (Linking).

HASKO, G.; PACHER, P.; DEITCH, E. A. et al. Shaping of monocyte and macrophage function by adenosine receptors. **Pharmacol Ther,** v. 113, n. 2, p. 264-75, Feb 2007. ISSN 0163-7258 (Print)
0163-7258 (Linking).

HOEBE, K.; JANSSEN, E.; BEUTLER, B. The interface between innate and adaptive immunity. **Nat Immunol,** v. 5, n. 10, p. 971-4, Oct 2004. ISSN 1529-2908 (Print). Disponível em: < http://www.ncbi.nlm.nih.gov/entrez/query.fcgi?cmd=Retrieve&db=PubMed&dopt=Citation&list_uids=15454919 >.

HONG, P. C.; TSOLIS, R. M.; FICHT, T. A. Identification of genes required for chronic persistence of *Brucella abortus* in mice. **Infect Immun,** v. 68, n. 7, p. 4102-7., 2000. Disponível em: < http://www.ncbi.nlm.nih.gov/htbin-post/Entrez/query?db=m&form=6&dopt=r&uid=10858227
http://iai.asm.org/cgi/content/full/68/7/4102
http://iai.asm.org/cgi/content/abstract/68/7/4102 >.

HUNT, A. C.; BOTHWELL, P. W. Histological findings in human brucellosis. **J Clin Pathol,** v. 20, n. 3, p. 267-72, May 1967. Disponível em: < http://www.ncbi.nlm.nih.gov/entrez/query.fcgi?cmd=Retrieve&db=PubMed&dopt=Citation&list_uids=5632572 >.

IWASAKI, A.; MEDZHITOV, R. Toll-like receptor control of the adaptive immune responses. **Nat Immunol,** v. 5, n. 10, p. 987-95, Oct 2004. ISSN 1529-2908 (Print)
1529-2908 (Linking).

JANG, S.; UEMATSU, S.; AKIRA, S. et al. IL-6 and IL-10 induction from dendritic cells in response to *Mycobacterium tuberculosis* is predominantly dependent on TLR2-mediated recognition. **J Immunol,** v. 173, n. 5, p. 3392-7, Sep 1 2004. ISSN 0022-1767 (Print) 0022-1767 (Linking).

JANKOVIC, D.; KULLBERG, M. C.; FENG, C. G. et al. Conventional T-bet+Foxp3(-) Th1 cells are the major source of host-protective regulatory IL-10 during intracellular protozoan infection. **The Journal of Experimental Medicine,** v. 204, n. 2, p. 273-283, February 19, 2007 2007. Disponível em: < http://jem.rupress.org/content/204/2/273.abstract >.

KAMANAKA, M.; KIM, S. T.; WAN, Y. Y. et al. Expression of Interleukin-10 in Intestinal Lymphocytes Detected by an Interleukin-10 Reporter Knockin tiger Mouse. **Immunity,** v. 25, n. 6, p. 941-952, 2006. ISSN 1074-7613. Disponível em: < http://linkinghub.elsevier.com/retrieve/pii/S1074761306005115 >.

KARAOGLAN, I.; PEHLIVAN, S.; NAMIDURU, M. et al. TNF-alpha, TGF-

beta, IL-10, IL-6 and IFN-gamma gene polymorphisms as risk factors for brucellosis. **New Microbiol,** v. 32, n. 2, p. 173-8, Apr 2009. ISSN 1121-7138 (Print) 1121-7138 (Linking).

KELLY, D.; CAMPBELL, J. I.; KING, T. P. et al. Commensal anaerobic gut bacteria attenuate inflammation by regulating nuclear-cytoplasmic shuttling of PPAR-gamma and RelA. **Nat Immunol,** v. 5, n. 1, p. 104-12, Jan 2004. ISSN 1529-2908 (Print) 1529-2908 (Linking).

KO, J.; GENDRON-FITZPATRICK, A.; SPLITTER, G. A. Susceptibility of IFN regulatory factor-1 and IFN consensus sequence binding protein-deficient mice to brucellosis. **J Immunol,** v. 168, n. 5, p. 2433-40., 2002. Disponível em: < http://www.ncbi.nlm.nih.gov/htbin-post/Entrez/query?db=m&form=6&dopt=r&uid=11859135 http://www.jimmunol.org/cgi/content/full/168/5/2433 http://www.jimmunol.org/cgi/content/abstract/168/5/2433 >.

KOHLER, S.; FOULONGNE, V.; OUAHRANI-BETTACHE, S. et al. The analysis of the intramacrophagic virulome of *Brucella suis* deciphers the environment encountered by the pathogen inside the macrophage host cell. **Proc Natl Acad Sci U S A,** v. 99, n. 24, p. 15711-6, Nov 26 2002. ISSN 0027-8424 (Print) 0027-8424 (Linking). Disponível em: < http://www.ncbi.nlm.nih.gov/pubmed/12438693 >.

KREIDER, T.; ANTHONY, R. M.; URBAN, J. F., JR. et al. Alternatively activated macrophages in helminth infections. **Curr Opin Immunol,** v. 19, n. 4, p. 448-53, Aug 2007. ISSN 0952-7915 (Print) 0952-7915 (Linking).

KREUTZER, D. L.; DREYFUS, L. A.; ROBERTSON, D. C. Interaction of polymorphonuclear leukocytes with smooth and rough strains of *Brucella abortus*. **Infect Immun,** v. 23, n. 3, p. 737-42., 1979. Disponível em: < http://www.ncbi.nlm.nih.gov/htbin-post/Entrez/query?db=m&form=6&dopt=r&uid=110680 >.

KUHN, R.; LOHLER, J.; RENNICK, D. et al. Interleukin-10-deficient mice develop chronic enterocolitis. **Cell,** v. 75, n. 2, p. 263-74, Oct 22 1993. ISSN 0092-8674 (Print) 0092-8674 (Linking).

LAPAQUE, N.; TAKEUCHI, O.; CORRALES, F. et al. Differential inductions of TNF-alpha and IGTP, IIGP by structurally diverse classic and non-classic lipopolysaccharides. **Cell Microbiol,** v. 8, n. 3, p. 401-13, Mar 2006. ISSN 1462-5814 (Print). Disponível em: < http://www.ncbi.nlm.nih.gov/entrez/query.fcgi?cmd=Retrieve&db=PubMed&dopt=Citation&list_uids=16469053 >.

LAWRENCE, T.; NATOLI, G. Transcriptional regulation of macrophage polarization: enabling diversity with identity. **Nat Rev Immunol,** v. 11, n. 11, p. 750-761, 2011. ISSN 1474-1733. Disponível em: < http://dx.doi.org/10.1038/nri3088 >.

LOKE, P.; GALLAGHER, I.; NAIR, M. G. et al. Alternative activation is an innate response to injury that requires CD4+ T cells to be sustained during chronic infection. **J Immunol,** v. 179, n. 6, p. 3926-36, Sep 15 2007. ISSN 0022-1767 (Print) 0022-1767 (Linking).

MACEDO, G. C.; MAGNANI, D. M.; CARVALHO, N. B. et al. Central role of MyD88-dependent dendritic cell maturation and proinflammatory cytokine production to control *Brucella abortus* infection. **J**

Immunol, v. 180, n. 2, p. 1080-7, Jan 15 2008. Disponível em: < http://www.ncbi.nlm.nih.gov/entrez/query.fcgi?cmd=Retrieve&db=PubMed&dopt=Citation&list_uids=18178848 >.

MAHAJAN, S.; DKHAR, H. K.; CHANDRA, V. et al. *Mycobacterium tuberculosis* modulates macrophage lipid-sensing nuclear receptors PPARgamma and TR4 for survival. **J Immunol,** v. 188, n. 11, p. 5593-603, Jun 1 2012. ISSN 1550-6606 (Electronic)
0022-1767 (Linking).

MARTINEZ, F. O.; SICA, A.; MANTOVANI, A. et al. Macrophage activation and polarization. **Front Biosci,** v. 13, p. 453-61, 2008. ISSN 1093-4715 (Electronic)
1093-4715 (Linking).

MARTIROSYAN, A.; MORENO, E.; GORVEL, J.-P. An evolutionary strategy for a stealthy intracellular *Brucella* pathogen. **Immunological Reviews,** v. 240, n. 1, p. 211-234, 2011. ISSN 1600-065X. Disponível em: < http://dx.doi.org/10.1111/j.1600-065X.2010.00982.x >.

MCCULLOUGH, N. B.; BEAL, G. A. Growth and manometric studies on carbohydrate utilization of *Brucella*. **J Infect Dis,** v. 89, n. 3, p. 266-71, Nov-Dec 1951. ISSN 0022-1899 (Print) 0022-1899 (Linking). Disponível em: < http://www.ncbi.nlm.nih.gov/pubmed/14888951 >.

MCKINNEY, J. D.; ZU BENTRUP, K. H.; MUNOZ-ELIAS, E. J. et al. Persistence of *Mycobacterium tuberculosis* in macrophages and mice requires the glyoxylate shunt enzyme isocitrate lyase. **Nature,** v. 406, n. 6797, p. 735-738, 2000. ISSN 0028-0836. Disponível em: < http://dx.doi.org/10.1038/35021074 >.

MOORE, K. W.; DE WAAL MALEFYT, R.; COFFMAN, R. L. et al. INTERLEUKIN-10 AND THE INTERLEUKIN-10 RECEPTOR. **Annual Review of Immunology,** v. 19, n. 1, p. 683-765, 2001. Disponível em: < http://www.annualreviews.org/doi/abs/10.1146/annurev.immunol.19.1.683 >.

MOSSER, D. M. The many faces of macrophage activation. **J Leukoc Biol,** v. 73, n. 2, p. 209-12, Feb 2003. ISSN 0741-5400 (Print) 0741-5400 (Linking).

MOSSER, D. M.; EDWARDS, J. P. Exploring the full spectrum of macrophage activation. **Nat Rev Immunol,** v. 8, n. 12, p. 958-69, Dec 2008. ISSN 1474-1741 (Electronic) 1474-1733 (Linking).

MURPHY, E. A.; SATHIYASEELAN, J.; PARENT, M. A. et al. Interferon-γ is crucial for surviving a *Brucella abortus* infection in both resistant C57BL/6 and susceptible BALB/c mice. **Immunology,** v. 103, n. 4, p. 511-518, 2001. ISSN 1365-2567. Disponível em: < http://dx.doi.org/10.1046/j.1365-2567.2001.01258.x >.

NETEA, M. G.; VAN DER GRAAF, C.; VAN DER MEER, J. W. et al. Toll-like receptors and the host defense against microbial pathogens: bringing specificity to the innate-immune system. **J Leukoc Biol,** v. 75, n. 5, p. 749-55, May 2004. Disponível em: < http://www.ncbi.nlm.nih.gov/entrez/query.fcgi?cmd=Retrieve&db=PubMed&dopt=Citation&list_uids=15075354 >.

O'CALLAGHAN, D.; CAZEVIEILLE, C.; ALLARDET-SERVENT, A. et al. A homologue of the *Agrobacterium tumefaciens* VirB and *Bordetella pertussis* Ptl type IV secretion systems is essential for intracellular survival of *Brucella suis*. **Mol Microbiol,** v. 33, n. 6, p. 1210-20., 1999. Disponível em: <

http://www.ncbi.nlm.nih.gov/htbin-post/Entrez/query?db=m&form=6&dopt=r&uid=10510235 >.

O'LEARY, S. N.; O'SULLIVAN, M. P.; KEANE, J. IL-10 Blocks Phagosome Maturation in *Mycobacterium tuberculosis*-Infected Human Macrophages. **American Journal of Respiratory Cell and Molecular Biology,** v. 45, n. 1, p. 172-180, July 1, 2011 2011. Disponível em: < http://ajrcmb.atsjournals.org/content/45/1/172.abstract >.

O'NEILL, L. A. J.; HARDIE, D. G. Metabolism of inflammation limited by AMPK and pseudo-starvation. **Nature,** v. 493, n. 7432, p. 346-355, 2013. ISSN 0028-0836. Disponível em: < http://dx.doi.org/10.1038/nature11862 >.

ODEGAARD, J. I.; RICARDO-GONZALEZ, R. R.; GOFORTH, M. H. et al. Macrophage-specific PPARgamma controls alternative activation and improves insulin resistance. **Nature,** v. 447, n. 7148, p. 1116-20, Jun 28 2007. ISSN 1476-4687 (Electronic)
0028-0836 (Linking). Disponível em: < http://www.ncbi.nlm.nih.gov/pubmed/17515919 >.

OSTERMAN, B.; MORIYON, I. International committee on systematics of prokaryotes: Subcommittee on the taxonomy of *Brucella*. **International Journal of Systematic and Evolutionary Microbiology,** v. 56, p. 1173-1175, 2006.

PAPPAS, G.; PAPADIMITRIOU, P.; AKRITIDIS, N. et al. The new global map of human brucellosis. **Lancet Infect Dis,** v. 6, n. 2, p. 91-9, Feb 2006. Disponível em: < http://www.ncbi.nlm.nih.gov/entrez/query.fcgi?cmd=Retrieve&db=PubMed&dopt=Citation&list_uids=16439329 >.

PASQUALI, P.; THORNTON, A. M.; VENDETTI, S. et al. CD4+CD25+ T regulatory cells limit effector T cells and favor the progression of brucellosis in BALB/c mice. **Microbes and Infection,** v. 12, n. 1, p. 3-10, 2010. ISSN 1286-4579. Disponível em: < http://www.sciencedirect.com/science/article/pii/S128645790900210X >.

PEYRON, P.; VAUBOURGEIX, J.; POQUET, Y. et al. Foamy macrophages from tuberculous patients' granulomas constitute a nutrient-rich reservoir for *M. tuberculosis* persistence. **PLoS Pathog,** v. 4, n. 11, p. e1000204, Nov 2008. ISSN 1553-7374 (Electronic)
1553-7366 (Linking). Disponível em: < http://www.ncbi.nlm.nih.gov/pubmed/19002241 >.

PILS, M. C.; PISANO, F.; FASNACHT, N. et al. Monocytes/macrophages and/or neutrophils are the target of IL-10 in the LPS endotoxemia model. **European Journal of Immunology,** v. 40, n. 2, p. 443-448, 2010. ISSN 1521-4141. Disponível em: < http://dx.doi.org/10.1002/eji.200939592 >.

PIZARRO-CERDA, J.; MERESSE, S.; PARTON, R. G. et al. *Brucella abortus* transits through the autophagic pathway and replicates in the endoplasmic reticulum of nonprofessional phagocytes. **Infect Immun,** v. 66, n. 12, p. 5711-24., 1998. Disponível em: < http://www.ncbi.nlm.nih.gov/htbin-post/Entrez/query?db=m&form=6&dopt=r&uid=9826346
http://iai.asm.org/cgi/content/full/66/12/5711 >.

RAES, G.; BRYS, L.; DAHAL, B. K. et al. Macrophage galactose-type C-type lectins as novel markers for alternatively activated macrophages elicited by parasitic infections and allergic airway inflammation. **J Leukoc Biol,** v. 77, n. 3, p. 321-7, Mar 2005. ISSN 0741-5400 (Print)
0741-5400 (Linking).

RAES, G.; NOEL, W.; BESCHIN, A. et al. FIZZ1 and Ym as tools to discriminate between differentially activated macrophages. **Dev Immunol,** v. 9, n. 3, p. 151-9, Sep 2002. ISSN 1044-6672 (Print) 1026-7905 (Linking).

RAFIEI, A.; ARDESTANI, S. K.; KARIMINIA, A. et al. Dominant Th1 cytokine production in early onset of human brucellosis followed by switching towards Th2 along prolongation of disease. **Journal of Infection,** v. 53, n. 5, p. 315-324, 2006. ISSN 0163-4453. Disponível em: < http://www.sciencedirect.com/science/article/pii/S016344530500407X >.

REDFORD, P. S.; MURRAY, P. J.; O'GARRA, A. The role of IL-10 in immune regulation during *M. tuberculosis* infection. **Mucosal Immunol,** v. 4, n. 3, p. 261-270, 2011. ISSN 1933-0219. Disponível em: < http://dx.doi.org/10.1038/mi.2011.7 >.

REYES, J. L.; TERRAZAS, L. I. The divergent roles of alternatively activated macrophages in helminthic infections. **Parasite Immunology,** v. 29, n. 12, p. 609-619, 2007. ISSN 1365-3024. Disponível em: < http://dx.doi.org/10.1111/j.1365-3024.2007.00973.x >.

RICOTE, M.; LI, A. C.; WILLSON, T. M. et al. The peroxisome proliferator-activated receptor-gamma is a negative regulator of macrophage activation. **Nature,** v. 391, n. 6662, p. 79-82, Jan 1 1998. ISSN 0028-0836 (Print) 0028-0836 (Linking).

RODRIGUEZ-PRADOS, J. C.; TRAVES, P. G.; CUENCA, J. et al. Substrate fate in activated macrophages: a comparison between innate, classic, and alternative activation. **J Immunol,** v. 185, n. 1, p. 605-14, Jul 1 2010. ISSN 1550-6606 (Electronic) 0022-1767 (Linking).

RODRIGUEZ-ZAPATA, M.; MATIAS, M. J.; PRIETO, A. et al. Human brucellosis is characterized by an intense Th1 profile associated with a defective monocyte function. **Infect Immun,** v. 78, n. 7, p. 3272-9, Jul 2010. ISSN 1098-5522 (Electronic)
0019-9567 (Linking).

ROERS, A.; SIEWE, L.; STRITTMATTER, E. et al. T Cell-specific Inactivation of the Interleukin 10 Gene in Mice Results in Enhanced T Cell Responses but Normal Innate Responses to Lipopolysaccharide or Skin Irritation. **The Journal of Experimental Medicine,** v. 200, n. 10, p. 1289-1297, November 15, 2004 2004. Disponível em: < http://jem.rupress.org/content/200/10/1289.abstract >.

ROLAN, H. G.; TSOLIS, R. M. Mice lacking components of adaptive immunity show increased *Brucella abortus* virB mutant colonization. **Infect Immun,** v. 75, n. 6, p. 2965-73, Jun 2007. Disponível em: < http://www.ncbi.nlm.nih.gov/entrez/query.fcgi?cmd=Retrieve&db=PubMed&dopt=Citation&list_uids=17420243 >.

ROLÁN, H. G.; TSOLIS, R. M. Inactivation of the Type IV Secretion System Reduces the Th1 Polarization of the Immune Response to *Brucella abortus* Infection. **Infection and Immunity,** v. 76, n. 7, p. 3207-3213, July 2008 2008. Disponível em: < http://iai.asm.org/content/76/7/3207.abstract >.

ROLÁN, H. G.; XAVIER, M. N.; SANTOS, R. L. et al. Natural Antibody Contributes to Host Defense against an Attenuated *Brucella abortus* virB Mutant. **Infect Immun,** v. 77, n. 7, p. 3004-3013, July 2009 2009. Disponível em: < http://iai.asm.org/content/77/7/3004.abstract >.

ROTHE, J.; LESSLAUER, W.; LOTSCHER, H. et al. Mice lacking the tumour necrosis factor receptor 1 are resistant to TNF-mediated toxicity but highly susceptible to infection by *Listeria monocytogenes*. **Nature,** v. 364, n. 6440, p. 798-802, Aug 26 1993. ISSN 0028-0836 (Print)
0028-0836 (Linking).

ROUX, C. M.; ROLAN, H. G.; SANTOS, R. L. et al. *Brucella* requires a functional Type IV secretion system to elicit innate immune responses in mice. **Cell Microbiol,** v. 9, n. 7, p. 1851-69, Jul 2007. Disponível em: < http://www.ncbi.nlm.nih.gov/entrez/query.fcgi?cmd=Retrieve&db=PubMed&dopt=Citation&list_uids=17441987 >.

SABAT, R.; GRÜTZ, G.; WARSZAWSKA, K. et al. Biology of interleukin-10. **Cytokine & Growth Factor Reviews,** v. 21, n. 5, p. 331-344, 2010. ISSN 1359-6101. Disponível em: < http://www.sciencedirect.com/science/article/pii/S1359610110000651 >.

SALCEDO, S. P.; MARCHESINI, M. I.; LELOUARD, H. et al. *Brucella* Control of Dendritic Cell Maturation Is Dependent on the TIR-Containing Protein Btp1. **PLoS Pathog,** v. 4, n. 2, p. e21, Feb 8 2008. ISSN 1553-7374 (Electronic). Disponível em: < http://www.ncbi.nlm.nih.gov/entrez/query.fcgi?cmd=Retrieve&db=PubMed&dopt=Citation&list_uids=18266466 >.

SARAIVA, M.; O'GARRA, A. The regulation of IL-10 production by immune cells. **Nat Rev Immunol,** v. 10, n. 3, p. 170-181, 2010. ISSN 1474-1733. Disponível em: < http://dx.doi.org/10.1038/nri2711 >.

SHEVACH, E. M. CD4+CD25+ suppressor T cells: more questions than answers. **Nat Rev Immunol,** v. 2, n. 6, p. 389-400, 2002. ISSN 1474-1733. Disponível em: < http://dx.doi.org/10.1038/nri821 >.

SHI, C.; PAMER, E. G. Monocyte recruitment during infection and inflammation. **Nat Rev Immunol,** v. 11, n. 11, p. 762-74, Nov 2011. ISSN 1474-1741 (Electronic)
1474-1733 (Linking). Disponível em: < http://www.ncbi.nlm.nih.gov/pubmed/21984070 >.

SHIREY, K. A.; COLE, L. E.; KEEGAN, A. D. et al. *Francisella tularensis* Live Vaccine Strain Induces Macrophage Alternative Activation as a Survival Mechanism. **The Journal of Immunology,** v. 181, n. 6, p. 4159-4167, September 15, 2008 2008. Disponível em: < http://jimmunol.org/content/181/6/4159.abstract >.

SIELING, P. A.; MODLIN, R. L. Cytokine patterns at the site of mycobacterial infection. **Immunobiology,** v. 191, n. 4-5, p. 378-87, Oct 1994. ISSN 0171-2985 (Print)
0171-2985 (Linking).

SIEWE, L.; BOLLATI-FOGOLIN, M.; WICKENHAUSER, C. et al. Interleukin-10 derived from macrophages and/or neutrophils regulates the inflammatory response to LPS but not the response to CpG DNA. **Eur J Immunol,** v. 36, n. 12, p. 3248-55, Dec 2006. ISSN 0014-2980 (Print)
0014-2980 (Linking).

SING, A.; ROST, D.; TVARDOVSKAIA, N. et al. *Yersinia* V-antigen exploits toll-like receptor 2 and CD14 for interleukin 10-mediated immunosuppression. **J Exp Med,** v. 196, n. 8, p. 1017-24, Oct 21 2002. ISSN 0022-1007 (Print)
0022-1007 (Linking).

SKENDROS, P.; BOURA, P.; CHRISAGIS, D. et al. Diminished percentage of CD4+ T-lymphocytes expressing interleukine-2 receptor alpha in chronic brucellosis.

Journal of Infection, v. 54, n. 2, p. 192-197, 2007. ISSN 0163-4453. Disponível em: < http://www.sciencedirect.com/science/article/pii/S016344530600140X >.

STARR, T.; NG, T. W.; WEHRLY, T. D. et al. *Brucella* Intracellular Replication Requires Trafficking Through the Late Endosomal/Lysosomal Compartment. **Traffic,** v. 9, n. 5, p. 678-694, 2008. ISSN 1600-0854. Disponível em: < http://dx.doi.org/10.1111/j.1600-0854.2008.00718.x >.

SURAUD, V.; OLIVIER, M.; BODIER, C. C. et al. Differential expression of homing receptors and vascular addressins in tonsils and draining lymph nodes: Effect of *Brucella* infection in sheep. **Veterinary Immunology and Immunopathology,** v. 115, n. 3,Äì4, p. 239-250, 2007. ISSN 0165-2427. Disponível em: < http://www.sciencedirect.com/science/article/pii/S0165242706003266 >.

SVETIC, A.; JIAN, Y. C.; LU, P. et al. *Brucella abortus* induces a novel cytokine gene expression pattern characterized by elevated IL-10 and IFN-g in CD4+ T cells. **International Immunology,** v. 5, n. 8, p. 877-883, August 1, 1993 1993. Disponível em: < http://intimm.oxfordjournals.org/content/5/8/877.abstract >.

SZANTO, A.; BALINT, B. L.; NAGY, Z. S. et al. STAT6 transcription factor is a facilitator of the nuclear receptor PPARgamma-regulated gene expression in macrophages and dendritic cells. **Immunity,** v. 33, n. 5, p. 699-712, Nov 24 2010. ISSN 1097-4180 (Electronic)
1074-7613 (Linking). Disponível em: < http://www.ncbi.nlm.nih.gov/pubmed/21093321 >.

TERWAGNE, M.; FEROOZ, J.; ROLAN, H. G. et al. Innate immune recognition of flagellin limits systemic persistence of *Brucella*. **Cell Microbiol,** v. 15, n. 6, p. 942-60, Jun 2013. ISSN 1462-5822 (Electronic) 1462-5814 (Linking).

TONTONOZ, P.; SPIEGELMAN, B. M. Fat and beyond: the diverse biology of PPARgamma. **Annu Rev Biochem,** v. 77, p. 289-312, 2008. ISSN 0066-4154 (Print)
0066-4154 (Linking).

TSOLIS, R. M.; YOUNG, G. M.; SOLNICK, J. V. et al. From bench to bedside: stealth of enteroinvasive pathogens. **Nat Rev Microbiol,** v. 6, n. 12, p. 883-92, Dec 2008. ISSN 1740-1534 (Electronic) 1740-1526 (Linking).

TUMITAN, A. R.; MONNAZZI, L. G.; GHIRALDI, F. R. et al. Pattern of macrophage activation in yersinia-resistant and yersinia-susceptible strains of mice. **Microbiol Immunol,** v. 51, n. 10, p. 1021-8, 2007. ISSN 0385-5600 (Print) 0385-5600 (Linking).

VAN DYKEN, S. J.; LOCKSLEY, R. M. Interleukin-4- and Interleukin-13-Mediated Alternatively Activated Macrophages: Roles in Homeostasis and Disease. **Annual Review of Immunology,** v. 31, n. 1, p. null, 2013. Disponível em: < http://www.annualreviews.org/doi/abs/10.1146/annurev-immunol-032712-095906 >.

VATS, D.; MUKUNDAN, L.; ODEGAARD, J. I. et al. Oxidative metabolism and PGC-1beta attenuate macrophage-mediated inflammation. **Cell Metab,** v. 4, n. 1, p. 13-24, Jul 2006. ISSN 1550-4131 (Print)
1550-4131 (Linking). Disponível em: < http://www.ncbi.nlm.nih.gov/pubmed/16814729 >.

VIEIRA, P. L.; CHRISTENSEN, J. R.; MINAEE, S. et al. IL-10-secreting regulatory T cells do not express Foxp3 but have comparable regulatory function to

naturally occurring CD4+CD25+ regulatory T cells. **J Immunol,** v. 172, n. 10, p. 5986-93, May 15 2004. ISSN 0022-1767 (Print) 0022-1767 (Linking).

WANG, P.; WU, P.; SIEGEL, M. I. et al. Interleukin (IL)-10 Inhibits Nuclear Factor B (NFB) Activation in Human Monocytes. **Journal of Biological Chemistry,** v. 270, n. 16, p. 9558-9563, April 21, 1995 1995. Disponível em: < http://www.jbc.org/content/270/16/9558.abstract >.

WAYNE, L. G.; LIN, K. Y. Glyoxylate metabolism and adaptation of *Mycobacterium tuberculosis* to survival under anaerobic conditions. **Infection and Immunity,** v. 37, n. 3, p. 1042-1049, September 1, 1982 1982. Disponível em: < http://iai.asm.org/content/37/3/1042.abstract >.

WEISS, D. S.; TAKEDA, K.; AKIRA, S. et al. MyD88, but not toll-like receptors 4 and 2, is required for efficient clearance of *Brucella abortus*. **Infect Immun,** v. 73, n. 8, p. 5137-43, Aug 2005. Disponível em: < http://www.ncbi.nlm.nih.gov/entrez/query.fcgi?cmd=Retrieve&db=PubMed&dopt=Citation&list_uids=16041030 >.

WELCH, J. S.; RICOTE, M.; AKIYAMA, T. E. et al. PPARgamma and PPARdelta negatively regulate specific subsets of lipopolysaccharide and IFN-gamma target genes in macrophages. **Proc Natl Acad Sci U S A,** v. 100, n. 11, p. 6712-7, May 27 2003. ISSN 0027-8424 (Print) 0027-8424 (Linking).

WEST, A. P.; BRODSKY, I. E.; RAHNER, C. et al. TLR signalling augments macrophage bactericidal activity through mitochondrial ROS. **Nature,** v. 472, n. 7344, p. 476-80, Apr 28 2011. ISSN 1476-4687 (Electronic) 0028-0836 (Linking).

WU, Z.; PUIGSERVER, P.; ANDERSSON, U. et al. Mechanisms controlling mitochondrial biogenesis and respiration through the thermogenic coactivator PGC-1. **Cell,** v. 98, n. 1, p. 115-24, Jul 9 1999. ISSN 0092-8674 (Print) 0092-8674 (Linking).

XAVIER, M. N.; PAIXÃO, T. A.; POESTER, F. P. et al. Pathological, Immunohistochemical and Bacteriological Study of Tissues and Milk of Cows and Fetuses Experimentally Infected with *Brucella abortus*. **Journal of Comparative Pathology,** v. 140, n. 2-3, p. 149-157, 2009. ISSN 0021-9975. Disponível em: < http://www.sciencedirect.com/science/article/pii/S0021997508001412 >. Acesso em: 2009/4//.

XAVIER, M. N.; PAXÃO, T. A.; DEN HARTIGH, A. B. et al. Pathogenesis of Brucella spp. **The Open Veterinary Science Journal,** v. 4, p. 109-118, 2010.

YKI-JÄRVINEN, H. Thiazolidinediones. **New England Journal of Medicine,** v. 351, n. 11, p. 1106-1118, 2004. Disponível em: < http://www.nejm.org/doi/full/10.1056/NEJMra041001 >.

YOUNG, E. J. An overview of human brucellosis. **Clin Infect Dis,** v. 21, n. 2, p. 283-9; quiz 290, Aug 1995. Disponível em: < http://www.ncbi.nlm.nih.gov/entrez/query.fcgi?cmd=Retrieve&db=PubMed&dopt=Citation&list_uids=8562733 >.

ZHAN, Y.; CHEERS, C. Endogenous interleukin-12 is involved in resistance to *Brucella abortus* infection. **Infect Immun,** v. 63, n. 4, p. 1387-90, Apr 1995. ISSN 0019-9567 (Print) 0019-9567 (Linking).

ZHAN, Y.; LIU, Z.; CHEERS, C. Tumor necrosis factor alpha and interleukin-12 contribute to resistance to the intracellular bacterium *Brucella abortus* by different

mechanisms. **Infect Immun,** v. 64, n. 7, p. 2782-6, Jul 1996. ISSN 0019-9567 (Print) 0019-9567 (Linking).

ZHANG, L.; CHAWLA, A. Role of PPARgamma in macrophage biology and atherosclerosis. **Trends Endocrinol Metab,** v. 15, n. 10, p. 500-5, Dec 2004. ISSN 1043-2760 (Print) 1043-2760 (Linking).

ZYGMUNT, M. S.; HAGIUS, S. D.; WALKER, J. V. et al. Identification of *Brucella melitensis* 16M genes required for bacterial survival in the caprine host. **Microbes Infect,** v. 8, n. 14-15, p. 2849-54, Nov-Dec 2006. Disponível em: < http://www.ncbi.nlm.nih.gov/entrez/query.fcgi?cmd=Retrieve&db=PubMed&dopt=Citation&list_uids=17090391 >.

Supplementary Material and Methods

Multiplex cytokine assays. Detection of IFNγ, IL-4 and IL-13 in the serum of C57BL/6J mice was performed using Multi-Plex cytokine assays (Bio-Rad, Hercules, CA), as previously described (Rolán and Tsolis, 2008). Groups of five C57BL/6 mice were infected i.p. with 5 x10^5 CFU of *Brucella abortus* 2308, and serum was obtained at necropsy at days 0, 3, 9, 15, 21 and 45 post-infection. Cytokine detection was performed according to the instructions provided by the kit's manufacturer. Multiplex assays were performed in the Animal Resources and Laboratory Services Core of the Pacific Southwest Regional Center of Excellence for Biodefense and Emerging Infectious Diseases.

Immunofluorescence microscopy. Immunofluorescence of *B. abortus* infected BMDM was performed as previously described (Starr *et al.*, 2008). Briefly, *B. abortus* MX2-infected BMDM were grown on 12-mm glass coverslips in 24-well plates. At 24h post-infection, cells were washed three times with PBS, fixed with 3% paraformaldehyde, pH 7.4, at 37°C for 20 min, washed three times with PBS and then incubated for 10 min in 50 mM NH_4Cl in PBS in order to quench free aldehyde groups. Samples were blocked and permeabilized in 10% goat serum and 0.1% saponin in PBS for 30 min at room temperature. Cells were labeled by inverting coverslips onto drops of DAPI (Invitrogen, Grand Island, NY) diluted 1:200 in 10% horse serum and 0.1% saponin in PBS and incubating for 45 min at room temperature. Cells were washed twice with 0.1% saponin in PBS, once in PBS, once in H_2O and then mounted in Mowiol 4-88 mounting medium (Calbiochem). Samples were observed on a Carl Zeiss LSM 510 confocal laser scanning microscope for image acquisition (Carl Zeiss Micro Imaging). Confocal images of 1024 × 1024 pixels were acquired as projections of three consecutive slices with a 0.38-µm step and assembled using Adobe Photoshop CS2 (Adobe Systems). For quantification of intracellular *Brucella* MX2, 50 BMDM/sample were counted. All experiments were performed independently in triplicate.

Growth in Tryptic Soy Broth in vitro. Tryptic soy broth (TSB) with or without glucose was prepared by adding 17g of enzymatic digest of casein (Difco/Becton-Dickinson, Sparks, MD), 3g of enzymatic digest of soybean meal (Difco/Becton-Dickinson, Sparks, MD), 5g of sodium chloride and 2.5g of dipotassium phosphate to 1 liter of purified water. The solution was autoclaved at 121°C for 30 min. Once TSB reached room temperature (RT), 12.5 mL of 20% glucose solution was added to reach a final glucose concentration of 0.25% (TSB + glucose). For *in vitro* growth essay, *B. abortus* 2308, and isogenic mutants BA159 (*gluP*) and MX6 (*gluP*::pGLUP1) overnight cultures were prepared using commercially available TSB containing glucose (Difco/Becton-Dickinson, Sparks, MD) as described in experimental procedures. Then, 1 mL of each overnight culture was washed 3 times in RT sterile PBS and the optical density (OD) was determined and adjusted to OD=1. All initial cultures were prepared by adding 100 µL of OD=1 solution to 9.9 mL of TSB or TSB + glucose, to reach starting OD of 0.01. Strains were further cultured at 37°C on a rotary shaker and the final OD was determined at 24 hours post inoculation. The experiment was performed independently in duplicate at least three times and the standard error for the 24h time point calculated.

Mass spectrometry analysis. RAW 264.7 macrophages were infected with *Brucella melitensis* 16M for 4 hours as described in Experimental procedures, then washed 3 times in 50 mM ammonium bicarbonate (AMBIC) to remove serum proteins. For mass spectrometry analysis, partially lysed cells in AMBIC were heat-treated at 100°C

for 5 min, placed into a Barocycler NEP2320 (Pressure Biosciences), then subjected to pressures alternating between 31,000 PSI and atmospheric pressure for 35 cycles (20 min total run time). Samples were centrifuged 10 min at 10,000 rpm on a microcentrifuge to separate soluble and insoluble broken cell components, the supernatant containing 50 mM AMBIC and soluble components (including proteins) was retained, then proteins reduced with 10mM TCEP (Pierce BondBreaker) at 90ºC for 20 min and afterward alkylated with 15 mM iodoacetamide (IAA) at room temperature in the dark for 1 hr. The IAA was deactivated with 5 mM dithiothreitol. Samples were then digested overnight with 1 ug of Promega modified sequencing grade trypsin, after which an equal amount of dichloromethane was added to each tube; each tube was vortexed vigorously for 2 min, then centrifuged 2 min at 15,000 rpm on a microcentrifuge to separate phases. The upper aqueous phase (containing digested peptides) was retained and the lower phase and interface (lipids and other small hydrophobics) were discarded. Samples were then dried completely in a vacuum centrifuge (Labconco), then resuspended in 2% ACN, 0.1% TFA. Samples were normalized using the A280 program on a ND-1000 Nanodrop spectrometer to roughly quantify, then loaded in equal amounts for LC-MS/MS. Digested peptides were analyzed by LC-MS/MS on a Thermo Finnigan LTQ with Michrom Paradigm LC and CTC Pal autosampler. Peptides were separated using a Michrom 200 µm x 150 mm Magic C_{18}AQ reversed phase column at 2 µl/min. Peptides were directly loaded onto a Agilent ZORBAX 300SB C_{18} reversed phase trap cartridge, which, after loading, was switched in-line with a Michrom Magic C_{18} AQ 200 um x 150 mm column connected to a Thermo-Finnigan LTQ iontrap mass spectrometer through a Michrom Advance Plug and Play nano-spray source. The nano-LC column was run with a 90 min-long gradient using a two buffer system, with Buffer A being 0.1% formic acid and Buffer B 100% acetonitrile. The gradient started with 1-10% buffer B for 5 min, then 10-35% buffer B for 65 min, 35-70% buffer B for 5 min, 70% buffer for 1 min, 1% buffer B for 14 min) at a flow rate of 2 mL min^{-1} for the maximum separation of tryptic peptides. MS and MS/MS spectra were acquired using a top 10 method, where the top 10 ions in the MS scan were subjected to automated low energy CID. An MS survey scan was obtained for the m/z range 375-1400. An isolation mass window of 2 Da was for the precursor ion selection, and a normalized collision energy of 35% was used for the fragmentation. A 2 min duration was used for the dynamic exclusion. Tandem mass spectra were extracted with Xcaliber version 2.0.7. Charge state deconvolution and deisotoping were not performed. All MS/MS samples were analyzed using X! Tandem (The GPM, thegpm.org; version CYCLONE (2013.02.01.1)). X! Tandem was set up to search a Uniprot mouse reference database appended to a decoy reversed database with the same number of entries (86070 entries total); the decoys allowing for the calculation of protein and peptide false discovery rates. Searches were conducted assuming the digestion enzyme trypsin. X! Tandem was searched with a fragment ion mass tolerance of 0.40 Da and a parent ion tolerance of 1.8 Da. Carbamidomethyl of cysteine was specified in X! Tandem as a fixed modification. Glu->pyro-Glu of the n-terminus, ammonia-loss of the n-terminus, gln->pyro-Glu of the n-terminus, deamidated of asparagine and glutamine, oxidation of methionine and tryptophan, dioxidation of methionine and tryptophan and acetyl of the n-terminus were specified in X! Tandem as variable modifications. Scaffold (version Scaffold_4.0.1, Proteome Software Inc., Portland, OR) was used to validate MS/MS based peptide and protein identifications. Peptide identifications were accepted if they could be established at greater than 80.0% probability by the

Scaffold Local FDR algorithm. Protein identifications were accepted if they could be established at greater than 95.0% probability and contained at least 2 identified peptides. Protein probabilities were assigned by the Protein Prophet algorithm (Nesvizhskii, Al et al Anal. Chem. 2003;75(17):4646-58). Proteins that contained similar peptides and could not be differentiated based on MS/MS analysis alone were grouped to satisfy the principles of parsimony. Proteins sharing significant peptide evidence were grouped into clusters. These parameters yielded a protein decoy false discovery rate (FDR) of 4.1% and a peptide decoy FDR of 0.61%, with 862 proteins identified in total. Differences between *Brucella* infected and control samples were observed using spectral counting and the T-test feature of the Scaffold program, with the weighted quantitative value (total spectra) of each sample as the criterion for differences in samples.

Supplementary table 1. qRT-PCR primers used in the present study

Target gene	Sequence
Actb	FWD: 5'-AGAGGGAAATCGTGCGTGAC-3'
	REV: 5'-CAATAGTGATGACCTGGCCGT-3'
Ym1	FWD: 5'-GGGCATACCTTTATCCTGAG-3'
	REV: 5'-CCACTGAAGTCATCCATGTC-3'
Fizz1	FWD: 5'-TCCCAGTGAATACTGATGAGA-3'
	REV: 5'-CCACTCTGGATCTCCCAAGA-3'
Pparg	FWD: 5'- CAGGCTTGCTGAACGTGAAG -3'
	REV: 5'- GGAGCACCTTGGCGAACA -3'
Il6	FWD: 5'-GCACAACTCTTTTCTCATTTCCACG-3'
	REV: 5'-GCCTTCCCTACTTCACAAGTCCG-3'
Nos2	FWD: 5'-TTGGGTCTTGTTCACTCCACGG-3'
	REV: 5'- CCTCTTTCAGGTCACTTTGGTAGG-3'
Tnfa	FWD: 5'-CATCTTGTCAAAATTCGAGTGACAA-3'
	REV: 5'-TGGGAGTAGACAAGGTACAACCC-3'
Hifa	FWD: 5'-TCTGGAAGGTATGTGGCATT-3' REV: 5'-AGGGTGGGCAGAACATTTAT-3'
Pfkfb3	FWD: 5'-AGCTGCCCGGACAAAACAT-3'
	REV: 5'-CTCGGCTTTAGTGCTTCTGGG-3'
Glut1	FWD: 5'-GCTGTGCTTATGGGCTTCTC-3'
	REV: 5'-CACATACATGGGCACAAAGC-3'
Pgc1b	FWD: 5'-CAAGCTCTGACGCTCTGAAGG-3'
	REV: 5'-TTGGGGAGCAGGCTTTCAC-3'
Acadm	FWD: 5'-GAAAGTTGCGGTGGCCTTGG-3'
	REV: 5'-AAGCACACATCATTGGCTGGC-3'

Acadl	FWD: 5'-GGGAAGAGCAAGCGTACTCC-3’
	REV: 5'-TCTGTCATGGCTATGGCACC-3’

Supplementary table 2. Histopathology score used in the present study

Score	Granuloma	Neutrophils	Necrosis	Vascular lesion
0	no lesion	no lesion	no lesion	no lesion
1	mild focal to multifocal granuloma formation	mild focal to multifocal neutrophilic infiltration	mild focal necrosis	mild focal vasculitis/thrombosis
2	mild to moderate focal to multifocal granuloma formation	mild to moderate muiltifocal neutrophilic infiltration	mild to moderate multifocal necrosis	mild to moderate multifocal vasculitis/thrombosis
3	moderate multifocal granuloma formation	moderate multifocal neutrophilic infiltration	moderate multifocal necrosis	moderate multifocal vasculitis/thrombosis
4	severe multifocal to coalescent granuloma formation	severe multifocal to coalescent neutrophilic infiltration	severe multifocal to coalescent necrosis	severe multifocal to diffuse vasculitis/thrombosis

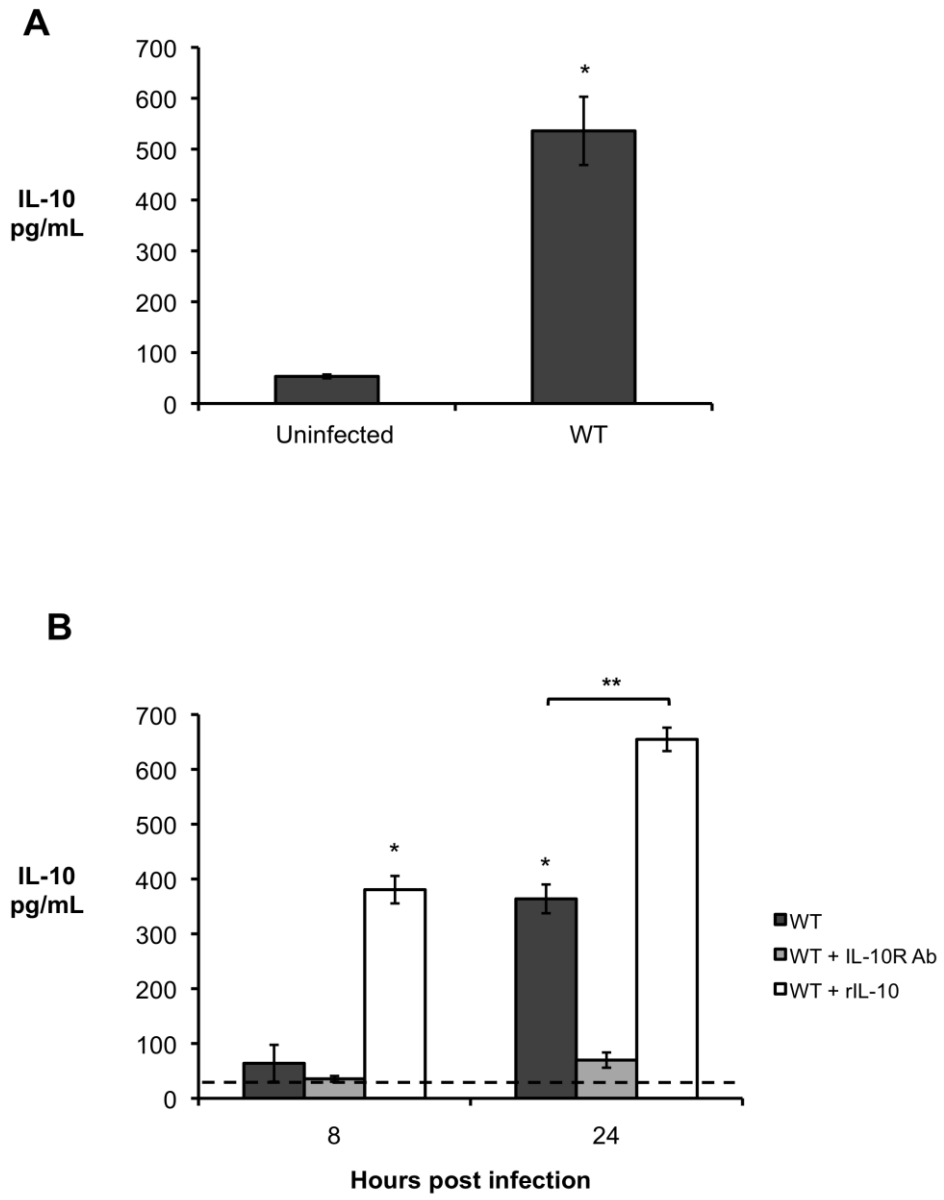

Fig S4

Supplementary figure 1. (A) ELISA essay for IL-10 production in supernatant from C57BL/6 wild type BMDM infected with *B. abortus* 2308 for 24h. (B) ELISA essay for IL-10 production in supernatant from RAW-Blue macrophages infected with *B. abortus* 2308 for 8h and 24h in the presence of IL-10 receptor blocking antibody (IL-10R Ab), isotype control (IgG Ab) or exogenous IL-10 (rIL-10)**.**

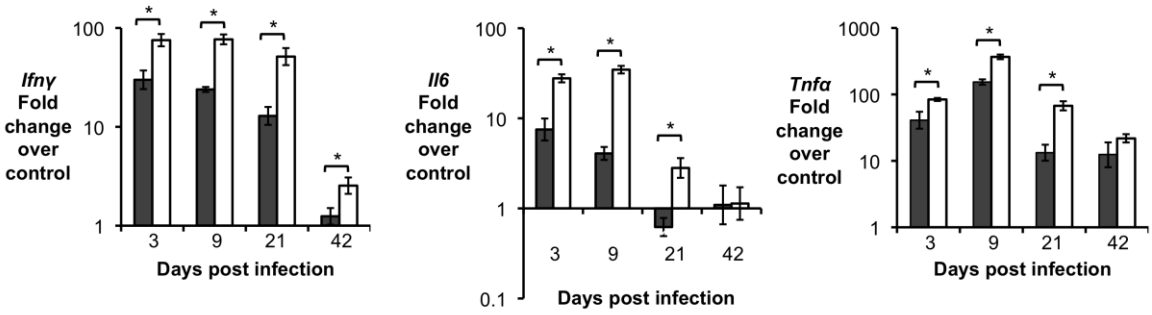

Supplementary figure 2. qRT-PCR analysis of pro-inflammatory cytokines in liver from littermate control (grey bars) compared with IL10Rflox/LysMCre mice (white bars) at 3, 9, 21 and 42 d.p.i. n=5. Values represent mean ± SEM. (*) represents $P<0.05$ relative to uninfected control using unpaired t-test statistical analysis.

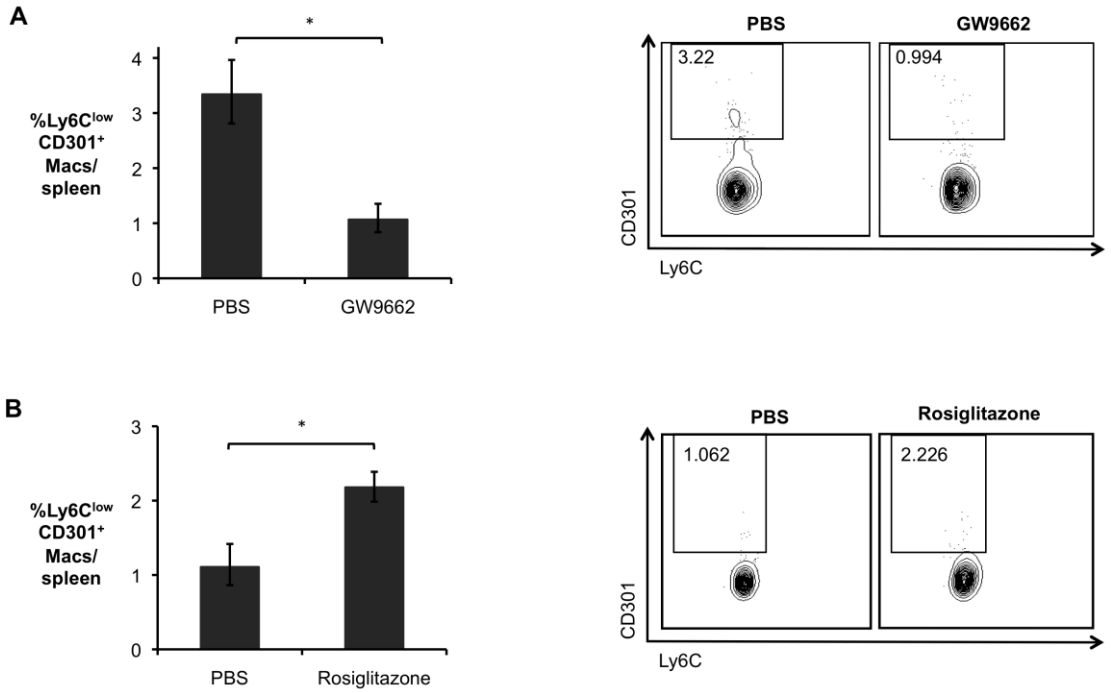

Fig.S3

Supplementary figure 3. Flow cytometry for AAM in mice treated with PPARg agonist and PPARg antagonist. AAM were CD3-B220-NK1.1-Ly6G-CD11b+F4/80+ cells that were Ly6Clow and CD301+. (A) AAM in C57BL/6 mice treated the PPARg antagonist GW9662 or mock treated with PBS from days 18-30 post *B. abortus* infection (n=4). (B) AAM in C57BL/6 mice treated the PPARg agonist Rosiglitazone or mock treated with PBS from 7 days before inoculation until 9 days post *B. abortus* infection (n=4). Gates were set using fluorescence-minus-one controls.

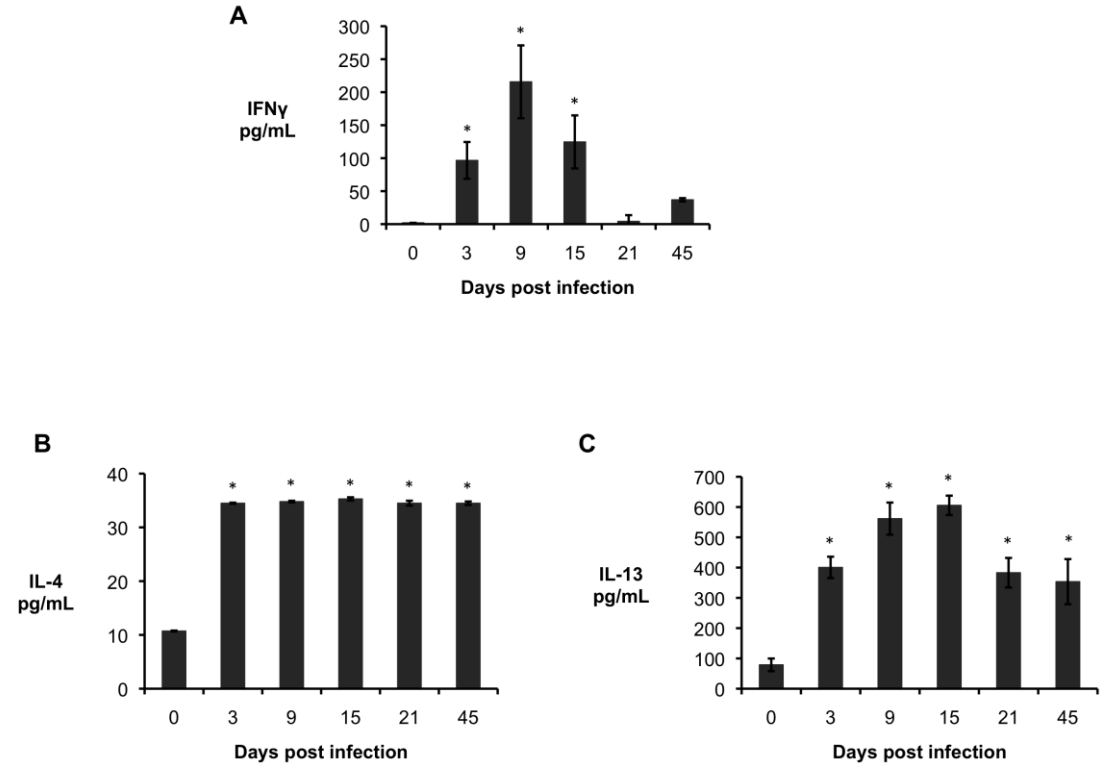

Fig.S2

Supplementary figure 4. Detection of IFN-g (A), IL-4 (B) and IL-13 (C) in serum from *B. abortus* infected C57BL/6J mice at 0, 3, 9, 15, 21 and 45 days post-infection using a multiplex cytokine array. n=5. Values represent mean ± SEM. (*) Represents $P<0.05$ using unpaired t-test statistical analysis.

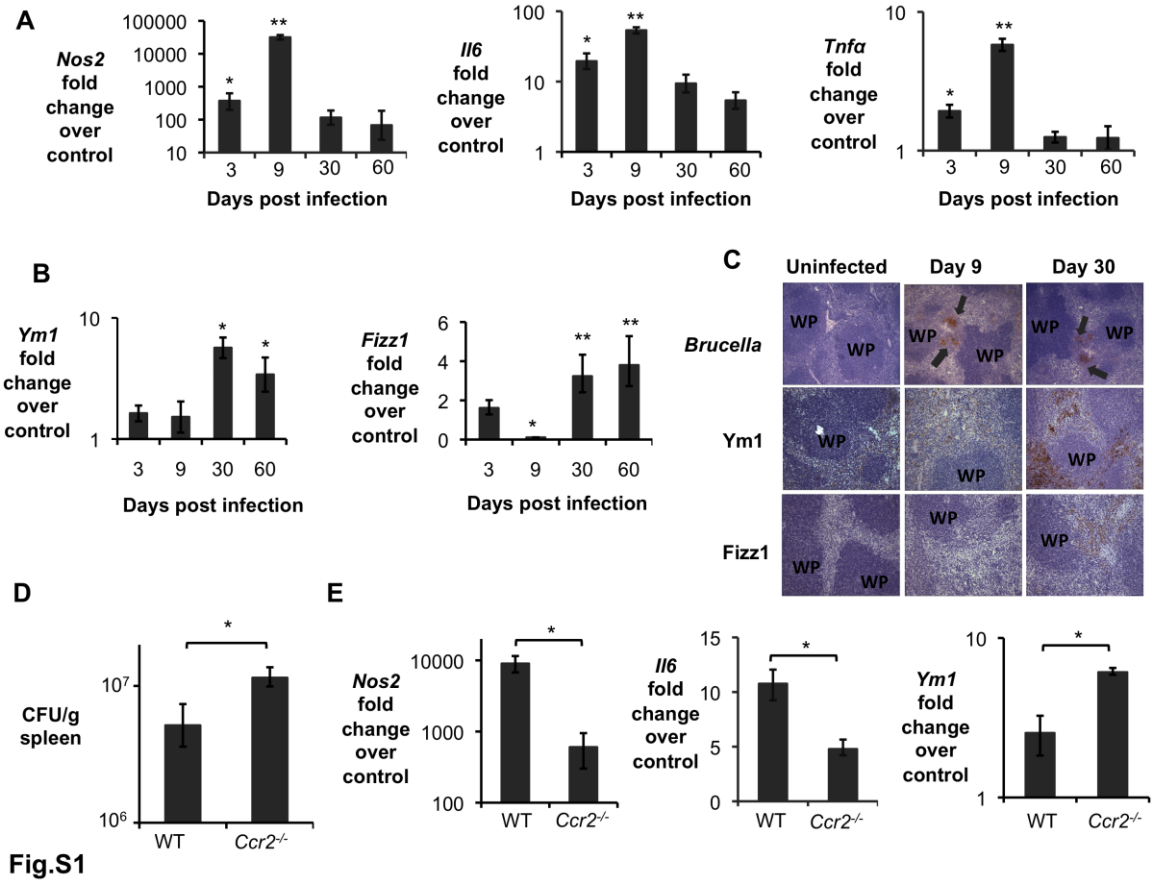

Supplementary figure 5. (A) Real time RT-PCR gene expression analysis of CAM genes *Nos2*, *Il6* and *Tnfa* in splenic CD11b^{+} cells from *B. abortus* infected C57BL/6J mice (n=5) at 3, 9, 30 and 60 d.p.i. **(B)** Real time RT-PCR gene expression analysis of AAM genes *Ym1* and *Fizz1* in CD11b^{+} splenic cells from *B. abortus* infected C57BL/6J mice (n=5) at 3, 9, 30 and 60 d.p.i. **(C)** Immunolabeling of *B. abortus* (first panel, black arrows) and AAM markers Ym1 and Fizz1 in spleens of *B. abortus* infected mice at 9 and 30 d.p.i. (x20). **(D)** *B. abortus* 2308 CFU counts in spleens from C57BL/6J and CCR2$^{-/-}$ mice (n=6) at 9 days post infection (d.p.i). **(E)** Real time RT-PCR gene expression analysis of CAM genes *Nos2* and *Il6* and AAM gene *Ym1* in CD11b+ splenic cells from *B. abortus* infected C57BL/6J and CCR2$^{-/-}$ mice (n=5) at 9 d.p.i. Values represent mean ± SEM. (*) Represents P<0.05 and (**) represents P<0.01 using one way ANOVA for (A-B) or unpaired t-test analysis for (D-E).

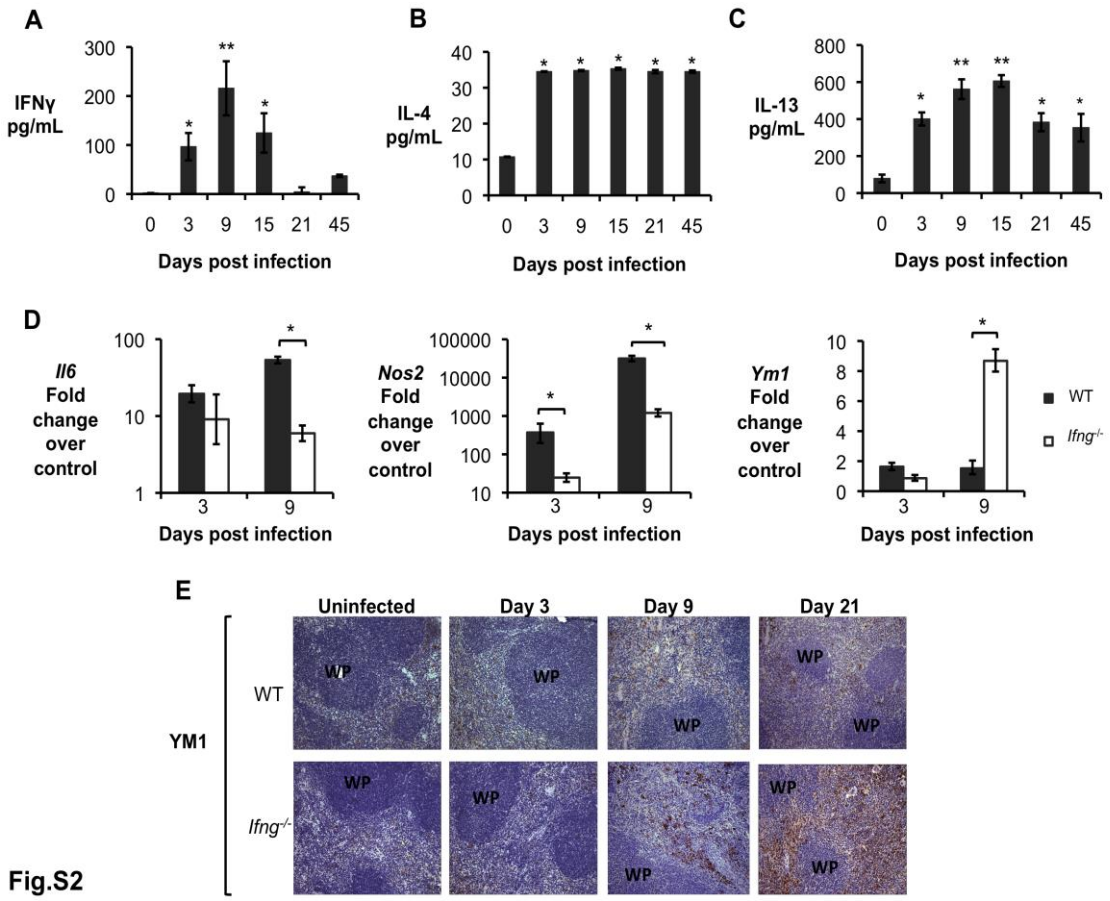

Fig.S2

Supplementary figure 6. Detection of IFN-γ **(A)**, IL-4 **(B)** and IL-13 **(C)** in serum from *B. abortus* infected C57BL/6J mice (n=5) at 0, 3, 9, 15, 21 and 45 days post-infection using a multiplex cytokine array. **(D)** Real time RT-PCR gene expression analysis of CAM genes *Il6* and *Nos2* and AAM gene *Ym1* in $CD11b^{+}$ splenocytes from *B. abortus*-infected C57BL/6J and congenic $Ifng^{-/-}$ mice (n=5) at 3 and 9 d.p.i. **(E)** Immunolabeling of AAM marker Ym1 in spleens of *B. abortus*-infected C57BL/6J and congenic $IFN\gamma^{-/-}$ mice at 3, 9 and 21 d.p.i. (x20). Values represent mean ± SEM. (*) Represents $P<0.05$ and (**) represents $P<0.01$ using one way ANOVA for (A-C) or unpaired t-test analysis for (D).

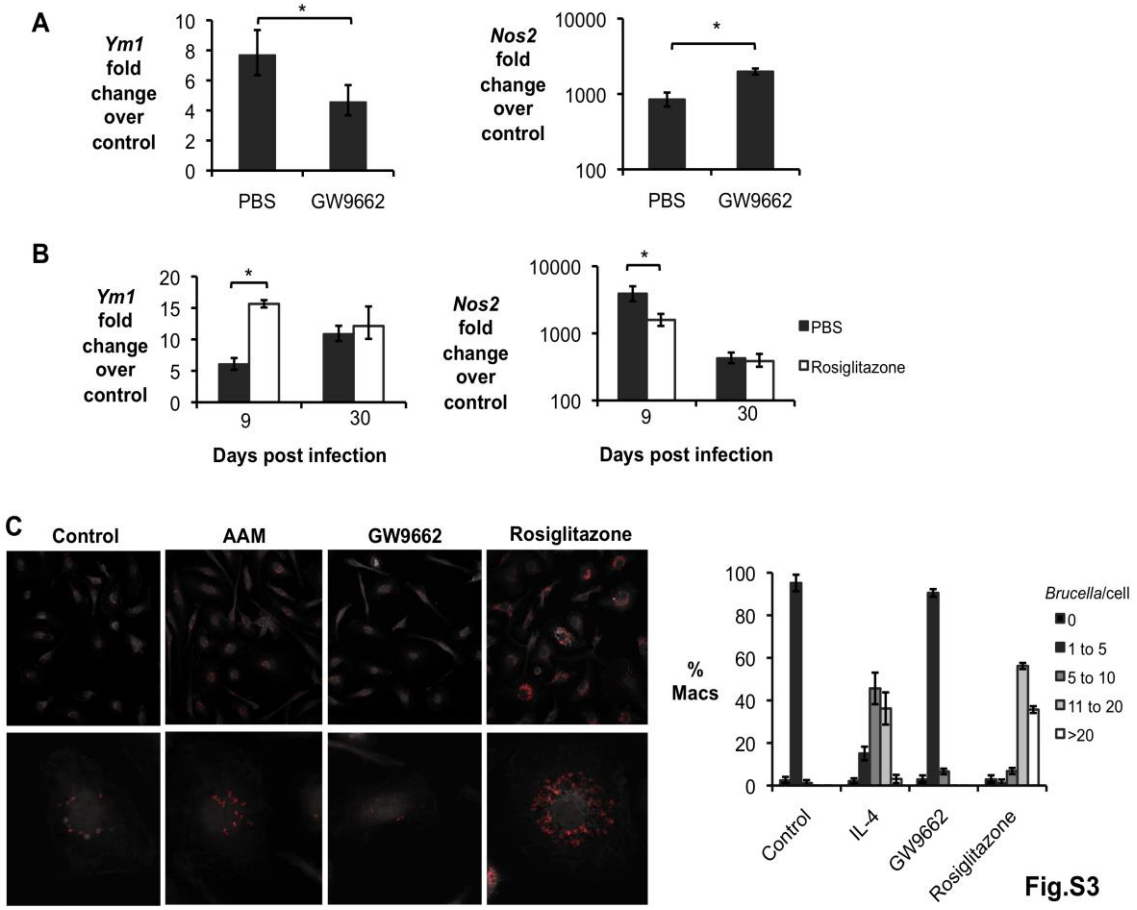

Supplementary figure 7. (A) Real time RT-PCR gene expression analysis of CAM marker *Nos2* and AAM marker *Ym1*. Transcripts were measured in $CD11b^{+}$ splenocytes obtained at 30 d.p.i.,from *B. abortus*-infected C57BL/6J mice (n=5) that had been treated daily from 18 to 30 d.p.i. with either PPARγ antagonist GW9662 or the diluent (PBS). **(B)** Real time RT-PCR gene expression analysis of CAM marker *Nos2* and AAM marker *Ym1*, measured at 9 and 30 d.p.i., in CD11b+ splenocytes from *B. abortus* infected C57BL/6J mice (n=5) treated daily for 7 days prior to infection with PPARγ agonist Rosiglitazone or PBS control. **(C)** Fluorescence microscopy of BMDM from C57BL/6J non-stimulated (Control), or stimulated with 10 ng/mL of rIL-4 (AAM) or with 10 ng/mL of IL-4 + 3µM of GW9662 or with 5µM of Rosiglitazone and infected with mCherry-expressing *B. abortus* 2308 (MX2; red) for 24h. Nuclei in white are stained with DAPI (left panel). Quantification of intracellular *B. abortus* MX2 in individual BMDM treated as described above (right panel). Values represent mean ± SEM from four independent experiments, each conducted in duplicate. (*) Represents $P<0.05$ using unpaired t-test analysis.

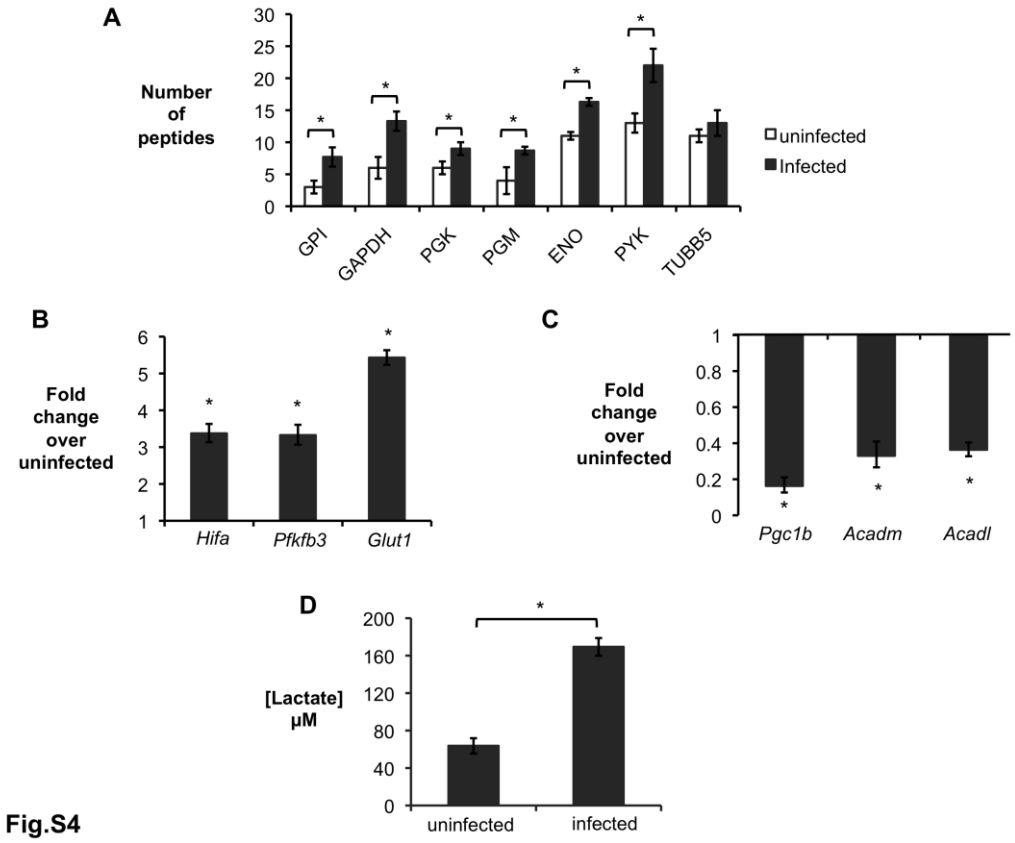

Fig.S4

Supplementary figure 8. (A) Mass spectrometry analysis of glycolytic pathway enzymes GPI (glucose phosphate isomerase), GAPDH (glyceraldehyde-3-phosphate-dehydrogenase), PGK (phosphoglycerate kinase), PGM (phosphoglycerate mutase), ENO (enolase 1), PYK (pyruvate kinase) and TUBB5 (Tubulin beta 5; loading control) as control in RAW 264.7 macrophages uninfected or infected with *Brucella* for 4 hours. Results shown are compiled from three independent experiments. **(B)** Real time RT-PCR gene expression analysis of glycolytic pathway genes *Hifa* (hypoxia inducible factor α), *Pfkfb3* (phosphofructokinase-3) and *Glut1* (glucose transporter 1) in BMDM from C57BL/6J infected with *B. abortus* for 8 hours. **(C)** Real time RT-PCR gene expression analysis of fatty acid β-oxidation pathway genes *Pgc1b* (PPARγ coactivator 1 β), *Acadm* (medium-chain acyl-CoA dehydrogenase) and *Acadl* (long-chain acyl-CoA dehydrogenase) in BMDM from C57BL/6J infected with *B. abortus* for 8 hours. **(D)** Measurement of lactate concentration in supernatant from BMDM from C57BL/6J uninfected or infected with *B. abortus* for 24 hours. Values represent mean ± SEM from four independent experiments, each conducted in duplicate. (*) Represents $P<0.05$ using one way ANOVA for (B-C) or unpaired t-test analysis for (A) and (D).

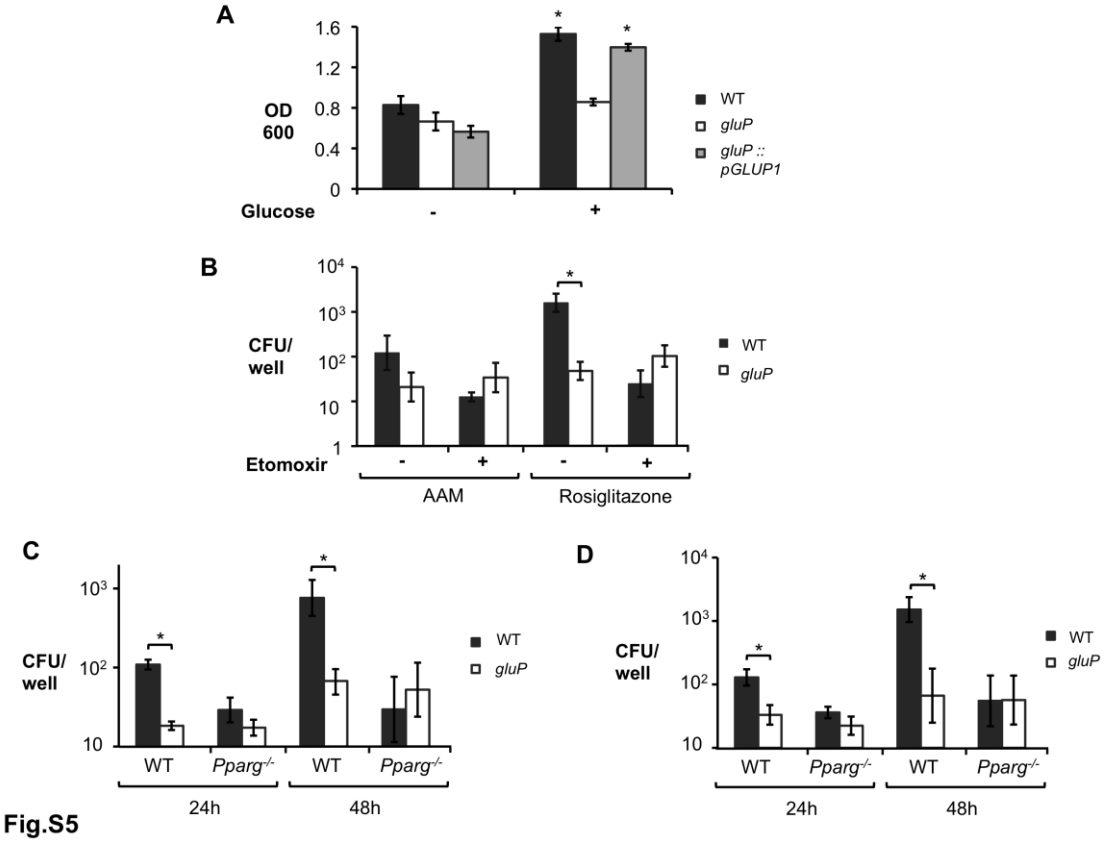

Fig.S5

Supplementary figure 9. (A) *In vitro* growth of *B. abortus* 2308 WT, isogenic *gluP* mutant and complemented *gluP* mutant (*gluP*::pGLUP1) in Tryptic Soy Broth formulated with (+) or without (-) glucose (0.25%), as measured by optical density (OD_{600}) at 24h. Data shown are compiled from three independent experiments, each conducted with duplicate samples. **(B)** Recovery of *B. abortus* from C57BL/6J BMDM treated with the β-oxidation inhibitor etomoxir (50 µM) or vehicle (PBS) in the presence of 10 ng/mL of rIL-4 (AAM) or 5µM of PPARγ agonist Rosiglitazone and infected with *B. abortus* 2308 WT or isogenic *gluP* mutant for 24h. **(C)** Recovery of *B. abortus* from WT or congenic *Pparg-/-* BMDM stimulated with 10 ng/mL of rIL-4 (AAM) and infected with *B. abortus* 2308 WT or isogenic *gluP* mutant for 24 and 48h. **(D)** Recovery of *B. abortus* from WT or congenic *Pparg-/-* BMDM stimulated with 5 µM of PPARγ agonist Rosiglitazone and infected with *B. abortus* 2308 WT or isogenic *gluP* mutant for 24 and 48h. Values shown in B-D represent mean ± SEM of four independent experiments conducted with duplicate samples. (*) Represents P<0.05 using one way ANOVA for (A) or unpaired t-test analysis for (B-D).